



# ASE 334 – PROPULSION SYSTEMS I

## TurboFan Engine Project

Performance Analysis and Optimization of a  
Supersonic, Low ByPass Ratio

16.07.2021

### Group Members:

Faruk Çorum 2021111

Berkay Cihan 2318020

Ömer Hakan Bozkurtoğlu 2156206

Brenda Muthusi 2278265

Ravian w. Simiyu 2337905

Instructor Name: Dr. Sıtkı Uslu

Course Assistant: Ali Mohaghegh

Group Name: FireFly Jetx

## TABLE OF CONTENTS

<b>ABSTRACT</b> .....	3
<b>NOMENCLATURE</b> .....	4
<b>1. INTRODUCTION</b> .....	5
<b>2. ENGINE PERFORMANCE AND MODELLING</b> .....	7
<b>3. COMPONENTS ANALYSIS AND DESIGN</b> .....	10
<b>3.1. INLET DESIGN</b> .....	10
<b>3.2. COMPRESSOR</b> .....	13
<b>3.3. COMBUSTION CHAMBER</b> .....	17
<b>3.4. TURBINE</b> .....	20
<b>3.4.1. Introduction</b> .....	20
<b>3.4.2. Turbine Blade, Disk Material Selection and Design Criteria</b> .....	20
<b>3.4.3. Geometry of Blades</b> .....	21
<b>3.4.4. Materials</b> .....	23
<b>3.4.5. Preliminary Turbine Design</b> .....	24
<b>3.4.6. History Over the Years</b> .....	25
<b>3.5. AFTERBURNER</b> .....	26
<b>3.5.1. Introduction</b> .....	26
<b>3.5.2. Operating of Afterburner</b> .....	27
<b>3.5.3. Materials</b> .....	27
<b>3.5.4. Advantages and Disadvantages of Afterburner</b> .....	27
<b>3.5.5. Mathematical Equations of the Afterburner</b> .....	29
<b>3.6. NOZZLE</b> .....	30
<b>4. CONCLUSION</b> .....	33
<b>REFERENCES</b> .....	34
<b>APPENDICES</b> .....	36
<b>A) The Analysis of Engine Performance and Modelling</b> .....	36
<b>B) CFD Analysis</b> .....	54
<b>B.1. CFD Analysis for Convergent-Divergent Nozzle</b> .....	54
<b>C) CAD Design</b> .....	56
<b>C.1. CAD Drawing for the Combustion Chamber</b> .....	56
<b>C.2. CAD Drawing for the Blade</b> .....	57
<b>C.3. CAD Drawing for the ConDi Nozzle</b> .....	58

## **ABSTRACT**

In this project, the turbofan jet engine "Turbo-Union RB199" is considered as our baseline engine. This engine has been improved in terms of TSFC and T/W to be used in the aircraft Panavia Tornado which will enter into service in 2030. Wet engine parameters are mainly focused on the comparison. The baseline wet engine has main design parameters as 23.5 OPR, 2.45 inner and 2.55 outer FPR, 1.1 BPR, 1600 K TET; but then, our improved engine has 32.54:1 OPR, 2.75 inner and 2.9 outer FPR, 1.1 BPR, 1745 K TET. Using these main parameters and other parameters on GasTurb 13, at sea level and stationary, TSFC has been decreased by 12.12 percent from 59.1187 g/(kN\*s) baseline wet engine to 51.9569 g/(kN\*s) FireFly Jetx wet engine, and T/W has been increased by 11.75 percent from 8.8893 baseline wet engine to 9.9336 FireFly Jetx wet engine. At 50000 ft and cruise speed 1800 km/hr, TSFC has been decreased by 7.59 percent from 65,7249 g/(kN\*s) baseline wet engine to 61,0890 g/(kN\*s) FireFly Jetx wet engine and increased T/W by 2.11 percent from 3, 5233 baseline wet engine to 3,5977 FireFly Jetx wet engine. Furthermore, detailed analyses were done for engine inlet design, oblique and normal shock, pressure ratio calculations for the new engine inlet design. Detailed analysis on engine exit nozzle, normal shock location calculated, and CFD analysis and nozzle design were done on ANSYS. Besides, further explanations were done about Compressor, Combustion, Turbine, and Afterburner parts of the engine.

## NOMENCLATURE

$A$ :	<i>Area</i> [ $m^2$ ]	$q$ :	<i>Dynamic pressure</i> [bar, Pa]
$A^*$ :	<i>Choked area</i> [ $m^2$ ]	$T$ :	<i>Temperature</i> [K]
$a$ :	<i>Local speed of sound</i> [m/s]	$T_t$ :	<i>Total temperature</i> [K]
$A_{ref}$ :	<i>The reference area</i> [ $m^2$ ]	$t$ :	<i>Time</i> [s]
$c_p$ :	<i>Pressure coefficient</i>	$u$ :	<i>Gas speed</i> [m/s]
$D_{add}$ :	<i>Additive drag</i> [N]	$V$ :	<i>Volume</i> [ $m^3$ ]
$D_r$ :	<i>Ram drag</i> [N]	$V$ :	<i>Speed</i> [m/s]
$F_g$ :	<i>Gross thrust</i> [N]	$V_m$ :	<i>Mean speed</i> [m/s]
$F_n$ :	<i>Net thrust</i> [N]	$V'$ :	<i>Relative speed</i> [m/s]
$H$ :	<i>Height</i> [m]	$W$ :	<i>Weight</i> [N]
$h$ :	<i>Specific enthalpy</i> [J/kg]	$W_a$ :	<i>The actual work</i> [J]
$h_t$ :	<i>Specific total enthalpy</i> [J/kg]	$W_{real}$ :	<i>The real compressor work</i> [J]
$L$ :	<i>Lift</i> [N]	$W_s$ :	<i>Isentropic compressor work</i> [J]
$M$ :	<i>Mach number</i>	$w$ :	<i>Specific work</i> [J/kg]
$\dot{m}$ :	<i>Mass flow rate</i> [kg/s]	$\gamma$ :	<i>Ratio of specific heats</i>
$\dot{m}_f$ :	<i>Fuel mass flow rate</i> [kg/s]	$\varphi$ :	<i>Cooling effectiveness parameter</i>
$\dot{m}_0$ :	<i>Air mass flow rate</i> [kg/s]	$\rho$ :	<i>Fluid density</i> [ $\frac{kg}{m^3}$ ]
$\dot{m}_p$ :	<i>Propellant mass flow rate</i> [kg/s]	$\mu$ :	<i>Coefficient of viscosity</i> [ $\frac{N*s}{m^2}$ ]
$p$ :	<i>Static pressure</i> [bar, Pa]	$\eta_o$ :	<i>Overall efficiency</i>
$p_t$ :	<i>Total pressure</i> [bar, Pa]	$\eta_{T_{HP}}$ :	<i>Turbine efficiency for the HP</i>
$Q_R$ :	<i>Fuel heating value</i> [kJ/kg]	$\eta_{T_{LP}}$ :	<i>Turbine efficiency for the LP</i>

### Abbreviations and acronyms

$AB$ :	<i>AfterBurner</i>
$AFR$ :	<i>Air Fuel Ratio</i>
$BPR$ :	<i>ByPass Ratio</i>
$ConDi$ :	<i>Convergent-Divergent Nozzle</i>
$FPR$ :	<i>Fan Pressure Ratio</i>
$HP$ C:	<i>High Pressure Compressor</i>
$HPT$ :	<i>High Pressure Turbine</i>
$LPC$ :	<i>Low Pressure Compressor</i>
$LPT$ :	<i>Low Pressure Turbine</i>
$Max Dry$ :	<i>W/o AB</i>
$OPR$ :	<i>Overall Pressure Ratio</i>
$SLS$ :	<i>Standard Sea-Level</i>
$T/W$ :	<i>Thrust to Weight Ratio</i>
$TET$ :	<i>Turbine Entry Temperature</i>

### Subscripts

$a$ :	<i>Actual</i>
$f$ :	<i>Fuel</i>
$g$ :	<i>Gross</i>
$m$ :	<i>Mean</i>
$max$ :	<i>Maximum</i>
$n$ :	<i>Net</i>
$p$ :	<i>Propellant</i>
$r$ :	<i>Relative</i>
$rev$ :	<i>Reversible</i>
$s$ :	<i>Isentropic</i>
$t$ :	<i>Total</i>

### Superscripts

$*$ :	<i>Critical or sonic state</i>
-------	--------------------------------

## 1. INTRODUCTION

The most contemporary variant of the fundamental gas turbine engine is a turbofan engine.[1] It is crucial in the production of thrust for both commercial and military aircraft. Since its inception in the 1950s, the turbofan engine has grown into the principal power source for today's commercial aviation fleet. It is often utilized on wide-body aircraft such as the Boeing 747 and the Airbus A300, as well as military aircraft.[2] A turbofan is a turbine engine with a huge low-pressure fan upstream of the compressor section, which allows low-pressure air to bypass the compressor and turbine, mixing with the jet stream and increasing the mass of accelerated air. This technology of moving enormous volumes of air at a slower speed improves efficiency while lowering fuel consumption and noise levels.[3]

- Fan

The shaft is driven by the expansion of gases in the combustion turbine stage, which spins the enormous fans. The fan forces air into the bypass and compression chambers, ensuring that it achieves the proper pressure and temperature to ignite and burn the fuel. The air that passes through the fan travels in two directions. A portion of the airflow is sent to the engine's core, while the rest, known as bypass air, is responsible for generating additional thrust and cooling engine components. The bypass stream mass flow rate ratio to the mass flow rate coming to the core is called the bypass ratio. It is a critical metric for categorizing the turbofan because engines with the largest bypass ratios achieve the highest propulsion efficiency.[4] Modern turbofan engines for airplane transport have bypass ratios ranging from 4 to 6 in most cases. The bypass ratio of a military-grade turbofan engine is less than one. The number of blades in a single fan stage can range from 20 to 50.[5] Crack resistance, stiffness, fatigue, and weight are the four most known criteria to consider when choosing a fan blade material. The corrosion resistance and strength of titanium alloys make them a desirable choice (See appendix C.2).

- Compressor

Before the incoming air enters the combustor, all turbine engines include a compressor to increase its pressure. The performance of the compressor has a significant impact on the overall efficiency of the engine. Compressors are classified as axial and centrifugal. Centrifugal compressors, which were initially employed in jet engines, are still utilized in tiny turbojets and turboshaft engines, as well as pumps in rocket engines. Axial compressors are used in most modern huge turbojet and turbofan engines.[6]

- Combustor

The high-pressure airflow enters the combustion chamber, where the fuel is injected after the accelerated airflow exits the compressor. After that, the fuel-air combination is ignited, and the hot gases that result in flow through turbines, which drive the compressors.

- Turbine

According to Saeed F. (2014), the high-pressure, high-temperature gas from the burner is directed to a turbine because the turbine has high-pressure gas on the one side and low-pressure

gas from the exhaust nozzle or exhaust pipe another side, the turbine may be thought of as a valve. As a result, the first valve in a gas turbine engine, the throttle station, is located in the turbine. The second and final throttle position on a supersonic aircraft is the throat of the exhaust nozzle. As a result, the flow process in a turbine (and exhaust nozzle) entails large (static) pressure drop, and thus significant (static) temperature drop, which is referred to as flow expansion. The compressor and the aircraft's propulsion are both powered by flow expansion. The turbine and the compressor are linked by a shared shaft, which delivers shaft power to the compressor (p. 168).[7]

- Nozzle

Saeed F. (2014) argues that the exhaust nozzle concept for aircraft jet engines has evolved from a basic convergent duct used to propel hot exhaust gases into a changeable geometry and multifunctional component in recent designs. Reversing thrust, thrust vectoring, noise suppression, and improved dynamic stability of maneuvering aircraft are among the new tasks. To meet these objectives, advancements in nozzle cooling, operation, and production were required (p. 168).[7]

- Mixer

The mixer lowers the velocity of the core as it emerges from the air, lowering the amount of noise created. Furthermore, the exhaust temperature is reduced, resulting in a reduction in the aircraft's thermal signature. When thermal sensing or heat-seeking weaponry are utilized in military airplanes, this capability is crucial. A mixer would also provide a performance gain in terms of enhanced thrust.[8]

- Multi-spool configuration

Saeed F. (2014) explains that two different and complementary systems were invented in the United States to establish a high-pressure compression system. The first is the Pratt & Whitney multi-spool idea, and the second is the variable stator (developed by GE). The multi-spool concept consists of the number of compressor stages divided into two or three groups: low-pressure compressor, medium pressure compressor, and high-pressure compressor. Each group is propelled by a separate shaft that rotates at different rates (p. 168).[7]

With the same fuel consumption, a low BPR engine can provide less thrust than a high BPR engine. Many military engines, on the other hand, now use low BPR engines with an afterburner. Afterburners mix the majority of the fuel with oxygen, heat it up, and fire it out of the nozzle. The addition of an afterburner boosts thrust by up to 50%. Although afterburners use a lot of fuel, they provide a lot of advantages for military aircraft since they provide a lot of thrusts. Turbofan engines frequently employ a mixer in low-pressure environments because it is difficult to ignite the cold air. The hot gas stream is mixed with cooled air in this mixing chamber.

For these reasons, the addition of an afterburner in our engine is an important point. Especially for military turbofan aircraft, take-off, maneuvering, and combat characteristics require more thrust. Afterburner has been added to our engine to fulfill these features.

## 2. ENGINE PERFORMANCE AND MODELLING

Baseline model:

Table 1. Baseline engine parameters.[27]

Engine type	Military turbofan
LPC stages	3 axial
IP stages	3 axial
HPC stages	6 axial
Combustion chamber	Annular throughflow
HP Turbine	1 axial
IP Turbine	1 axial
LP Turbine	2 axial
Max. Dry thrust	~ 40 kN
Max. AB thrust	~ 70 kN
TET	Approx. 1600 K
A/B Temperature	Approx. 2000 K
Air Flow Rate	72 kg/s
Max. Dry SFC (SLS, ISA)	~ 17 g/kNs
Max. A/B (SLS, ISA)	~ 59 g/kNs
OPR	23.5:1
BPR	1.1
Max. Engine diameter	73.1 cm
Max. Engine length	3.3 meter
Engine weight	1084 kg

As can be seen in the table 1, the design parameters of our baseline engine Turbo-Union RB199 which is a 3-spool military type turbofan engine from 1970's.

Table 2. Properties and values for the baseline engine.[GasTurb]

Property	Unit	Value	Comment			
Intake Pressure Ratio		0,995				
No (0) or Average (1) Core dP/P		1				
Inner Fan Pressure Ratio		2,45				
Outer Fan Pressure Ratio		2,55				
Core Inlet Duct Press. Ratio		1				
IP Compressor Pressure Ratio		2				
Compr. Interduct Press. Ratio		0,99				
HP Compressor Pressure Ratio		4,85				
Bypass Duct Pressure Ratio		0,97				
Inlet Corr. Flow W2Rstd	kg/s	72				
Design Bypass Ratio		1,1				
Burner Exit Temperature	K	1600				
Burner Design Efficiency		0,999				
Burner Partload Constant		1,6	used for off design only			
Fuel Heating Value	MJ/kg	43,124				
Overboard Bleed	kg/s	0				
Power Offtake	kW	50				
HP Spool Mechanical Efficiency		1				
IP Spool Mechanical Efficiency		1				
LP Spool Mechanical Efficiency		1				
Burner Pressure Ratio		0,97				
IPT Interd. Ref. Press. Ratio		0,99				
LPT Interd. Ref. Press. Ratio		0,99				
Turbine Exit Duct Press Ratio		0,98				
Hot Stream Mixer Press Ratio		0,99				
Cold Stream Mixer Press Ratio		0,99				
Mixed Stream Pressure Ratio		1				
Mixer Efficiency		0,5				
Design Mixer Mach Number		0,24				
Design Mixer Area	m <sup>2</sup>	0				

As seen in the table 2 is GasTurb 13 software in which we tried to create our baseline engine with approximate parameters inside GasTurb 13 program. The parameters above are used to find the other design parameters and engine performance on GasTurb. The new engine has 23.5 OPR, 2.45 inner and 2.55 outer FPR, 1.1 BPR and 1600 K TET for the main design parameters.

Station	W kg/s	T K	P kPa	WRstd kg/s	Reheat on			
amb		288,15	101,325			FN = 70,03 kN		
2	71,640	288,15	100,818	72,000	TSFC = 59,1187 g/(kN*s)			
13	37,526	388,24	257,087	17,168	WF Burner= 0,66874 kg/s			
21	34,114	384,50	247,005	16,165	s NOx = 0,82223			
22	34,114	384,50	247,005	16,165	BPR = 1,1000			
24	34,114	482,08	494,010	9,050	Core Eff = 0,4251			
25	34,114	482,08	489,070	9,142	Prop Eff = 0,0000			
3	31,044	782,57	2371,989	2,185	P3/P2 = 23,527			
31	27,462	782,57	2371,989		P2/P1 = 0,99500			
4	28,131	1600,00	2300,830	2,919	P22/P21 = 1,00000			
41	29,836	1557,01	2300,830	3,054	P25/P24 = 0,99000			
42	29,836	1275,25	865,317		P4/P3 = 0,97000			
43	31,542	1250,41	865,317		P44/P43 = 0,99000			
44	31,542	1250,41	856,664		P48/P47 = 0,99000	Input:		
45	32,907	1228,00	856,664	8,035	P6/P5 = 0,98000	HPC Tip Speed m/s	420,00000	
46	32,907	1142,99	610,921		P16/P13 = 0,97000	HPC Inlet Radius Ratio	0,80000	
47	33,589	1133,98	610,921		P5/P2 = 0,92882	HPC Inlet Mach Number	0,50000	
48	33,589	1133,98	604,812	11,163	P8/P64 = 0,88868	min HPC Inlet Hub Diameter m	0,00000	
49	33,589	955,79	273,965		P16/P6 = 0,92882	Output:		
5	34,612	947,67	273,965	23,215	A63 = 0,17251 m <sup>2</sup>	HPC Tip circumf. Mach No	0,98073	
64	70,637	674,56	255,171		A163 = 0,27731 m <sup>2</sup>	HPC Tip relative Mach No	1,10084	
7	74,108	2040,00	226,766		A64 = 0,44981 m <sup>2</sup>	Design HP Spool Speed [RPM]	18900,96	
8	75,609	2013,00	226,766	89,293	WF total = 4,13981 kg/s	HPC Inlet Tip Diameter m	0,42439	
Bleed	0,171	782,57	2371,985		A8 = 0,38786 m <sup>2</sup>	HPC Inlet Hub Diameter m	0,33951	
					WBld/W2 = 0,00238	Calculated HPC Radius Ratio	0,80000	
					Ang8 = 5,13 °	Corr.Flow/Area HPC kg/(s*m <sup>2</sup> )	179,51654	
Efficiencies:	isentr	polytr	RNI	P/P	P8/Pamb = 2,23801			
Outer LPC	0,8800	0,8946	0,995	2,550	PWX = 50,00 kw			
Inner LPC	0,8700	0,8852	0,995	2,450	W1kLP/W25= 0,00000			
IP Compressor	0,8500	0,8636	1,729	2,000	WHDB1/W22= 0,00000			
HP Compressor	0,8600	0,8857	2,614	4,850	WCWN/W25 = 0,05000			
Burner	0,9990			0,970	Loading = 100,00 %			
HP Turbine	0,9000	0,8892	3,165	2,659	WCWR/W25 = 0,05000			
IP Turbine	0,9000	0,8963	1,547	1,402	WCIN/W25 = 0,04000			
LP Turbine	0,9004	0,8913	1,197	2,208	WCIR/W25 = 0,02000			
Reheat	0,9000			0,889	WF Reheat= 3,47107 kg/s			
					XM64 = 0,24001			
					XM7 = 0,60724			
					far7 = 0,05917			
					WCLR/W25 = 0,03000			
HP Spool mech Eff	1,0000	Nom Spd	18901 rpm					
IP Spool mech Eff	1,0000	Nom Spd	16700 rpm					
LP Spool mech Eff	1,0000	Nom Spd	14600 rpm					
hum [%]	0,0	war0	FHV	Fuel				
			43,124	Generic				

Figure 1. The result of the wet baseline engine.[GasTurb]

After running the simulation at sea level conditions with zero velocity, this figure 1 results from the wet baseline engine. The most important values from this figure are thrust which is 70.03 kN force, and TSFC, which is 59,1187 g/(kN \* s).

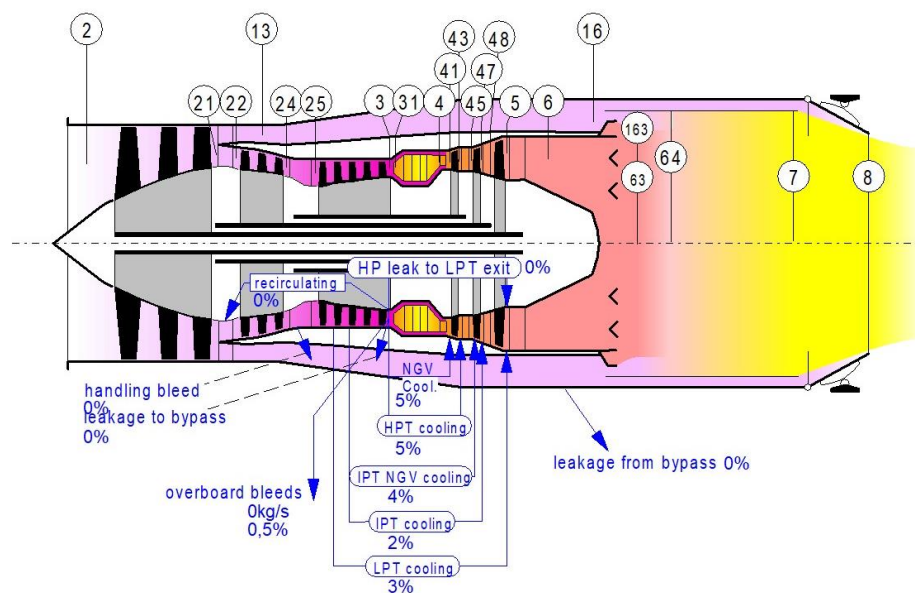


Figure 2. Rough drawing of the baseline engine.[GasTurb]

As shown in the figure 2, it has an afterburner and a divergent nozzle. Also, this shows which numbers represent which part of the engine through this report.

**Table 3. Main Thermo-fluid variables.[GasTurb]**

Units	SI 2	SI 21	SI 24	SI 25	SI 3	SI 4	SI 43	SI 45	SI 47	SI 48	SI 5	SI 6	SI 13	SI 16	SI 64	SI 7	SI 8		
Mass Flow kg/s	71,64	34,1143	34,1143	34,1143	31,044	28,1307	31,5422	32,9067	33,589	33,589	34,6124	34,6124	37,5257	37,5257	70,6371	74,1082	75,6092		
Total Temperature K	288,15	384,496	482,076	482,076	782,566	1600	1250,41	1228	1133,98	1133,98	947,668	947,668	388,245	388,245	674,56	2040	2013		
Static Temperature K	274,407	366,293	459,622	459,622	777	1579,26	1204,24	1182,31	1091,1	1091,1	910,355	935,66	369,866	369,866	667,576	1947,07	1779,78		
Total Pressure kPa	100,818	247,005	494,01	489,07	2371,99	2300,83	865,317	856,664	610,921	604,812	273,965	268,486	257,087	249,374	255,171	226,766	226,766		
Static Pressure kPa	84,9889	208,322	416,933	412,763	2308,76	2171,67	736,986	729,441	519,815	514,617	232,761	254,947	216,829	210,324	245,407	180,724	125,199		
Velocity m/s	166,055	191,614	214,126	214,125	109,992	229,608	336,386	333,544	321,126	321,126	294,893	167,289	192,535	192,535	122,619	509,486	803,681		
Area m <sup>2</sup>	0,399849	0,089859	0,050415	0,050924	0,027266	0,025574	0,04398	0,045901	0,063022	0,063658	0,131772	0,217964	0,095434	0,098386	0,449826	0,449826	0,383884		
Mach Number	0,5	0,5	0,5	0,5	0,2	0,3	0,5	0,5	0,5	0,5	0,5	0,5	0,28	0,5	0,5	0,24	0,607214		
Density kg/m <sup>3</sup>	1,07897	1,98129	3,16014	3,12854	10,3514	4,79059	2,13203	2,14935	1,65971	1,64311	0,890731	0,949248	2,04228	1,98101	1,28085	0,323362	0,24507		
Spec Heat @ T J/(kg*K)	1004,52	1012,15	1026,63	1026,63	1094,55	1276,26	1225,39	1220,06	1203,28	1203,28	1164,7	1164,7	1012,48	1012,48	1082,63	1400,52	1395,27		
Spec Heat @ Ts J/(kg*K)	1004,19	1010,57	1023,04	1023,04	1093,23	1273,96	1218,19	1212,6	1195,55	1195,55	1156,45	1162,04	1010,88	1010,88	1080,89	1392,69	1373,66		
Enthalpy @ T J/kg	-10032,3	87070	186503	186503	504823	1,5131266	1,070866	1,0418566	927371	927371	708033	708033	90850,6	90850,5	392292	2,197236E	2,15541E6		
Enthalpy @ Ts J/kg	-23819,4	68712	163578	163578	498774	1,4867666	1,0140266	986229	875810	875810	875810	875810	662552	692040	72315,7	72315,6	384774	2,067446E	1,83246E6
Entropy Function @ T -0,11924	0,893073	1,69566	1,69566	1,69566	3,47836	6,58273	5,48742	5,40405	5,06506	5,06506	4,32142	4,32142	0,927145	0,927145	2,95022	8,05588	7,97751		
Entropy Function @ Ts -0,29004	0,722749	1,52603	1,52603	1,52603	3,45134	6,52496	5,3269	5,24326	4,90356	4,90356	4,15843	4,15843	4,26968	4,756842	4,756841	2,9112	7,82893	7,3835	
Exergy J/kg	-414,6	87074,4	177456	176624	478094	1,227166	794288	771611	657204	656373	431041	429369	91345,6	88826,2	224835	1,59773E6	1,56239E6		
Gas Constant J/(kg*K)	287,05	287,05	287,05	287,05	287,05	287,046	287,047	287,047	287,047	287,047	287,047	287,047	287,047	287,047	287,049	287,04	287,041		
Fuel-Air-Ratio	0	0	0	0	0	0,024351	0,021661	0,020744	0,020314	0,020314	0,019701	0,019701	0	0	9,5577E-3	0,059167	0,057924		
Water-Air-Ratio	0	0	0	0	0	0	0	0	0	0	0	0	0	0	0	0	0		
Inner Radius m	0,112195	0,163765	0,147389	0,169757	0,173876	0,1753	0,1753	0,1753	0,1753	0,1753	0,166535	0	0,240419	0,268401	0	0	0		
Outer Radius m	0,373983	0,235419	0,194209	0,212196	0,19858	0,197156	0,211493	0,212934	0,225367	0,225817	0,263966	0,263401	0,292916	0,321491	0,378397	0,378397	0,351327		
Axial Position m	0,186992	0,186992	1,06878	1,12773	1,41689	1,56958	1,64244	1,6775	1,74022	1,82787	1,99626	2,33942	0,779595	2,33942	2,66091	3,94746	4,21233		

Main Thermo-fluid variables in every part of the wet engine at sea level stationary can be seen from the table 3.

After finalizing the engine performance calculations, the total performance change data has been obtained. However, for the rest graphs, figures and intermediate calculations (See Appendix A.1).

### Total Performance Change:

**Table 4. Comparison among SLS TSFC, SLS T/W, Cruise TSFC and Cruise T/W.**

	<b>Baseline Wet</b>	<b>FireFly Jetx Wet</b>	<b>Net Change</b>	<b>Baseline Dry</b>	<b>FireFly Jetx Dry</b>	<b>Net Change</b>
SLS TSFC	59.1187	51.9569	<b>-12.12%</b>	16.7	17.1	<b>~0%</b>
SLS T/W	8.8893	9.9336	<b>+11.75%</b>	6.2042	7.3421	<b>+15.5%</b>
Cruise TSFC	65.7249	61.0890	<b>-7.59%</b>	32.014	32.2889	<b>~0%</b>
Cruise T/W	3.5233	3.5977	<b>+2.11%</b>	1.3032	1.4702	<b>+11.359%</b>

As it can be seen from the table 4, we achieved our goal with 12.12% decrease in TSFC and an 11.75% increase in T/W at sea level wet conditions. Also, at cruise speed (50,000 ft, 1800 km/hr) wet conditions, we got a 7.59% decrease in TSFC and a 2.11% increase in T/W. Furthermore, we also made simulations for the dry engines, which are not mainly focused on. However, besides not much of a change we got in TSFC values, we achieved a significant T/W increase at both sea level and cruise speed conditions. For more detailed information (See Appendix A.1).

### Parametric Studies and Optimization Tools:

The optimization tool is mainly used on the GasTurb 13 software, especially for the nozzle and other parameters. For example, by setting the main design parameters of the nozzle as variables and setting the net thrust between 73 and 75 as constraints. Lastly, after selecting TSFC as the figure of merit, GasTurb software starts a simulation. The software sets different values for the variables randomly to minimize the figure of merit by not exceeding the constraints. This tool was very useful for optimizing the engine. For more detailed information (See Appendix A.1).

### 3. COMPONENTS ANALYSIS AND DESIGN

#### 3.1. INLET DESIGN

The inlet of a gas turbine engine takes in air and supplies it at decelerated, more pressurized and higher Mach number values. In the flow, air at a supersonic speed goes through the inlet, causing a series of oblique shock waves which are followed by a normal shock wave. To obtain the different stagnation temperatures, stagnation pressures and Mach numbers at each point, equations from isentropic relations, normal shock jump relations, oblique shock relations, and area to throat area relations are used. All equations for the inlet design is taken from reference 26.

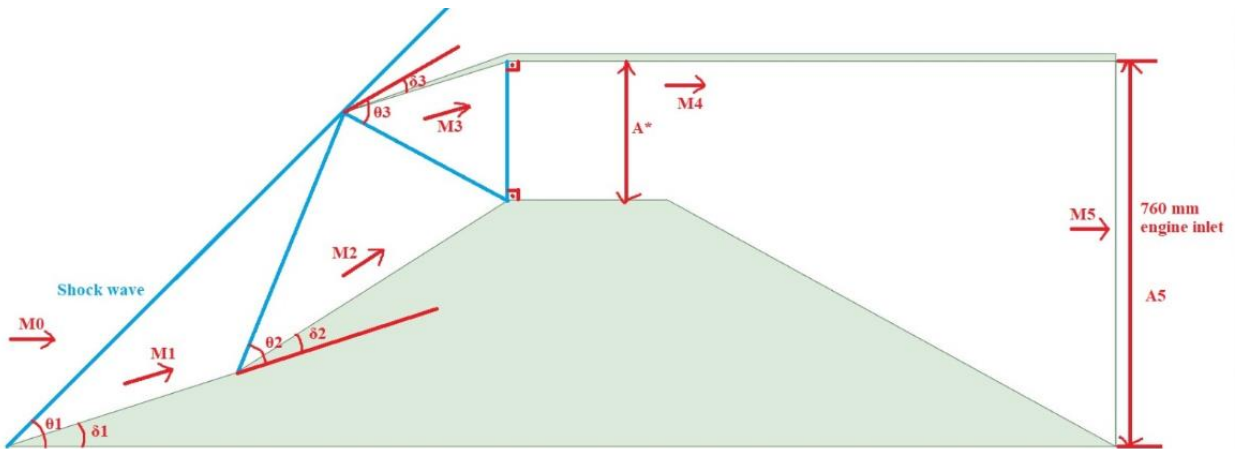


Figure 3. The representation of engine inlet.[ANSYS]

It can be seen from the figure 3, the drawing illustrates the engine inlet where  $M$  is the mach number,  $\delta$  is the deflection angle,  $\theta$  is the shock angle,  $A^*$  is the critical area where the normal shock occurs and  $A_5$  is the area where the fan is located.

At the maximum speed of  $2400 \text{ km/hr}$  the value of the Mach number ( $M_0$ ) =  $2.2$  and  $\gamma=1.4$ . Using these values and the equation below, the first oblique shock angle and the Mach number ( $M_1$ ) are obtained.

$$M_1^2 = \frac{(\gamma+1)^2 M_0^4 \sin^2 \theta_1 - 4(M_0^2 \sin^2 \theta_1 - 1)(\gamma M_0^2 \sin^2 \theta_1 + 1)}{[2\gamma M_0^2 \sin^2 \theta_1 - (\gamma+1)][(\gamma-1)M_0^2 \sin^2 \theta_1 + 2]} \quad (1)$$

The value of  $\theta_1 = 44.8^\circ$  and  $M_1 = 1.8209$

The pressure ratio for the first oblique wave is obtained from the equation below as  $0.9131$ .

$$PR_i = \left[ \frac{(\gamma+1)M_{i-1}^2 \sin^2 \theta_i}{(\gamma-1)M_{i-1}^2 \sin^2 \theta_i + 2} \right]^{\frac{\gamma}{\gamma-1}} \left[ \frac{(\gamma+1)}{2\gamma M_{i-1}^2 \sin^2 \theta_i - (\gamma-1)} \right]^{\frac{1}{\gamma-1}}, i = 1-3 \quad (2)$$

Using the equation 3, the value of the deflection angle  $\delta$  is obtained from its relation to  $\theta_1 = 44.8^\circ$  and the initial Mach number ( $M_0$ ).

$$\tan \delta_1 = \frac{2 \cot \theta_1 (M_0^2 \sin^2 \theta_1 - 1)}{2 + M_0^2 (\gamma + 1 - 2 \sin^2 \theta_1)} \quad (3)$$

The value of the deflection angle at this point is  $17.7844^\circ$ .

For the second oblique shock wave, similar equations (as shown in the figures below) are used to obtain the 3<sup>rd</sup> Mach number, the second shock wave angle, pressure ratio and the deflection angle.

$$M_2^2 = \frac{(\gamma + 1)^2 M_1^4 \sin^2 \theta_2 - 4(M_1^2 \sin^2 \theta_2 - 1)(\gamma M_1^2 \sin^2 \theta_2 + 1)}{[2\gamma M_1^2 \sin^2 \theta_2 - (\gamma + 1)][(\gamma - 1)M_1^2 \sin^2 \theta_2 + 2]} \quad (4)$$

The value of  $M_2 = 1.6506$  and the value of  $\theta_2 = 50^\circ$ . The pressure ratio after the 2<sup>nd</sup> shock wave is 0.9595.

The deflection angle at this point is obtained as  $14.6617^\circ$  using the following formula.

$$\tan \delta_2 = \frac{2 \cot \theta_2 (M_1^2 \sin^2 \theta_2 - 1)}{2 + M_1^2 (\gamma + 1 - 2 \sin^2 \theta_2)} \quad (5)$$

For the 3<sup>rd</sup> oblique shock wave, the Mach number, pressure ratio and oblique shock angle are obtained as shown in the following formula:

$$M_3^2 = \frac{(\gamma + 1)^2 M_2^4 \sin^2 \theta_3 - 4(M_2^2 \sin^2 \theta_3 - 1)(\gamma M_2^2 \sin^2 \theta_3 + 1)}{[2\gamma M_2^2 \sin^2 \theta_3 - (\gamma + 1)][(\gamma - 1)M_2^2 \sin^2 \theta_3 + 2]} \quad (6)$$

The value of  $M_3 = 1.2986$  and the value of  $\theta_3 = 60.2^\circ$ . The pressure ratio after the 2<sup>nd</sup> shock wave is 0.9498. The deflection angle at this point is  $15.1924^\circ$  from the following formula.

$$\tan \delta_3 = \frac{2 \cot \theta_3 (M_2^2 \sin^2 \theta_3 - 1)}{2 + M_2^2 (\gamma + 1 - 2 \sin^2 \theta_3)} \quad (7)$$

At this point a normal shock wave occurs where the value of  $\theta_4 = 90^\circ$ . and the deflection angle is  $0^\circ$ . The mach number  $M_4 = 0.7966$ . The pressure ratio across a normal shock is calculated using the following formula.

$$PR_4 = \left[ \frac{(\gamma + 1)M_4^2 - up}{(\gamma - 1)M_4^2 - up + 2} \right]^{\frac{\gamma}{\gamma-1}} \left[ \frac{(\gamma + 1)}{2\gamma M_4^2 - up - (\gamma - 1)} \right]^{\frac{1}{\gamma-1}} \quad (8)$$

The value of the pressure ratio is obtained as 0.9796.

The total pressure ratio after 3 oblique shocks and 1 normal shock is obtained by multiplying all the individual pressure ratios for each shock.

$$PR = PR1 * PR2 * PR3 * PR4 = 0.8152$$

To obtain the value of the area ratio where  $M_5 = 0.6$  and  $\gamma = 1.4$ , the following formula is used.

$$\left(\frac{A_5}{A^*}\right)^2 = \frac{1}{M_5^2} \left[ \frac{2}{\gamma+1} \left( 1 + \frac{\gamma-1}{2} M_5^2 \right) \right]^{\frac{\gamma+1}{\gamma-1}} \quad (9)$$

Where the value of  $A_5$  is calculated as shown below:

$$A_5 = \pi * (R)^2 \quad (10)$$

$$A_5 = \pi * \left( \frac{0.76m}{2} \right)^2 = 0.4536 m^2$$

With the values of  $A_5$ ,  $M_5$  and  $\gamma$ ; the value of  $A^*$  is obtained as  $0.38175 m^2$  and the radius at this point is  $348.6 mm$ .

### 3.2. COMPRESSOR

The compression process is divided into three parts in the 3-spool mixed spool turbofan engine.

- Low Pressure Compressor (LPC)
- Intermediate Pressure Compressor (IPC)
- High Pressure Compressor (HPC)

These three parts can be observed clearly in the figure below:

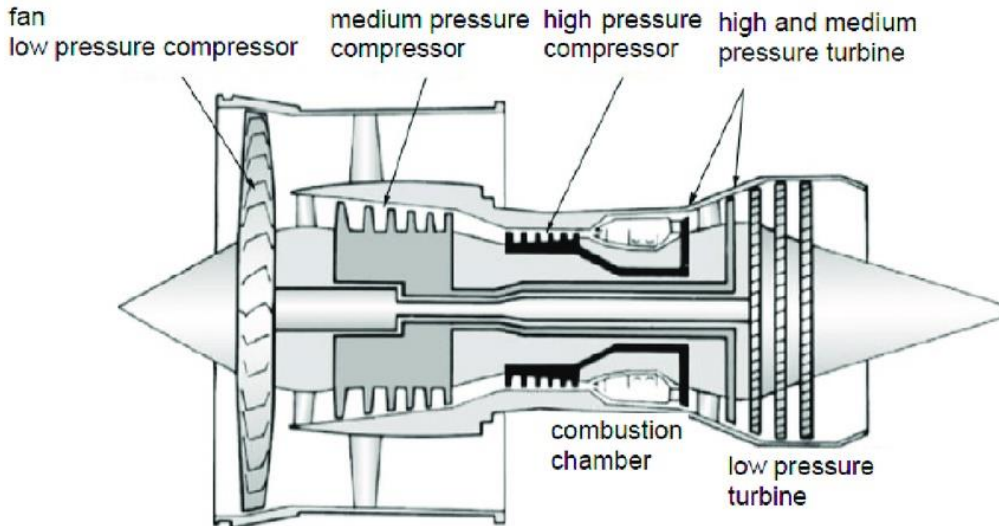


Figure 4. LPC, IPC and HPC.[9]

The figure 4 clearly shows the position of the low pressure, intermediate pressure and high pressure compressors in a three spool turbofan engine.

#### Low Pressure Compressor:

The value of the inner LPC pressure ratio is calculated by the following formula.

$$\pi_{cl} = \tau^{\left(\frac{\gamma}{\gamma-1}\right)} \quad (11)$$

where  $\gamma = 1.4$  and  $\tau = 1.335$

The inner LPC pressure ratio= 2.750.

Table 5. Summary of the compressor duct input and the respective characteristics.[9]

Compressor Duct Input		
Number of Struts		8
Length/Inlet Inner Radius		0.4
Inner Annulus Slope@Exit [deg]		0
Relative Strut Length [%]		60
Casing Thickness	m	0.005
Casing Material Density	kg/m <sup>3</sup>	8000
Compr Interduct Mass Factor		1

The table 5 illustrates the compressor duct input and specifications with respect to the parameters.

Table 6. Summary of the compressor duct output and the respective characteristics.[9]

Compressor Duct Output		
Length	m	0.0600151
Outer Casing Mass	kg	2.82368
Strut Mass	kg	0.858885
Inner Casing Mass	kg	2.26154
Total Mass	kg	5.9441

The table 6 demonstrates the basic respective characteristics such as length and total mass of the compressor duct output.

#### Intermediate Pressure Compressor:

The value of the IPC pressure ratio is calculated by the following formula.

$$\pi_I = \tau^{\left(\frac{\gamma}{\gamma-1}\right)} \quad (12)$$

where  $\gamma = 1.4$  and  $\tau = 1.284$

The IPC pressure ratio = 2.40.

To obtain the value of the isentropic efficiency in the intermediate pressure compressor, the following formula is used.

$$\eta_{isentropic} = \frac{\pi_{cl}}{\pi_I} = \left[ \tau^{\left(\frac{\gamma}{\gamma-1}\right)} \right] / \left[ \tau^{\left(\frac{\gamma}{\gamma-1}\right)} \right] \quad (13)$$

The value of the isentropic efficiency in IPC = 0.873.

The polytropic efficiency is generally slightly higher than the isentropic efficiency. To obtain the value of the polytropic efficiency in the intermediate pressure compressor, the following formula is used.

$$\eta_{polytropic} = \frac{\left[ R * \ln \left( \frac{P_2}{P_1} \right) \right]}{(s_2 - s_1)} \quad (14)$$

Where  $P_1, T_1, s_1$ : Pressure, temperature and specific entropy in state 1 and  $P_2, T_2, s_2$ : Pressure, temperature and specific entropy in state 2.  $R$  is the gas constant. The value of the polytropic efficiency = 0.887.

#### High Pressure Compressor:

The value of the HPC pressure ratio is calculated by the following formula.

$$\pi_{ch} = \tau^{\left(\frac{\gamma}{\gamma-1}\right)} \quad (15)$$

where  $\gamma = 1.4$  and  $\tau = 1.577$

The HPC pressure ratio = 4.930.

To obtain the value of the isentropic efficiency in the high pressure compressor, the following formula is used.

$$\eta_{isentropic} = \eta_c = \frac{\left[ \pi_c^{\left( \frac{\gamma-1}{\gamma} \right)} - 1 \right]}{[\tau c - 1]} \quad (16)$$

The value of the isentropic efficiency in IPC = 0.860.

To obtain the value of the polytropic efficiency in the HPC, the following formula is used.

$$e_c = \frac{\frac{dp_t}{dh_t}}{\frac{p_t}{RT_t}} = \frac{\frac{dp_t}{p_t}}{\frac{C_p dT_t}{RT_t}} = \frac{\frac{dp_t}{p_t}}{\frac{\gamma}{\gamma-1} \frac{dT_t}{T_t}} \quad (17)$$

The value of the polytropic efficiency = 0.8856.

Table 7. Summary of the high-pressure compressor input and the respective characteristics.[9]

HPC Input				
Number of Stages	5	Casing Thickness	m	0.005
Number of Radial Stages	0	Casing Material Density	kg/m <sup>3</sup>	4000
Number of Variable Guide Vanes	1	Rel Work of Radial End Stage		0.3
Inlet Guide Vanes (IGV) 0/1	1	Duct Inner Radius Ratio		1
IGV Profile Thickness [%]	5	Duct Length/Inlet Inner Radius		0
IGV Material Density	kg/m <sup>3</sup>	Number of Duct Struts		8
Annulus Shape Descriptor 0..1	0.3	Relative Duct Strut Length [%]		60
Given Radius Rat: Inl/Exit 0/1	0	Rad Diffusor/Rotor Blade Length		0.5
Inlet Radius Ratio	0.243	Rotor Inlet Swirl Angle		0
Exit Radius Ratio	0.9	Rotor Blade Backsweep Angle		20
Blade and Vane Sweep 0/1	0	Diffusor Wall Thickness	m	0.0025
First Stage Aspect Ratio	1.5	Casing Thermal Exp Coeff	E-6/K	10
Last Stage Aspect Ratio	2	Casing Specific Heat	J/(kg*K)	500
Blade Gapping: Gap/Chord	0.1	Casing Time Constant		10
Pitch/Chord Ratio	0.5	Blade and Vane Time Constant		0.5
Disk Bore / Inner Inlet Radius	0.25	Platform Time Constant		1
Diffuser Area Ratio	1.5	Design Tip Clearance [%]		1.5
Rel Thickness Inner Air Seal	0.04	d Flow / d Tip Clear.		2
Compressor Mass Factor	1	d Eff / d Tip Clear.		2
Outer Casing Thickness	m	d Surge Margin / d Tip Clear.		5
Outer Casing Material Density	kg/m <sup>3</sup>			

The table 7 gives information about the characteristics of the high pressure compressor at the input.

Table 8. Summary of the high-pressure compressor output and the respective characteristics.[9]

HPC Output Summary		
Length (w/o Diffusor)	m	0.193196
Number of Inlet Guide Vanes		85
Total Number of Blade and Vanes		1807
Diffusor Length	m	0.0291415
Casing Mass	kg	4.3696
Outer Casing Mass	kg	3.48187
Total Vane Mass	kg	2.47175
Total Blade Mass	kg	2.9481
Inner Air Seal Mass	kg	0.591898
Rotating Mass	kg	15.5533
IGV Mass	kg	0.397095
Exit Diffusor Mass	kg	1.21254
Total Mass	kg	27.4862
Polar Moment of Inertia	kg*m <sup>2</sup>	0.237105

The table 8 shows the characteristics of the high pressure compressor at the output.

## Design:

Generally, in gas turbine engines, the air is compressed by two types of compressors: Axial flow compressors and centrifugal flow compressors. The axial flow compressors contain blades and rotors that facilitate the air acceleration until the required pressure value is achieved. The centrifugal compressors facilitate acceleration by means of a propeller and increase the pressure using a diffuser.[10,11]

Table 9. Difference between the axial and centrifugal compressor.[9]

Variables	Centrifugal Compressor	Axial Compressor
Pressure Ratio per Stage-Efficiency	$\approx 10$ – low efficiency $<5$ – high efficiency	$<1.5$ – high efficiency
Mass Flow Rate	Low	High
Overall Pressure Ratio	Moderate	High

As seen in the table 9, The axial compressor is preferred as it produces a higher pressure overall ratio and a higher isentropic efficiency. The difference between the centrifugal and axial compressor in terms of pressure ratio per stage efficiency, mass flow rate and overall pressure ratio. The differences assist in making the decision on which compressor is favorable in this situation.

Table 10. Range and typical values of each design parameters for compression systems.[9]

Parameter	Range of Values	Typical Value
Flow Coefficient, $\phi$	$0.3 \leq \phi \leq 0.9$	0.6
Axial Mach Number, $M_z$	$0.3 \leq M_z \leq 0.6$	0.55
Degree of Reaction, $^oR$	$0.1 \leq ^oR \leq 0.90$	0.5 (for $M < 1$ )
D-Factor, D	$D \leq 0.6$	0.45
Tip Tangential Mach Number, $M_T$	1.0-1.5	1.3
Reynolds Number Based on chord, $Re_c$	$300,000 \leq Re_c$	$>500,000$
Stage Average Aspect Ratio, AR	$1.0 \leq AR \leq 4.0$	$< 2.0$
Stage Average Solidity, $\sigma$	$1.0 \leq \sigma \leq 2.0$	1.4
Loading Coefficient, $\psi$	$0.2 \leq \psi \leq 0.5$	0.35
Polytropic Efficiency, $e_c$	$0.85 \leq e_c \leq 0.92$	0.9
Tip Relative Mach Number (1 <sup>st</sup> Rotor), $(M_{1r})_{tip}$	$(M_{1r})_{tip} \leq 1.7$	1.3-1.5
Hub rotational speed, $\omega r_h$	$\omega r_h \leq 380$ m/s	300 m/s
Tip rotational speed, $\omega r_t$	$450 \leq \omega r_t \leq 500$ m/s	500 m/s
De Haller Criterion, $W_2 / W_1$	$W_2 / W_1 \geq 0.72$	0.75
Compressor Pressure Ratio per Spool	$\Pi_c < 20$	up to 20
Aspect Ratio, Fan	$\sim 2 - 5$	$< 1.5$
Aspect Ratio, Compressor	$\sim 1 - 4$	$\sim 2$
DCA Blade (Range)	$0.8 \leq M \leq 1.2$	Same
Axial Gap Between Blade Rows	$0.23c_z$ to $0.25c_z$	$0.25c_z$
NACA-65 Series (Range)	$M \leq 0.8$	Same
Taper Ratio	$\sim 0.8 - 1.0$	0.8

As indicated in the table 10, the ranges of values for the design parameters are related to the two compressors. The range and typical values of each design parameter for compression systems, as shown in the table 10, give an estimate of the attainable values in the compressor.

### 3.3. COMBUSTION CHAMBER

Air and fuel mixture react each other in what is known as the primary zone in the principal stage. Subsequent stages of air are introduced through the combustion chamber for dilution and cooling purposes. These stages lead to stable combustion, reducing air pollution and also a combustion chamber exit temperature profile. The section we use for the combustion chamber is called the direct flow combustion chamber. Combustion chamber can be designed in different shapes such as multi-can combustor, can-annular and annular. For our engine, we prefer to use the annular combustion chamber as it burns more smoothly and is shorter because of that, it will be lighter. Also, limited configurations require the use of more material, which further increases the weight clearance. Moreover, annular burners are closer to more uniform temperature output and lower pressure among the three designs.[12,13]

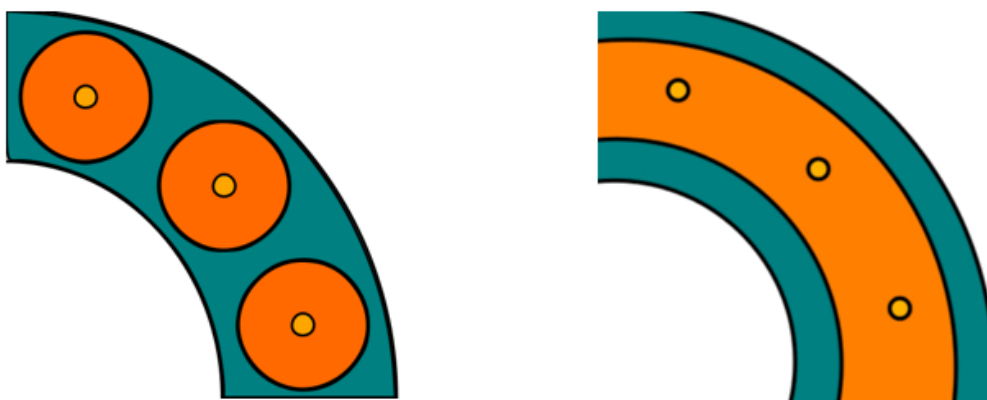


Figure 5. Can-annular combustor and annular combustor.[14]

The figure 5 depicts the view of can-annular combustor and annular combustor.

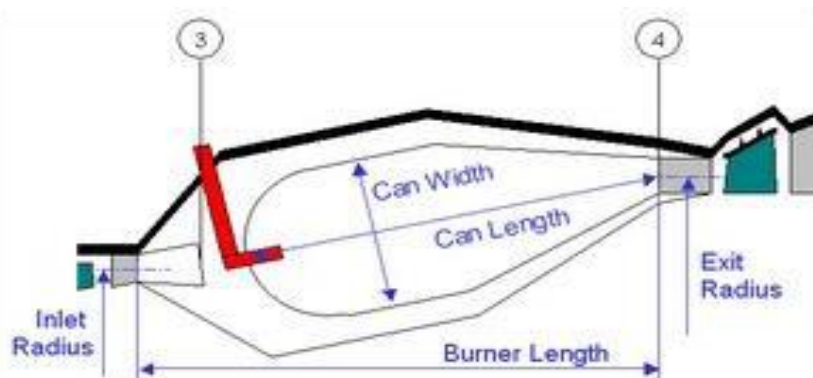


Figure 6. Annular burner dimensions.[15]

The figure 6 shows the geometry of annular burner is described by the proportions of the dimensions.

Table 11. Parameters for the combustion chamber.[GasTurb]

Exit/Inlet Radius	1	Mean Radius, Exit	m	0,164322
Length/Inlet Radius	1	Length	m	0,164322
Can Width/Can Length	0,4	Can Volume	m³	0,00491859
Inner Casing Thickness	m	Can Mass	kg	11,0484
Outer Casing Thickness	m	Can Surface Area / Mass	m²/kg	0,05
Casing Material Density	kg/m³	Fuel Injector Mass	kg	1,50247
Can Wall Thickness	m	Inner Casing Mass	kg	2,46425
Can Material Density	kg/m³	Outer Casing Mass	kg	8,35918
Can Thermal Exp Coeff	E-6/K	Total Mass	kg	23,3743
Can Specific Heat	J/(kg*K)	Can Heat Soakage	kW	0
Can Time Constant				
Mass of Fuel Inj. / Fuel Flow	2			
Burner Mass Factor	1			

The table 11 indicates the parameters which are related to the combustion chamber.

The following formula is used to measure the pressure loss of the combustion chamber.

$$\frac{p_{t3} - p_{t4}}{p_{t3}} \quad (18)$$

$$\frac{p_{t3} - p_{t4}}{p_{t3}} = \frac{3263.944 - 3166.026}{3263.944} = 0.02999 \text{ (Relative to the inlet total pressure)}$$

Since the pressure loss in this part of the engine is very small, so it rises to the minimum value of 0.02999, which is mostly seen in the combustion chambers.

Combustion efficiency can be found by a multi-step process that starts with finding the cooling efficiency with the following equation.

$$\phi = \frac{T_g - T_w}{T_g - T_c} \quad (19)$$

Where " $T_g$ " is the temperature of hot gas, " $T_w$ " is the average wall temperature and " $T_c$ " is the compressor discharge temperature. Next, the reaction rate "b" can be found using the following formula.

$$b = 382 \left( \sqrt{2} \pm \frac{\phi}{1.03} \right) \quad (20)$$

where [ (+) for  $\phi < 1.03$  and (-) for  $\phi > 1.03$ ]

As a result, the burner loading parameter CLP can be found, which is well related to the combustion efficiency and defined as follows:

$$CLP = \theta = \frac{p_{t3}^{1.75} A_{ref} H e^{\frac{T_{t3}}{b}}}{\dot{m}} \quad (21)$$

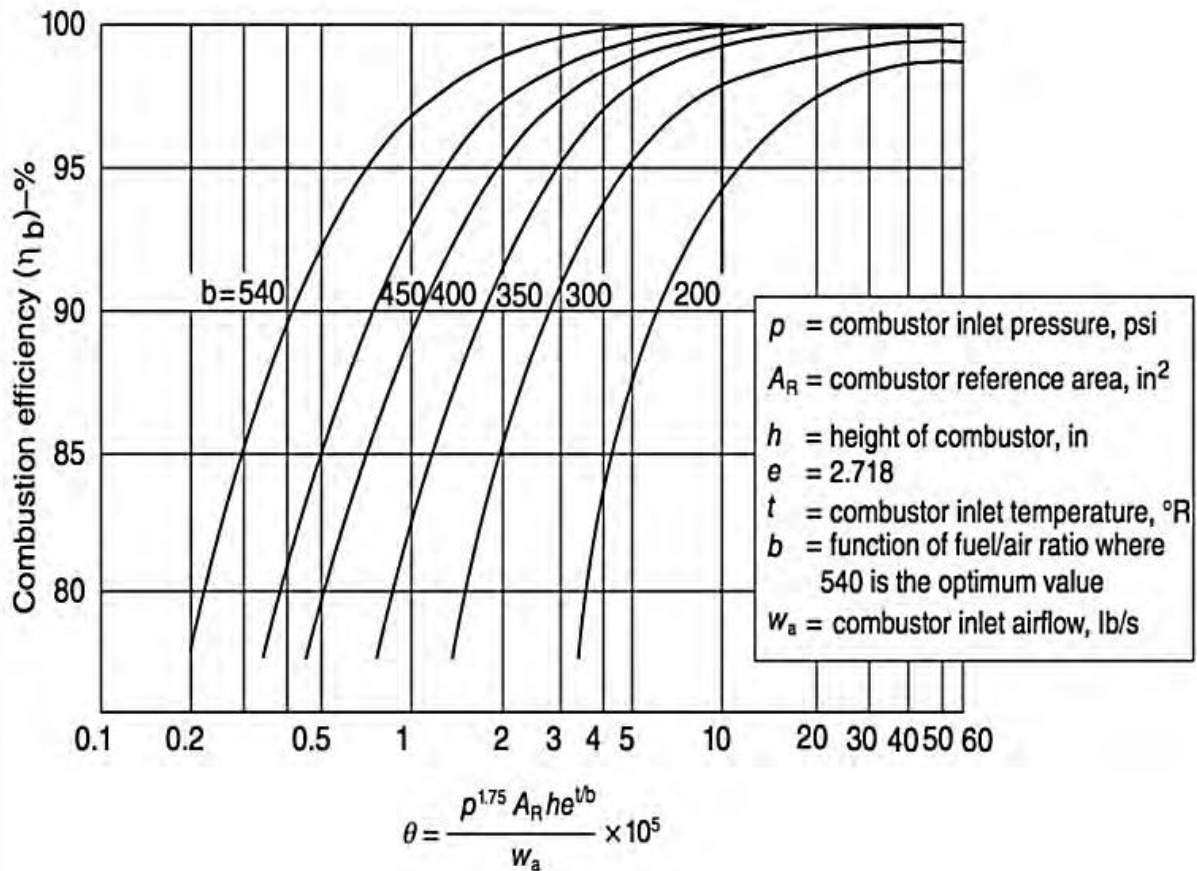


Figure 7. Combustion Efficiency.[15]

The figure 7 gives information about the combustion efficiency. The reaction rate parameter “b” depends on  $\Phi$ , and is calculated by the “CLP”. As a result of many studies, we found titanium alloy is an excellent choice for the combustion chamber. It works for long periods of extreme heat due to its very limited space and use.

Table 12. The important parameters for the combustion chamber.

Parameters	Value
b	475.290268
$\Phi$	1.22
CLP	$51.37 * 10^5$
Estimated Combustor Efficiency	Tends to 100%
Design Combustor Efficiency	99.70%

As can be seen from the table 12, the combustion efficiency is close to 100% with a value of “b”. According to the source 5, titanium alloy is an excellent choice for the combustion chamber material (See Appendix C.1).

### 3.4. TURBINE

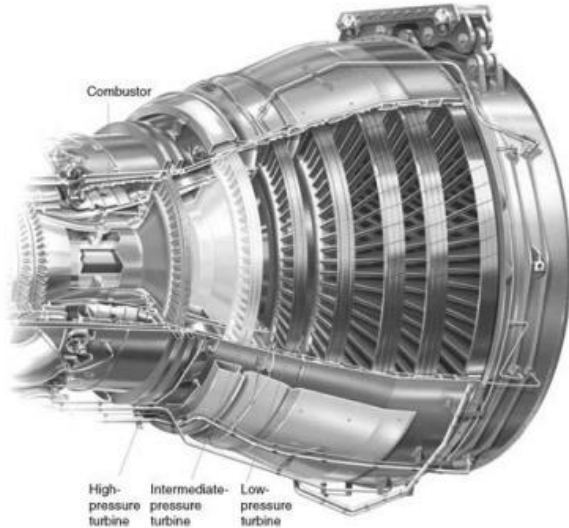


Figure 8. A three-shaft turbine system.[7]

The figure 8 shows the three-shaft turbine system. Also, the system has combustor, high pressure turbine, intermediate pressure turbine and low pressure turbine.

#### 3.4.1. Introduction

The turbine is required to supply the necessary power for the compressors to operate. A High-Pressure Turbine drives a High-Pressure Compressor, a Low-Pressure Turbine drives a Low-Pressure Compressor, and an Intermediate Pressure Turbine drives an Intermediate Pressure Compressor all of which are part of the three-spool turbofan. This is accomplished by obtaining energy from the hot gases produced by combustion. The turbine may be divided into many stages, each with one row of stationary nozzle guiding vanes and one row of moving blades to generate the driving torque. The number of stages is determined by the ratio between the amount of power required through the gas flow.

Additionally, the rotational speed at which it must be generated, and the maximum diameter of the turbine that may be used. Engines with higher turbine inlet temperatures are more efficient thermally and have a better power-to-weight ratio. By-pass engines have higher propulsive efficiency, allowing for a smaller turbine to produce the same thrust.

#### 3.4.2. Turbine Blade, Disk Material Selection and Design Criteria

The materials used in the disks and turbine blades and the year of development are depicted in the figure 9. Materials that are necessarily resistant to high temperatures are required. Some alloys, such as nickel-based alloys used to relieve thermal stress in blades and disks, have a high thermal conductivity. Some materials, like ceramics, have limited thermal conductivity and so reduce heat transfer to the blades. Thermal protection coatings are used on various materials, particularly turbine blades, to reduce surface operating temperatures and thus, extend component life.

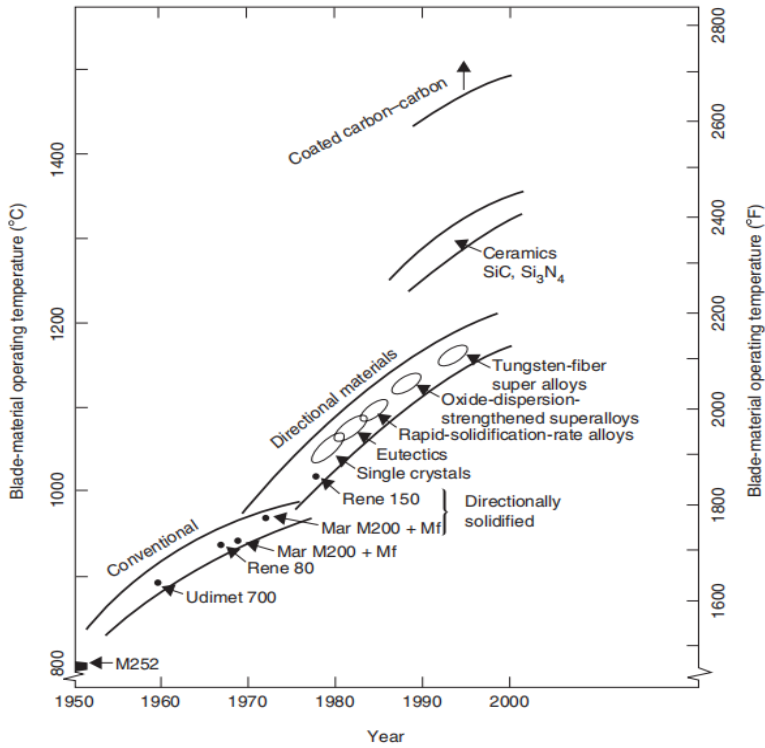


Figure 9. The relation of blade-material operating temperature over the years.[16]

The figure 9 illustrates the progression of the turbine material development from 1950 to 2000. It can be seen that the blade material operating temperature is improving every year, meaning that by 2030 it would be approximately 3000 Kelvin. This is an optimistic projection for our design which relies on better quality material to withstand higher temperatures at the turbine inlet.

A blade profile is created in the blade design process that ensures a smooth pressure and match distribution by minimizing sudden pressure drops and flow separation.

### 3.4.3. Geometry of Blades

The next stage is to calculate an axial chord, stator and rotor spacing, and turbine blade height (Fig.10). The continuity equation will be used to determine the height of turbine blades. The axial chord and axial spacing can both be approximated based on calculated height in early design.[20]

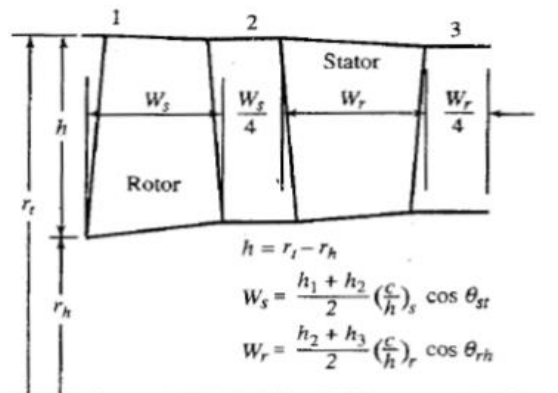


Figure 10. The axial chord, the spacing among stator, rotor and the height of turbine blades.[19]

The figure 10 shows the geometry of the turbine. Turbines contain a rotor and stator blade. The shape of the rotor blades directly affects the performance of the turbines. The stator blades are usually stationary as opposed to the rotor blades, which move. After the rotor blades impel the air, it goes through the stator blades. The stator blades act as diffusers at each stage. They partially convert high-velocity air into high pressure.

The working fluid velocities in a turbomachine can be displayed as a graph called a "velocity triangle" or a "velocity diagram".[19]

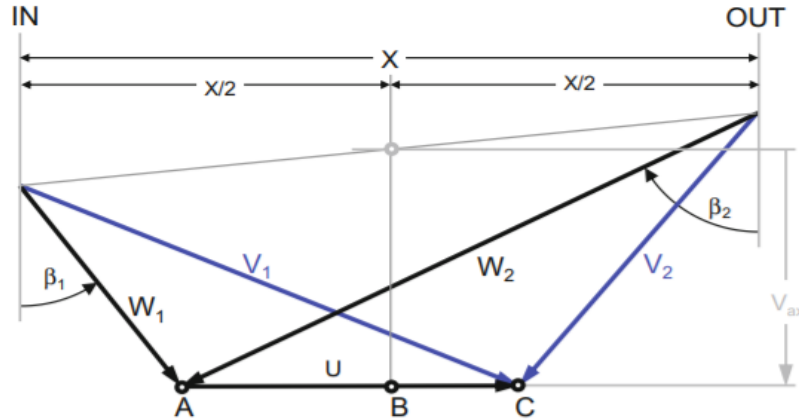


Figure 11. General velocity of diagram for a turbine.[19]

The figure 11 demonstrates the velocity triangle of one stage of the axial flow turbine. Let us restrict our attention to designs in which the axial velocity  $C_a$  is constant through the rotor. This will imply an annulus flared as in the figure 11. To accommodate the decrease in density as the gas expands through the stage. The velocity triangle is used to analyze equations and the velocity of flow on compressors and turbines. Therefore, the useful equations can be obtained to aid as in calculation.

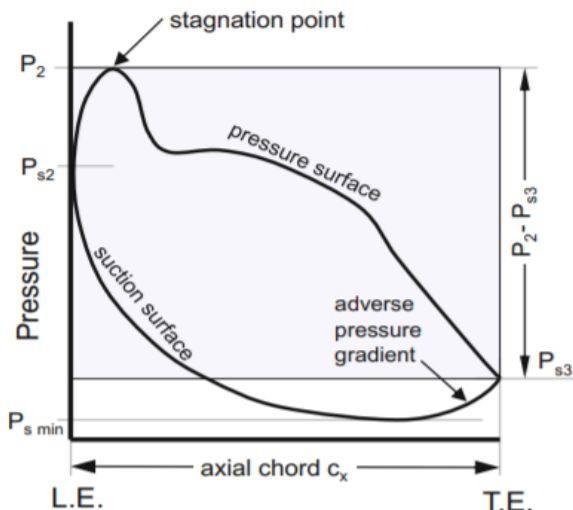


Figure 12. Pressure distribution around turbine airfoil.[19]

The figure 12 illustrates the pressure distribution over the axial chord around the turbine aerofoil. By studying the pressure distribution, we can better understand how to design the turbine blade. Nevertheless, one significant result of the study is a summary of the pressure,

velocity, and temperature distributions for typical situations. The conventional blading is shown in Figure 12. The vital feature is the magnitude of the opposing pressure gradient on the convex (suction) surface. If the amount becomes too great, it may result in a large wake, a separation of the boundary layer, and an increase in profile loss coefficient. Suppose you want to design with highly aerodynamic blade loads and also low suction surface pressures. In that case, you need to know what limiting pressure or velocity distribution will give separate trailing edges.

Table 13. Typical multi-stage turbine inlet and outlet parameters.[21]

Parameters	Front stages (HP)	Last stages (LP)
$\alpha_2$	$75^0 - 70^0$	$65^0 - 60^0$
Degree of reaction	0.20-0.25	0.35-0.45
Exit Mach number (M3)	0.25-0.35	0.5 for turbojet and turbofan engines 0.65 – 0.70 for turbo-prop engine
Exit swirl angle ( $\alpha_3$ )		$0-10^0$

The table 13 shows the typical multistage turbine inlet and outlet parameters. The journal suggests that the figures outlined are normal for a turbofan with reheat under normal conditions.[21] Parameters such as degree of reaction, exit Mach number, and exit swirl angle are highlighted per both front and last stages of high pressure and low-pressure turbines.

### 3.4.4. Materials

The effects of these temperatures on the nozzle guiding vanes and turbine blades have always been a limiting issue in adopting higher turbine entrance temperatures. The high speed of rotation, which transmits tensile stress to the turbine disc and blades, is also a limiting factor.[17]

#### 1. Nozzle guide vanes

Because of their immobility, the turbine blades are subjected to the same rotating stresses as the nozzle guide vanes. As a result, heat resistance is the most significant attribute. Although cooling is essential to prevent melting, nickel alloys are utilized. Ceramic coatings can improve heat resistance while also reducing the amount of cooling air required under the same conditions, enhancing engine efficiency.[17]

#### 2. Turbine discs

A turbine disc is subjected to significant rotational stresses and must rotate at high speed in a relatively cold environment. The resistance to fatigue cracking is the limiting element that limits the practical disc life. Turbine discs were previously produced of ferritic and austenitic steels, but nickel-based alloys are now utilized. Increased fatigue resistance extends the life of a disc by adding alloying elements in nickel. Alternatively, more expensive powder metallurgy discs, which contribute 10% to the strength, allow for quicker rotational speeds.[17]

### 3. Turbine blades

While the blades are glowing red-hot, they must be sturdy enough to sustain the centrifugal loads caused by high-speed rotation. Turbine blades must also be resistant to thermal shock and fatigue, as well as corrosion and oxidation resistant, in order to avoid failure due to high-frequency changes in gas conditions. The turbine blades gradually lengthen over time as they are used. This is referred to as creep, and there is a finite usable life limit before breakdown. High-temperature steel forgings were utilized in the beginning, but they were quickly replaced with cast nickel-base alloys, which have better creep and fatigue qualities.[17]

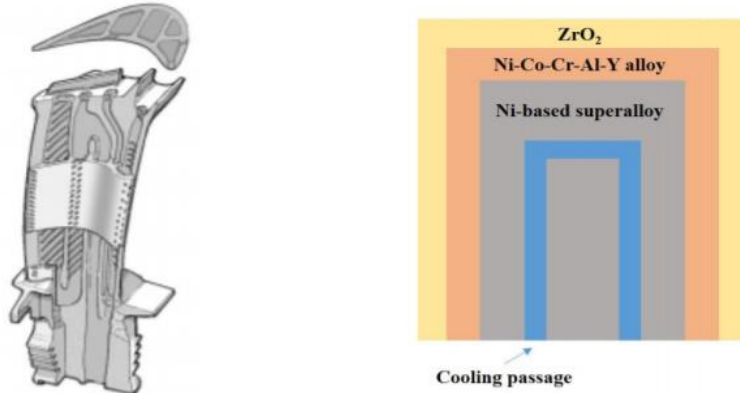


*Figure 13. Design for turbine blade cooling passages (left side) and rough design of thermal barrier coating (Right side).[17]*

The figure 13 shows the turbine blade design and materials of turbine blades. Also, figure 13 portrays how the turbine blade cooling is designed to increase the material lifespan. The opposite is a thermal coating that is applied to the turbine blade to withstand the high temperatures that are subjected to it.

#### 3.4.5. Preliminary Turbine Design

Stage Characteristics and Loading Coefficient;

$$\Psi = \frac{UV_{ax}(\tan \beta_1 - \tan \beta_2)}{U_m^2} = \frac{V_{ax}(\tan \beta_1 - \tan \beta_2)}{U_m} = \frac{\Delta V_U}{U_m} \quad (22)$$

Flow Coefficient;

$$\phi = \frac{V_{ax}}{U_m} \quad (23)$$

Stage Reaction;

$$A = \frac{1/2 V_{ax}^2 (\tan^2 \beta_2 - \tan^2 \beta_1)}{UV_{ax}(\tan \beta_1 - \tan \beta_2)} = -\frac{V_{ax}}{2U} (\tan \beta_1 + \tan \beta_2) \quad (24)$$

### 3.4.6. History Over the Years

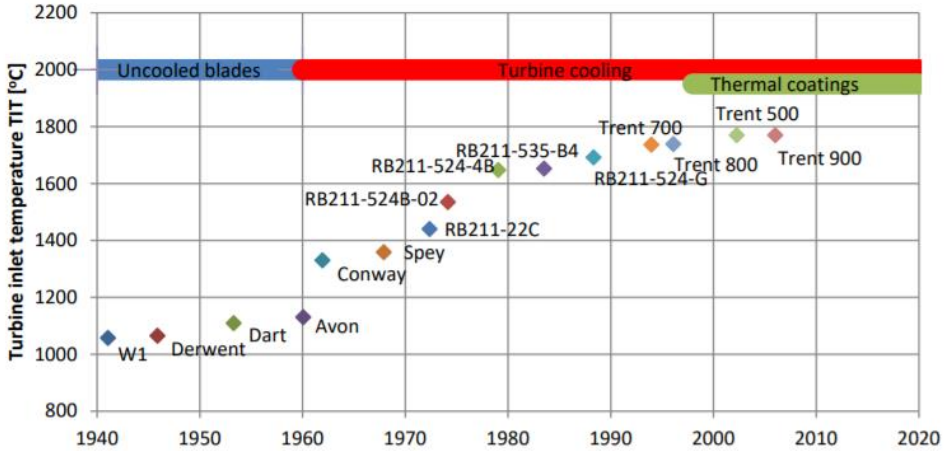


Figure 14. The development turbine inlet temperature over the years for the Rolls-Royce engines.[22]

The figure 14 shows how the turbine inlet temperature increased steadily through the years with each engine from 1940 - 2020. We can only anticipate that the trend will continue so that by 2030 the TIT reaches 2200K. This will significantly improve the thrust of the engine, both with and without an afterburner.

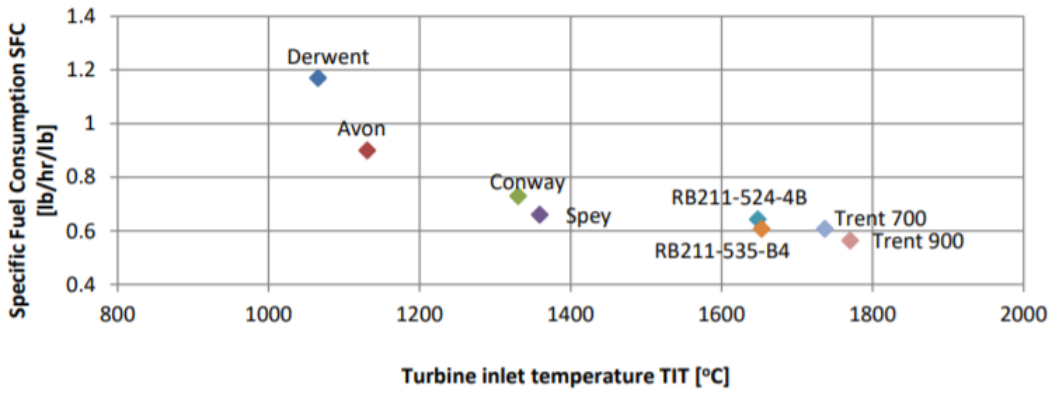


Figure 15. Specific fuel consumption versus turbine inlet temperature.[22]

It can be seen from the figure 15, with increased turbine inlet temperature, the specific fuel consumption is seen to decrease with the increase in turbine inlet temperature.

## 3.5. AFTERBURNER

### 3.5.1. Introduction

Afterburning (or reheat) is a technique for increasing an engine's basic thrust to increase an aircraft's take-off, climb, and combat capability (for military aircraft). Increased power may be produced by using a larger engine, but this would raise frontal area, weight and overall fuel consumption. Hence afterburning is the optimum technique of thrust augmentation for a short time.[18] As a result of the higher temperature of the exhaust gas, the velocity of the jet leaving the propelling nozzle increases, increasing engine performance.

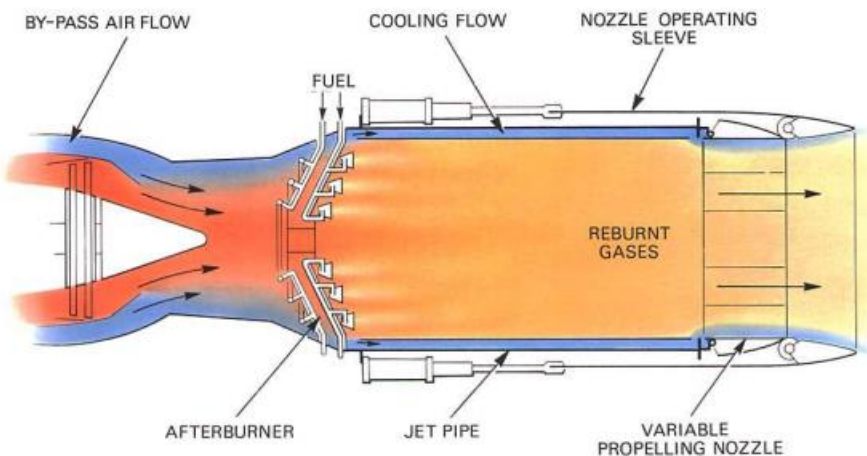


Figure 16. The visualization of afterburner.[19]

The figure 16 shows the process of introducing and burning fuel between the engine turbine and the propelling nozzle of a jet pipe, with the unburned oxygen in the exhaust gas being used to support combustion.

On low by-pass engines, afterburning is accomplished by mixing the by-pass and turbine streams before reaching the afterburner fuel injection and stabilizer system, allowing combustion to occur in the mixed exhaust stream. Another option is to inject fuel and stabilize the flame in each by-pass and turbine stream separately, then burn the available gases up to a single exit temperature at the final nozzle.

Because of the additional constraints in the jet pipe, the thrust of an afterburning engine is slightly lower than that of a similar engine without afterburning equipment. Also, due to the bigger jet pipe and afterburning equipment, the power plant's overall weight has grown as well.

The diffuser, flame holder, spray ring, duct liner and augmenter duct must all be included in the basic design if early estimations of afterburner weight and dimensions are required. The latter serves as a screech damper (a high-frequency oscillation that may quickly damage an afterburner) as well as a cooling air conduit for the nozzle.[19]

### 3.5.2. Operating of Afterburner

The gas stream from the engine turbine reaches the jet pipe at a velocity of 750 to 1,200 feet per second. Still, this is too fast for a stable flame to be maintained. Then, the flow is diffused before entering the afterburner combustion zone, reducing the flow velocity while increasing the pressure. However, kerosine burns at only a few feet per second at standard mixture ratios, any fuel burned in the dispersed air stream would be swept away. As a result, a type of flame stabilizer is situated downstream of the fuel burners to provide a zone where turbulent eddies are formed to aid combustion. Besides, The local gas velocity is further decreased to a figure at which flame stabilization occurs while combustion is in operation.[17]

### 3.5.3. Materials

The propelling nozzle and jet pipe are both comprised of a nickel alloy material that is heat resistant.

### 3.5.4. Advantages and Disadvantages of Afterburner

- Thrust Increase

The ratio of absolute jet pipe temperatures before and after the extra fuel is burned determining the increase in thrust. The thrust gain can be computed as follows, ignoring tiny losses due to afterburner equipment and gas flow momentum variations. Low by-pass engines with afterburning technology can provide static thrust gains of up to 70%. [19]

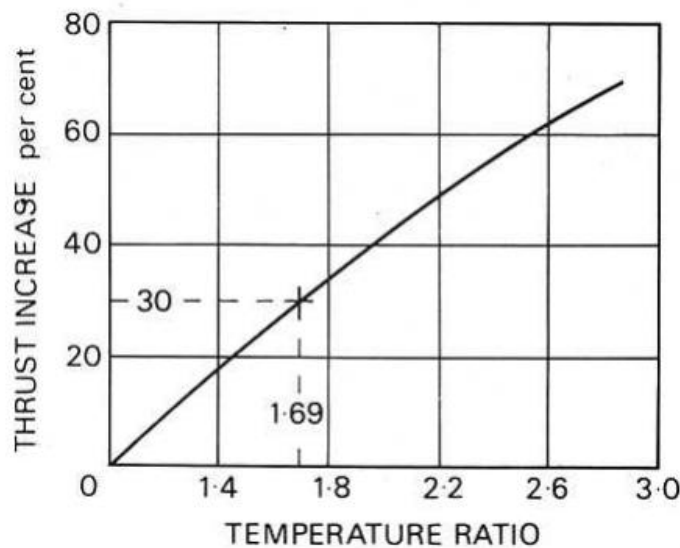


Figure 17. The relation between thrust and temperature ratio.[19]

The figure 17 illustrates how the increase in thrust affects the temperature ratio proportionally. An increase in temperature ratio results in an increase in the thrust.

- Increase in Specific Fuel Consumption

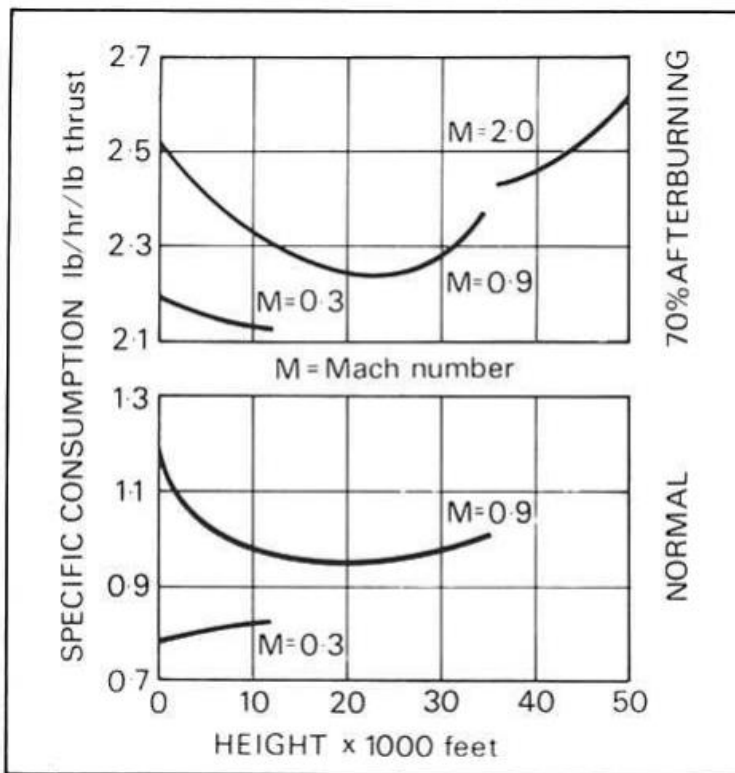


Figure 18. Specific fuel consumption comparison.[17]

The figure 18 shows the addition of the afterburner results in unwanted effects such as an increase in the specific fuel consumption. This is a trade-off in performance that we chose to accept since we also obtain an added increase in thrust. Therefore it is acceptable.

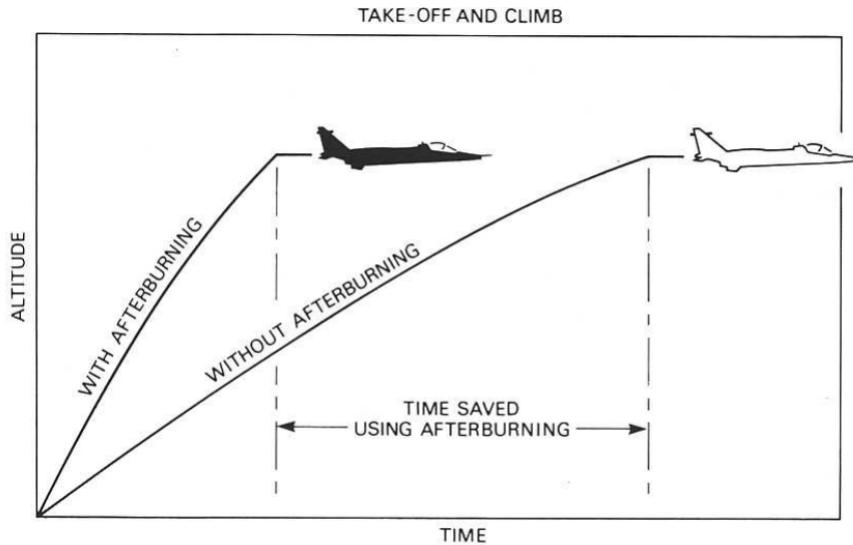


Figure 19. Afterburning and its effect on the rate of climb.[17]

It can be seen clearly from the figure 19, the effect of afterburner on time saved during flight. More time is being saved with the addition of an afterburner. Therefore, the team chose to add an afterburner to our engine so as to save time during both take-off and climb.

### 3.5.5. Mathematical Equations of the Afterburner

Application of the energy equation to the afterburner yields an expression for the fuel-to-air ratio in the afterburner in terms of known parameters as follows:

$$(\dot{m}_{6M} + \dot{m}_{fAB})h_{t7} - \dot{m}_{6M}h_{t6M} = \dot{m}_{fAB}Q_{R,AB}\eta_{AB} \quad (25)$$

$$f_{AB} \equiv \frac{\dot{m}_{fAB}}{\dot{m}_{6M}} = \frac{h_{t7} - h_{t6M}}{Q_{R,AB}\eta_{AB} - h_{t7}} = \frac{\tau_{\lambda AB} - h_{t6M}/h_0}{\frac{Q_{R,AB}\eta_{AB}}{h_0} - \tau_{\lambda AB}} \quad (26)$$

The total pressure at the exit of the afterburner is known via the loss parameter according to

$$p_{t7} = p_{t6M} \cdot \pi_{AB} \quad (27)$$

Note that we need two afterburner total pressure loss parameters, one for the afterburner on and the second for the afterburner off, that is, AB-On and AB-Off.

We define afterburner (or reheat) efficiency as a ratio of fuel mass flows, namely:

$$\eta_{W2} = \frac{W_{F,RH,equi}}{W_{F,RH}} = \frac{far_{7,equi} - far_{64}}{far_7 - far_{64}} \quad (28)$$

Here, WF,RH,equi is the fuel flow required by an ideal afterburner to achieve the chemical equilibrium temperature T7,equi.[7]

- Change in Performance

Table 14. Change in parameters with respect to the afterburner.[7]

Parameters	With Afterburner	Without Afterburner
FN (kN)	74.51	43.89
TSFC ( $\frac{g}{kN} * s$ )	51.9569	17.1148

The table 14 portrays the change in performance of two parameters which are thrust and thrust specific fuel consumption. As can be seen from the table, the effect of the afterburner is an increase in net thrust and an undesired increase in TSFC.

### 3.6. NOZZLE

Jet engines power the majority of military and commercial aircraft from the past to the present. Despite the fact that turbine engines come in various shapes and sizes, they all have some characteristics. A nozzle is used in all gas turbine engines to generate thrust, return exhaust gases to free flow, and regulate the mass flow rate through the engine. The power turbine is placed downstream of the nozzle. In comparison to other engine parts, such as a compressor, it is a primary device. The nozzle is simply a specifically designed part that allows hot gases to flow through it. When it comes to the arithmetic calculations for the nozzle, though, it does take some consideration. A co-annular nozzle is widely used in several turbofan engines. The core flow exits the central nozzle, while the annular nozzle exits the fan flow. The nozzles that combine the two streams produce more thrust and are quieter than convergent nozzles. Convergent-divergent nozzles with adjustable geometry are required for afterburning turbofans. [25]

At this nozzle, the flow first converges to the minimum area or throat, then expands from the diverging section to the outlet on the right. The flow is subsonic above the throat, but supersonic below the throat. Variable geometry nozzles are heavier than fixed geometry nozzles. All the nozzles we have discussed so far are round tubes. In order to increase the maneuverability of the aircraft, the thrust direction is changed with the nozzle.

Because the nozzle conducts hot exhaust back into the free flow, there can be serious interactions between the engine exhaust flow and the airflow around the aircraft. Especially on fighter planes, large friction penalties can occur near the nozzle exits. As in the intake part, the outer nozzle configuration is often designed by the airframe and subjected to wind tunnel testing to determine performance effects on the airframe. The engine manufacturer usually takes care of the internal nozzle.[25]

There are two types of nozzles: convergent (CO) and convergent-divergent (ConDi). Converging nozzles are utilized for streams below Mach 1 (subsonic) because the region along the converging part shrinks, increasing the velocity in the throat until Mach 1 is reached. A divergent component follows the converging part at the throat of the ConDi nozzle, causing the area to begin to rise rather than shrink. If the flow has not yet reached Mach 1, the flow velocity will start to drop as the retreating part grows in size. If the flow in the throat (choked flow) hits Mach 1, the area in the throat will continue to grow, increasing the velocity.[24]

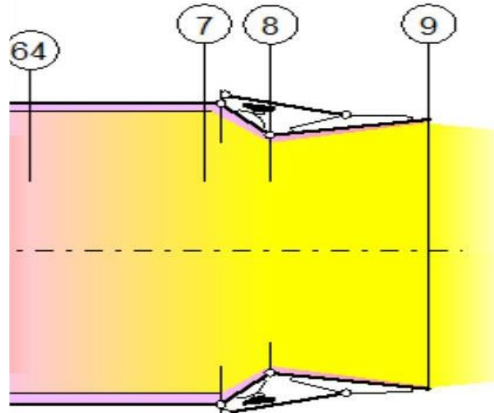


Figure 20. Nozzle section of engine Turbo-Union RB199.[GasTurb]

As can be seen from the figure 20, the nozzle of the Turbo-Union RB199 engine consists of 4 parts. The section 64 is the entry area of the nozzle without afterburner. The section 7 is the area of the afterburner entrance. The section 8 is the throat area. The section 9 is the exit area. The diameters of sections 64 and 7 do not change, they are fixed. However, the diameters of sections 8 and 9 may vary depending on the pushing force if desired.

ConDi nozzle is needed for our Turbo-Union RB199 engine, which we designed according to the previous explanation, to accelerate the flow even more and to achieve higher thrust values. The area ratio is  $\left(\frac{A_0}{A_8}\right) = 1.075$ , and the Mach speed is 1.306. As a result, the field must start increasing again to reach higher velocities, because our engine moves supersonic speed, so a diverging section is needed. This is why we used the ConDi nozzle for our Turbo-Union RB199 design (See Appendix C.3).

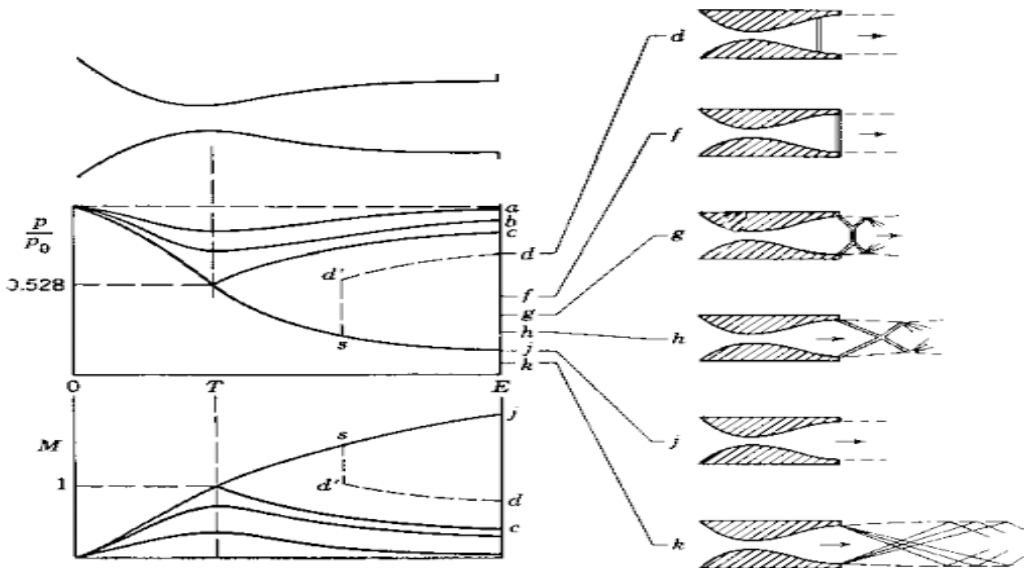


Figure 21. Flow output states at the nozzle outlet.[23]

The figure 21 illustrates the flow output states for the nozzle outlet. To get the best thrust, we need to eliminate shocks in or out of the nozzle. That is, the flow should expend ideally once exiting the nozzle. Thus, we need to choose the "j" nozzle.

$$\frac{A}{A^*} = \left(\frac{k+1}{2}\right)^{\frac{-k+1}{2(k-1)}} * \frac{(1+\frac{M^2(k-1)}{2})^{\frac{k+1}{2(k-1)}}}{M} \quad (29)$$

$$\frac{p}{p_t} = (1 + M^2 \frac{k-1}{2})^{\frac{-k}{k-1}} \quad (30)$$

$$M = \frac{v}{(kRT)^{0.5}} \quad (31)$$

$$F = \dot{m}_e V_e - \dot{m}_0 V_0 + (p_e + p_0) A_e \quad (32)$$

The analysis is started by considering a very narrow throat to ensure ideal expansion at the outlet. Then, expanding the area is started with the above equations. Until an ideal pressure value is reached  $\left(\frac{P_8}{P_0}\right) = 0.534$ , the pressure ratio should decrease. This value is the critical stagnation pressure ratio of the throat at Mach 1. After that, it will start to increase isentropically once again without any shock accruing. Since the area ratio should be  $\left(\frac{A_9}{A_8}\right) = 1.075$  for ideal expansion, the Mach number at the output is calculated as 1.306. At this Mach number, our velocity is calculated as 987.889 m/s. Finally, the thrust can be calculated with this velocity.

## 4. CONCLUSION

The objective of the project was to achieve lowering TSFC by 10% and raising the Thrust to Weight Ratio. To achieve this, we first modeled the generic engine design to the GasTurb software and began optimization. In-depth cycle analysis is done on the process to determine where efficiency can be improved. The main parameters considered that affect thrust is Overall Pressure Ratio, Bypass Ratio, Turbine Entry Temperature and Fan Pressure Ratio. To achieve 74KN thrust, the bypass duct pressure ratio was increased from 0.97 to 0.975, and the reheat temperature was reduced from 2040 to 1950 Kelvin. In the inlet design, we analyzed the effects of shocks, and this guided our design. The inlet shape should be designed such that it slows down the speed of the flow to a speed that can be handled throughout the engine. The flow slows down by a number of oblique shocks, so it can enter the fan and then the compressor without causing any damage to the combustion. For the compressor design, the decision to go with axial compressors was due to the fact that they have a high overall pressure ratio and higher isentropic pressure. The type of material used in these designs was ceramic coatings and nickel-based alloys, which are used in turbines to withstand excess temperature. CFD analysis is also needed to verify and optimize the performance of designs. Reheat/Afterburner is added to improve thrust but negatively affects TSFC.

Therefore, a tradeoff was made in terms of performance. Materials used to make the afterburner include nickel alloys. We also anticipated that better quality material would have been discovered by the year of entry into service. Thus, the material used in the turbine would allow for higher Turbine Entry Temperature.

The table 4 concludes the overall improvement of the engine. Hence, we achieved our goal at sea level wet engines by decreasing the TSFC 12.12% and T/W 11.75%, as we mainly focused on. To achieve this, GasTurb 13 parametric tool and optimization tool were used. We checked whether our calculations agree with the real cases by running CFD simulations in ANSYS. Further information about the material, the geometry and theoretical background, etc., were given in the engine inlet, compressor, combustion chamber, turbine, afterburner and nozzle parts.

## REFERENCES

- [1] “*Turbofan Engine*” (2021, May 13). NASA Glenn Research Center. Retrieved from: <https://www.grc.nasa.gov/www/k-12/airplane/aturbf.html>
- [2] Joosung J.LeeStephen P.LukachkoIan A.Waitz. (2004). “*Aircraft and Energy Use*”. ScienceDirect.com | Science, health and medical journals, full text articles and books. Retrieved from: <https://www.sciencedirect.com/science/article/pii/B012176480X001947>
- [3] “*Propulsion systems*” (n.d.). Encyclopedia Britannica. Retrieved from: <https://www.britannica.com/technology/airplane/Propulsion-systems#ref528078>
- [4] “*Jet engine - medium-bypass turbofans, high-bypass turbofans, and ultrahigh-bypass engines*” (n.d.). Encyclopedia Britannica. Retrieved from: <https://www.britannica.com/technology/jet-engine/Medium-bypass-turbofans-high-bypass-turbofans-and-ultrahigh-bypassengines#ref135185>
- [5] “*Quest for Performance: The Evolution of Modern Aircraft*” (n.d.). NASA History Division | NASA. Retrieved from: <https://history.nasa.gov/SP-468/ch10-3.htm>
- [6] “*Compressors*” (2015, May 5). NASA Glenn Research Center. Retrieved from: <https://www.grc.nasa.gov/www/k-12/airplane/compress.html>
- [7] Farokhi, S. (2014). *Aircraft propulsion*. John Wiley & Sons.
- [8] “*Exhaust mixer*” (2005, October 14). Wikipedia, the free encyclopedia. Retrieved July 14, 2021, from: [https://en.wikipedia.org/wiki/Exhaust\\_mixer](https://en.wikipedia.org/wiki/Exhaust_mixer)
- [9] “*Figure 4. Typical modern three-spool turbofan jet engine: Compressor on...*” (2020, June 24). ResearchGate. Retrieved from: [https://www.researchgate.net/figure/Typical-modern-three-spool-turbofan-jet-engine-compressor-on-the-left-turbine-on-the\\_fig2\\_322904838](https://www.researchgate.net/figure/Typical-modern-three-spool-turbofan-jet-engine-compressor-on-the-left-turbine-on-the_fig2_322904838)
- [10] “*Comparison of centrifugal and axial flow compressors for small gas turbine applications*” (1966). K-REx Home. Retrieved from: <https://krex.k-state.edu/dspace/handle/2097/22584>
- [11] Baxter, A. D. and Ehrich, . Fredric F. (2015, September 27). “*jet engine*”. Encyclopedia Britannica. Retrieved from: <https://www.britannica.com/technology/jet-engine>
- [12] Razak, A. (2007). “*Industrial Gas Turbines*”, 137-173. Retrieved from: <https://doi.org/10.1533/9781845693404.1.137>
- [13] Akash J. (n.d.). *Gas Turbine Combustion Chamber*. Gas Turbine Theory. Retrieved from: [https://www.rajagiritech.ac.in/Home/mech/Course\\_Content/Semester%20IV/ME%2020204%20Thermal%20Engineering/Module%206.pdf](https://www.rajagiritech.ac.in/Home/mech/Course_Content/Semester%20IV/ME%2020204%20Thermal%20Engineering/Module%206.pdf)
- [14] Peacewise. (2021, February 28). “*Annular combustor for a gas turbine engine*”. Retrieved from: <https://en.wikipedia.org/wiki/Combustor#/media/File:AnnularCombustorNew.png>
- [15] Wang Yingjun. (n.d.). “*Combustion Efficiency*”. Retrieved from: [https://www.aiaa.org/docs/default-source/uploadedfiles/education-and-careers/university-students/design-competitions/1stplace\\_beihang-university\\_design\\_report.pdf?sfvrsn=9393aae1\\_0](https://www.aiaa.org/docs/default-source/uploadedfiles/education-and-careers/university-students/design-competitions/1stplace_beihang-university_design_report.pdf?sfvrsn=9393aae1_0), pp. 31

- [16] Wilson, D. G., & Korakianitis, T. (2014). *The design of high-efficiency Turbomachinery and gas turbines*. MIT Press.
- [17] Kurzke, J., & Halliwell, I. (2018). *Propulsion and power: An exploration of gas turbine performance modeling*. Springer.
- [18] Royce, R. (2015). *The jet engine*. John Wiley & Sons.
- [19] Rogers, G. F., Cohen, H., Saravanamuttoo, H. I., Straznicky, P., & Nix, A. (2017). *Gas turbine theory*.
- [20] Okura, T. (2015). *Materials for Aircraft Engines*. ASEN 5063 Aircraft Propulsion Final Report Retrieved from: [https://www.colorado.edu/faculty/kantha/sites/default/files/attached-files/73549-116619\\_-\\_takehiro\\_okura\\_-\\_dec\\_17\\_2015\\_1027\\_am\\_-\\_asen\\_5063\\_2015\\_final\\_report\\_okura.pdf](https://www.colorado.edu/faculty/kantha/sites/default/files/attached-files/73549-116619_-_takehiro_okura_-_dec_17_2015_1027_am_-_asen_5063_2015_final_report_okura.pdf)
- [21] Wygonik, P. (2015). Journal of kones powertrain and transport, Vol. 19, No. 2 2012 influence of the gas turbine engine design parameters on the energy consumption of the MULTIROLE aircraft missions. *Journal of KONES. Powertrain and Transport*, 19(2), 569-573. Retrieved from: <https://doi.org/10.5604/12314005.1138277>
- [22] Strobridge, T. R., Moulder, J. C., & Clark, A. F. (1979). “Titanium combustion in turbine engines”, 4. Retrieved from: <https://doi.org/10.6028/nbs.ir.79-1616>
- [23] Nordqvist, M., Kareliusson, J., Da Silva, E. R., Kyprianidis, K. G (2017). “Conceptual Design of a Turbofan Engine for a Supersonic Business Jet”. Mälardalen University Future Energy Center. Retrieved from: <https://www.diva-portal.org/smash/get/diva2:1305926/FULLTEXT01.pdf>
- [24] “Nozzles” (2021, May 13). NASA Glenn Research Center. Retrieved from: <https://www.grc.nasa.gov/www/k-12/airplane/nozzle.html>
- [25] James Rushbrooke. (2020, April 14). “*Shock wave arrangements in CD nozzles*” SoftInWay. Retrieved from: <https://blog.softinway.com/an-introduction-to-shock-waves/>
- [26] Ran, H., & Mavris, D. (2005). “Preliminary design of a 2D supersonic inlet to maximize total pressure recovery”. *AIAA 5th ATIO and 16th Lighter-Than-Air Sys Tech. and Balloon Systems Conferences*. Retrieved from: <https://doi.org/10.2514/6.2005-7357>
- [27] ASE 334 Propulsion Systems – I, Project, Performance Analysis and Optimization of a Supersonic, Low ByPass Ratio TurboFan Engine Project Manual. Middle East Technical University Northern Cyprus Campus, 2021.

## APPENDICES

### A) The Analysis of Engine Performance and Modelling

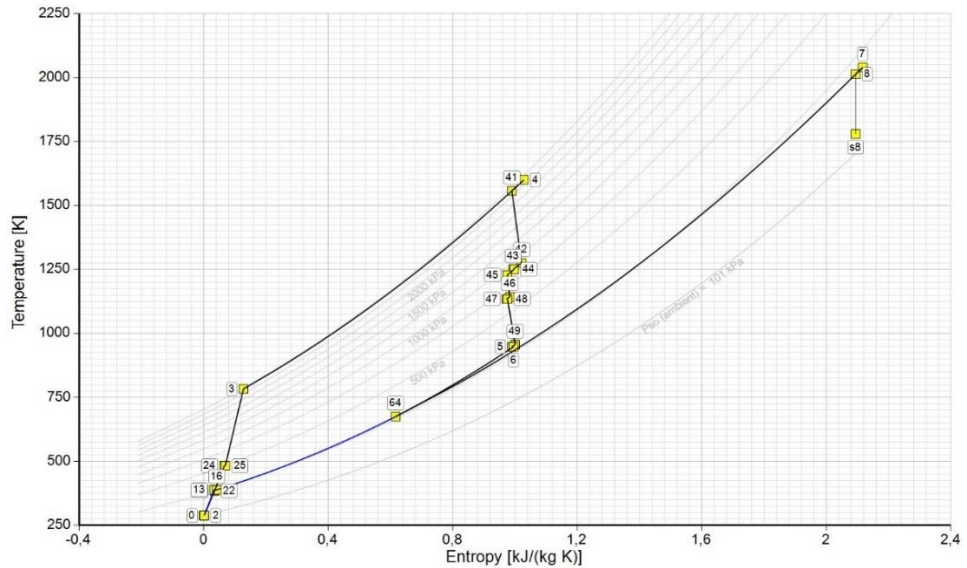


Figure 22. The relation between temperature and entropy.[GasTurb]

This cycle shows the temperature and entropy values at every part of the baseline wet engine at sea level.

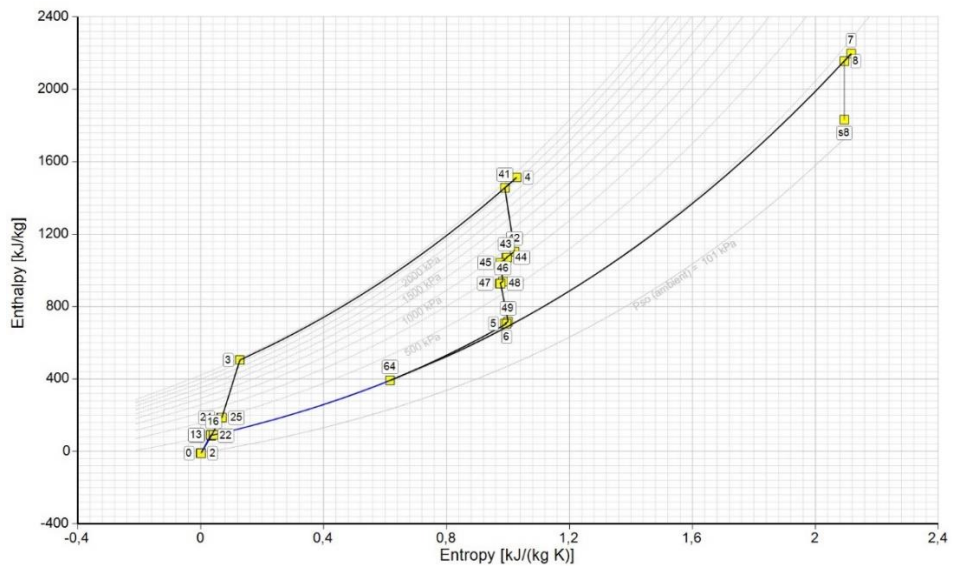


Figure 23. The relation between enthalpy and entropy.[GasTurb]

This is the cycle analysis of the baseline wet engine at sea level. This figure 23 shows the enthalpy and entropy at every part of the engine.

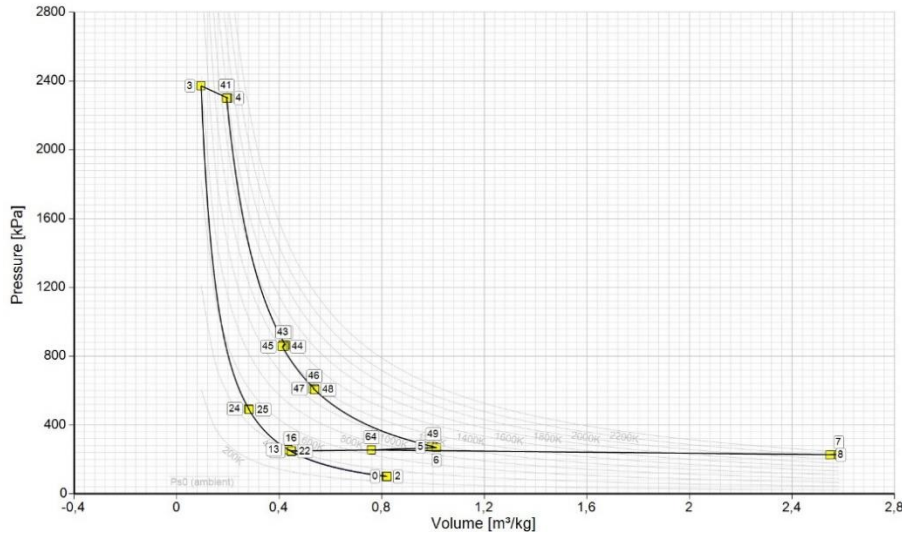


Figure 24. The relation between pressure and volume.[GasTurb]

The final cycle shows the pressure and volume at every part of the baseline wet engine at sea level conditions.

$$\eta_{\text{thermal}} = \frac{\text{rate of production of kinetic energy}}{\text{fuel power}} = \frac{\left( \frac{\dot{m}_e u_e^2}{2} - \frac{\dot{m}_o u_o^2}{2} \right)}{\dot{m}_f h} \quad (33)$$

Using the formula 33, when  $\dot{m}_e = 71.64 \text{ kg/s}$ ,  $u_e = 166.055 \text{ m/s}$ ,  $\dot{m}_o = 75.6092 \text{ kg/s}$ ,  $u_o = 803.681 \text{ m/s}$ ,  $\dot{m}_f = 0.66874 + 3.47107 = 4.13981 \text{ kg/s}$  and  $h = 43.124 \text{ MJ/kg}$  the thermal efficiency can be found as 13.1244% for the baseline wet engine.

Station	W kg/s	T K	P kPa	WRstd kg/s	
amb		288,15	101,325		FN = 40,05 kN
2	71,640	288,15	100,818	72,000	TSFC = 16,6960 g/(kN*s)
13	37,526	388,24	257,087	17,168	WF_Burner= 0,66874 kg/s
21	34,114	384,50	247,005	16,165	s_NOx = 0,82223
22	34,114	384,50	247,005	16,165	BPR = 1,1000
24	34,114	482,08	494,010	9,050	Core_Eff = 0,4251
25	34,114	482,08	489,070	9,142	Prop_Eff = 0,0000
3	31,044	782,57	2371,989	2,185	P3/P2 = 23,527
31	27,462	782,57	2371,989		P2/P1 = 0,99500
4	28,131	1600,00	2300,830	2,919	P25/P24 = 0,99000
41	29,836	1557,01	2300,830	3,054	P4/P3 = 0,97000
42	29,836	1275,25	865,317		P44/P43 = 0,99000
43	31,542	1250,41	865,317		P48/P47 = 0,99000
44	31,542	1250,41	856,664		P6/P5 = 0,98000
45	32,907	1228,00	856,664	8,035	P16/P13 = 0,97000
46	32,907	1142,99	610,921		P5/P2 = 0,92882
47	33,589	1133,98	610,921		P8/P64 = 1,00000
48	33,589	1133,98	604,812	11,163	P16/P6 = 0,92882
49	33,589	955,79	273,965		A63 = 0,17218 m²
5	34,612	947,67	273,965	23,215	A163 = 0,28543 m²
64	72,138	668,81	254,999		A64 = 0,45761 m²
8	72,138	668,81	254,999	43,670	A8 = 0,19001 m²
Bleed	0,171	782,57	2371,985		wBld/w2 = 0,00238
<hr/>					
Efficiencies:	isentr	polytr	RNI	P/P	Anq8 = 20,00 °
Outer LPC	0,8800	0,8946	0,995	2,550	P8/Pamb = 2,51665
Inner LPC	0,8700	0,8852	0,995	2,450	PwX = 50,00 kw
IP Compressor	0,8500	0,8636	1,729	2,000	WtLp/W25= 0,00000
HP Compressor	0,8600	0,8857	2,614	4,850	WHDbl/W22= 0,00000
Burner	0,9990			0,970	WCnH/W25 = 0,05000
HP Turbine	0,9000	0,8892	3,165	2,659	Loading = 100,00 %
IP Turbine	0,9000	0,8963	1,547	1,402	WCnR/W25 = 0,05000
LP Turbine	0,9004	0,8913	1,197	2,208	WCir/W25 = 0,02000
<hr/>					
HP Spool mech Eff	1,0000	Nom Spd	18901 rpm		far7 = 0,00936
IP Spool mech Eff	1,0000	Nom Spd	16700 rpm		Wclr/W25 = 0,03000
LP Spool mech Eff	1,0000	Nom Spd	14600 rpm		
<hr/>					
hum [%]	war0	FHV	Fuel		
0,0	0,00000	43,124	Generic		

Figure 25. The results for the dry baseline engine at sea level stationary condition.[GasTurb]

The figure 25 represents the dry baseline engine at sea level stationary conditions. The thrust drops to 40.05 kN, and the TSFC also decreases to 16.696 g/(kN\*s).

**Table 15. Thermo-fluid variables of the dry baseline engine.[GasTurb]**

Units	St 2	St 21	St 24	St 25	St 3	St 4	St 43	St 45	St 47	St 48	St 5	St 6	St 13	St 16	St 64	St 8
Mass Flow	kg/s	71,64	34,1143	34,1143	34,1143	31,044	28,1307	31,5422	32,9067	33,589	33,589	34,6124	34,6124	37,5257	37,5257	72,1381
Total Temperature	K	288,15	384,496	482,076	482,076	782,566	1600	1250,41	1228	1133,98	1133,98	947,668	947,668	388,245	388,245	668,814
Static Temperature	K	274,407	366,293	459,622	459,622	777	1579,26	1204,24	1182,31	1091,1	1091,1	910,355	935,66	369,866	369,866	661,884
Total Pressure	kPa	100,818	247,005	494,01	489,07	2371,99	2300,83	865,317	856,664	610,921	604,812	273,965	268,486	257,087	249,374	254,999
Static Pressure	kPa	84,9889	208,322	416,933	412,763	2308,76	2171,67	736,986	729,441	519,815	514,617	232,761	254,947	216,829	210,324	245,236
Velocity	m/s	166,055	191,614	214,126	214,125	109,992	229,608	336,386	333,544	321,126	321,126	294,893	167,289	192,535	192,535	122,13
Area	m <sup>2</sup>	0,399849	0,089859	0,050415	0,050924	0,027266	0,025574	0,04398	0,045901	0,063022	0,063658	0,131772	0,217964	0,095434	0,098386	0,457611
Mach Number		0,5	0,5	0,5	0,5	0,2	0,3	0,5	0,5	0,5	0,5	0,5	0,5	0,28	0,5	0,24
Density	kg/m <sup>3</sup>	1,07897	1,98129	3,16014	3,12854	10,3514	4,79059	2,13203	2,14935	1,65971	1,64311	0,890731	0,949248	2,04228	1,98101	1,29077
Spec Heat @ T	J/(kg*K)	1004,52	1012,15	1026,63	1026,63	1094,55	1276,26	1225,39	1220,06	1203,28	1203,28	1164,7	1164,7	1012,48	1012,48	1080,91
Spec Heat @ Ts	J/(kg*K)	1004,19	1010,57	1023,04	1023,04	1093,23	1273,96	1218,19	1212,6	1195,55	1195,55	1156,45	1162,04	1010,88	1010,88	1079,18
Enthalpy @ T	J/kg	-10032,3	87070	186503	504823	1,51312E6	1,0706E6	1,04185E6	927371	927371	706033	706033	90850,6	90850,6	386020	386020
Enthalpy @ Ts	J/kg	-23819,4	68712	163578	498774	1,48676E6	1,01402E6	986229	875810	875810	662552	692040	72315,7	72315,6	378562	374687
Entropy Function @ T	-0,11924	0,893073	1,69566	1,69566	3,47836	6,58273	5,48742	5,40405	5,06506	5,06506	4,32142	4,32142	0,927146	0,927145	2,91751	2,91751
Entropy Function @ Ts	-0,29004	0,722749	1,52603	1,52603	3,45134	6,52496	5,3269	5,24328	4,90356	4,90356	4,15843	4,26968	0,756842	0,756841	2,87847	2,28756
Exergy	J/kg	-414,6	87074,4	177456	176624	478094	1,2271E6	794288	771611	657204	656373	431041	429369	91345,6	88826,2	221212
Gas Constant	J/(kg*K)	267,05	287,05	287,05	287,05	287,05	287,046	287,047	287,047	287,047	287,047	287,047	287,047	287,047	287,047	287,049
Fuel-Air-Ratio		0	0	0	0	0	0,024351	0,021661	0,020744	0,020314	0,020314	0,019701	0,019701	0	0	9,3570E-3
Water-Air-Ratio		0	0	0	0	0	0	0	0	0	0	0	0	0	0	0
Inner Radius	m	0,112195	0,163765	0,147389	0,169757	0,173876	0,1753	0,1753	0,1753	0,1753	0,166535	0	0,240419	0,268401	0	0
Outer Radius	m	0,373983	0,235419	0,194209	0,212196	0,19858	0,197156	0,211493	0,212934	0,225367	0,225817	0,263966	0,263401	0,292916	0,321491	0,381657
Axial Position	m	0,186992	0,186992	1,06878	1,12773	1,41689	1,56958	1,64244	1,6775	1,74022	1,82787	1,99626	2,33942	0,779595	2,33942	2,66091

The table 15 shows the thermo-fluid variables of the dry baseline engine at sea level stationary.

Using the formula 33, when  $\dot{m}_e = 71.64 \text{ kg/s}$ ,  $u_e = 166.055 \text{ m/s}$ ,  $\dot{m}_o = 72.1381 \text{ kg/s}$ ,  $u_o = 471.875 \text{ m/s}$ ,  $\dot{m}_f = 0.66874 \text{ kg/s}$  and  $h = 43.124 \text{ MJ/kg}$  the thermal efficiency can be found as 24.424% for the baseline dry engine.

### FireFly Jetx Turbofan Jet Engine:

**Table 16. the new parameter of the FireFly Jetx engine.[GasTurb]**

Property	Unit	Value	Comment													
Intake Pressure Ratio		-1														
No (0) or Average (1) Core dP/P		1														
Inner Fan Pressure Ratio		2,75														
Outer Fan Pressure Ratio		2,9														
Core Inlet Duct Press. Ratio		1														
IP Compressor Pressure Ratio		2,4														
Compr. Interduct Press. Ratio		0,99														
HP Compressor Pressure Ratio		4,93														
Bypass Duct Pressure Ratio		0,97														
Inlet Corr. Flow W2Rstd	kg/s	72														
Design Bypass Ratio		1,1														
Burner Exit Temperature	K	1745														
Burner Design Efficiency		0,999														
Burner Partload Constant		1,6	used for off design only													
Fuel Heating Value	MJ/kg	43,124														
Overboard Bleed	kg/s	0														
Power Offtake	kW	50														
HP Spool Mechanical Efficiency		0,995														
IP Spool Mechanical Efficiency		0,995														
LP Spool Mechanical Efficiency		0,995														
Burner Pressure Ratio		0,97														
IPT Interd. Ref. Press. Ratio		0,99														
LPT Interd. Ref. Press. Ratio		0,99														
Turbine Exit Duct Press Ratio		0,98														
Hot Stream Mixer Press Ratio		0,99														
Cold Stream Mixer Press Ratio		0,99														
Mixed Stream Pressure Ratio		1														
Mixer Efficiency		0,5														
Design Mixer Mach Number		0,24														
Design Mixer Area	m <sup>2</sup>	0														

The table 16 shows the new parameter of the baseline engine which is used in our FireFly Jetx engine. For the main design parameters new engine has, 32.54 OPR, 2.75 inner and 2.9 outer FPR, 1.1 BPR and 1745 K TET.

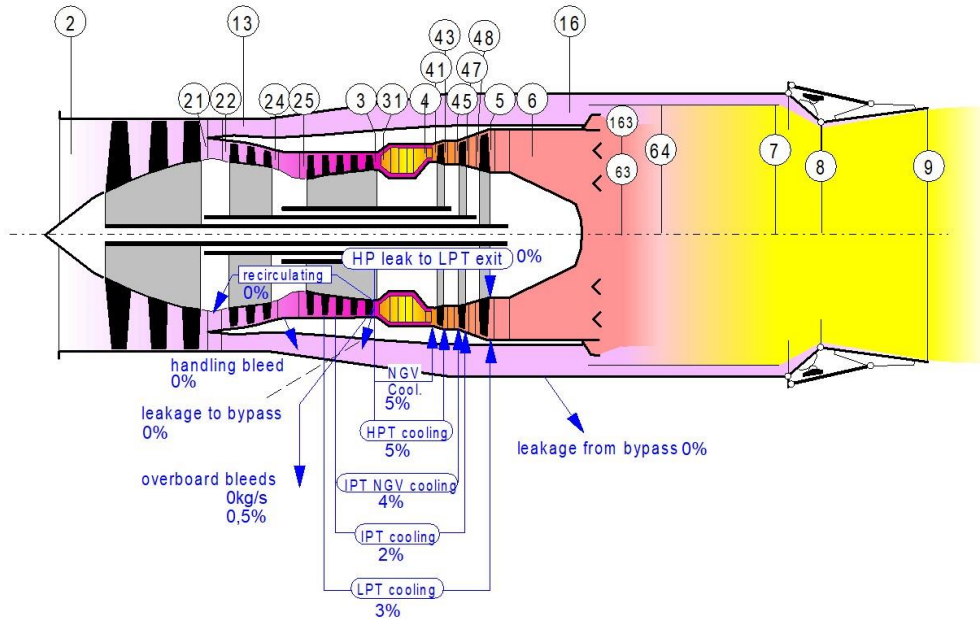


Figure 26. The new engine.[GasTurb]

From the figure 26, it can be seen that this new engine has con-di type of nozzle to get more thrust with less TSFC.

Station	W kg/s	T K	P kPa	WRstd kg/s	Reheat on	
amb	288,15	101,325			FN = 74,51 kN	
2	72,000	288,15	101,325	72,000	TSFC = 51,9569 g/(kN*s)	
13	37,714	404,14	293,843	15,402	WF Burner = 0,75123 kg/s	
21	34,286	398,79	278,644	14,667	s NOx = 1,37729	
22	34,286	398,79	278,644	14,667	BPR = 1,1000	
24	34,286	529,23	668,745	7,040	Core Eff = 0,4538	
25	34,286	529,23	662,058	7,111	Prop Eff = 0,0000	
3	31,200	858,02	3263,944	1,671	P3/P2 = 32,213	
31	27,500	858,02	3263,944		P2/P1 = 1,00000	
4	28,351	1745,00	3166,026	2,233	P22/P21 = 1,00000	
41	30,066	1698,83	3166,026	2,336	P25/P24 = 0,99000	
42	30,066	1391,08	1169,237		P4/P3 = 0,97000	
43	31,780	1364,34	1169,237		P44/P43 = 0,99000	
44	31,780	1364,34	1157,545		P48/P47 = 0,99000	
45	33,151	1340,15	1157,545	6,258	P6/P5 = 0,98000	
46	33,151	1227,51	759,625		P16/P13 = 0,97000	
47	33,837	1218,19	759,625		P5/P2 = 0,91281	
48	33,837	1218,19	752,029	9,374	P8/P64 = 0,90988	
49	33,837	1015,13	318,626		P16/P6 = 0,91281	
5	34,866	1007,26	318,626	20,730	Input:	
64	71,071	714,39	293,529		HPC Tip Speed m/s	420,00000
7	74,191	1950,00	267,077		HPC Inlet Radius Ratio	0,80000
8	75,700	1924,36	267,077	74,217	HPC Inlet Mach Number	0,50000
Bleed	0,171	858,02	3263,934		min HPC Inlet Hub Diameter m	0,00000
Efficiencies:	isentr polytr RNI				Output:	
Outer LPC	0,8800	0,8964	1,000	2,900	HPC Tip circumf. Mach No	0,93693
Inner LPC	0,8700	0,8870	1,000	2,750	HPC Tip relative Mach No	1,06199
IP Compressor	0,8500	0,8669	1,867	2,400	HPC Inlet Tip Diameter m	0,80000
HP Compressor	0,8600	0,8856	3,166	4,930	Design HP Spool Speed [RPM]	21414,54
Burner	0,9990				A63 = 0,40566 m <sup>2</sup>	0,50000
HP Turbine	0,9000	0,8892	3,935	2,708	HPC Inlet Tip Diameter m	0,37458
IP Turbine	0,9000	0,8955	1,891	1,524	Wt total = 3,87127 kg/s	0,29966
LP Turbine	0,9004	0,8907	1,371	2,360	HPC Inlet Hub Diameter m	0,80000
Reheat	0,9000				Calculated HPC Radius Ratio	0,80000
					Corr.Flow/Area HPC kg/(s*m <sup>2</sup> )	179,25399
Ang8				7,00 °		
P8/Pamb						
PWx						
WTkLP/W25						
WHDB1/W22						
WCWN/W25						
Loading						
WCWR/W25						
WCIN/W25						
WCIR/W25						
WF Reheat						
XM64						
XM7						
far7						
WCLR/W25						
Con-Di Nozzle:						
A9*(Ps9-Pamb)	-0,274					
hum [%]	war0	FHV	Fuel			
0,0	0,00000	43,124	Generic			

Figure 27. The results for new wet baseline engine.[GasTurb]

The figure 27 shows the final results of the new wet engine simulation at sea level condition, stationary position. It can be seen that new engine has 74.51 kN thrust and 51,9569 g/(kN\*s) TSFC.

**Table 17. Thermo-fluid variables of the wet baseline engine.[GasTurb]**

	Units	St 2	St 21	St 24	St 25	St 3	St 4	St 43	St 45	St 47	St 48	St 5	St 6	St 13	St 16	St 64	St 7	St 8	St 9
Mass Flow	kg/s	72	34,2857	34,2857	34,2857	31,2	28,3512	31,7798	33,1512	33,8369	33,8369	34,8655	34,8655	37,7143	37,7143	71,0712	74,1912	75,6998	75,6998
Total Temperature	K	288,15	398,794	529,225	529,225	858,022	1745	1364,34	1340,15	1218,19	1218,19	1007,26	1007,26	404,143	404,143	714,392	1950	1924,36	1924,36
Static Temperature	K	274,407	379,922	505,07	505,07	852,078	1722,94	1314,99	1291,44	1172,89	1172,89	968,037	994,733	385,069	385,069	707,201	1879,56	1698,14	1565,49
Total Pressure	kPa	101,325	278,644	668,745	662,058	3263,94	3166,03	1169,24	1157,54	759,625	752,029	318,626	312,254	293,843	285,027	293,529	267,077	267,077	267,077
Static Pressure	kPa	85,416	235,024	564,674	559,027	3177,34	2989,21	996,535	986,396	646,849	640,38	270,988	296,576	247,847	240,411	282,338	223,759	147,23	100,526
Velocity	m/s	166,055	195,102	224,137	224,137	114,87	239,264	350,558	347,637	332,127	332,127	303,385	172,08	196,402	196,402	125,965	440,959	786,54	987,889
Area	m <sup>2</sup>	0,399849	0,081544	0,039275	0,039671	0,020908	0,019605	0,034338	0,035839	0,053027	0,053562	0,11788	0,195069	0,085639	0,088288	0,405671	0,318636	0,342533	
Mach Number		0,5	0,5	0,5	0,5	0,2	0,3	0,5	0,5	0,5	0,5	0,28	0,5	0,5	0,24	0,534009	1	1,30602	
Density	kg/m <sup>3</sup>	1,08439	2,15506	3,89482	3,85588	12,9905	6,04413	2,64008	2,66087	1,92128	1,90207	0,974904	1,03867	2,24226	2,17499	1,39082	0,414745	0,302051	0,223709
Spec Heat @ T	J/(kgK)	1004,52	1013,4	1035,78	1035,78	1111,58	1297,12	1247,41	1241,87	1222,45	1222,45	1181,88	1181,88	1014,16	1014,16	1094,25	1382,8	1377,76	1377,76
Spec Heat @ Ts	J/(kgK)	1004,19	1011,75	1030,59	1030,59	1110,26	1295,11	1240,51	1234,95	1214,78	1214,78	1179,24	1179,24	1012,2	1012,2	1092,45	1376,55	1355,45	1339,4
Enthalpy @ T	J/kg	-10032,3	101489	235194	235194	588176	1,706646	1,215446	1,183856	1,032576	1,032576	777913	777913	106935	106935	436097	2,0596E	2,02016E	2,02016E
Enthalpy @ Ts	J/kg	-23819,4	82458,7	210075	210075	581579	1,678026	1,15468	1,123236	977412	977412	731891	731891	87648,1	87648,1	428164	1,96178E6	1,71078E6	1,53214E6
Entropy Function @ T	-0,11924	1,02129	2,03117	2,03117	3,83265	6,99805	5,88134	5,79614	5,3831	5,3831	4,58214	4,58214	1,06854	1,06854	3,17106	7,79335	7,71763	7,71763	
Entropy Function @ Ts	-0,29004	0,851042	1,86202	1,86202	3,80575	6,94058	5,72152	5,63614	5,22239	5,22239	4,41987	4,53063	0,889303	0,889303	3,13219	7,61638	7,12209	6,74051	
Exergy	J/kg	4,6855E-3	100857	223444	222813	558545	1,41288E6	931453	905878	754112	753281	493847	492176	106788	104289	261958	1,49475E6	1,46211E6	1,46211E6
Gas Constant	J/(kgK)	287,05	287,05	287,05	287,05	287,05	287,046	287,046	287,046	287,046	287,046	287,047	287,047	287,05	287,05	287,048	287,041	287,041	287,041
Fuel-Air-Ratio		0	0	0	0	0	0,027219	0,024211	0,023186	0,022706	0,022706	0,022021	0,022021	0	0	0,010683	0,055052	0,053896	0,053896
Water-Air-Ratio		0	0	0	0	0	0	0	0	0	0	0	0	0	0	0	0	0	0
Inner Radius	m	0,112195	0,166709	0,150038	0,149831	0,153587	0,154828	0,154828	0,154828	0,154828	0,154828	0,147086	0	0,236836	0,254184	0	0	0	0
Outer Radius	m	0,373983	0,231836	0,186948	0,187289	0,175056	0,173816	0,186882	0,188094	0,202115	0,202537	0,243222	0,249184	0,284619	0,304487	0,359345	0,359345	0,320727	0,332536
Axial Position	m	0,186992	0,186992	1,01605	1,07607	1,32989	1,46507	1,52836	1,55933	1,61477	1,69219	1,85122	2,1674	0,763424	2,1674	2,47189	3,69367	3,94521	4,58666

The table 17 has the main thermo-fluid variables at every part of the wet engine done at sea level stationary position.

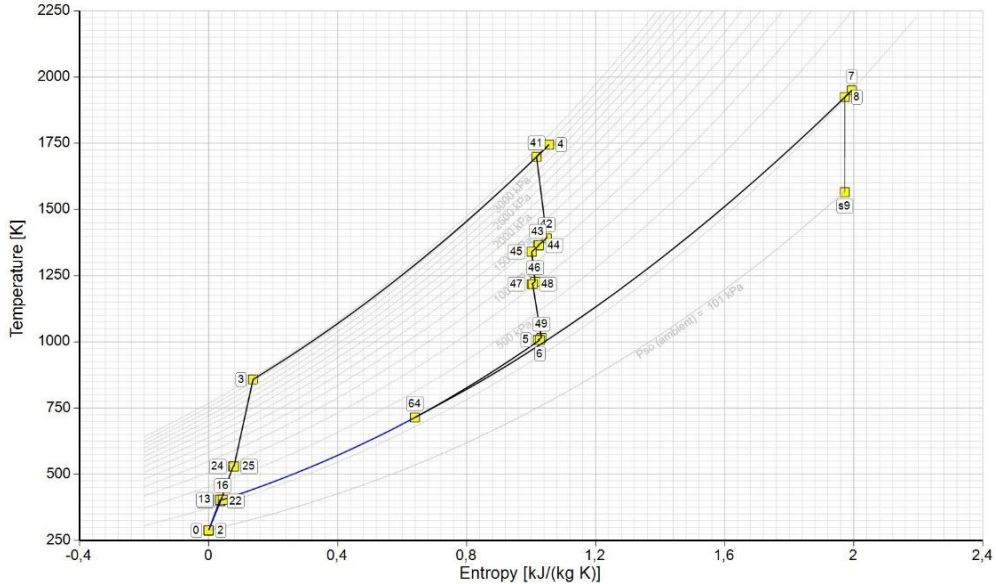


**Figure 28. The relation between temperature and entropy.[GasTurb]**

The figure 28 is the cycle analysis of the new wet engine at sea level. From the temperature versus entropy, the graph can be seen at every part of the engine.

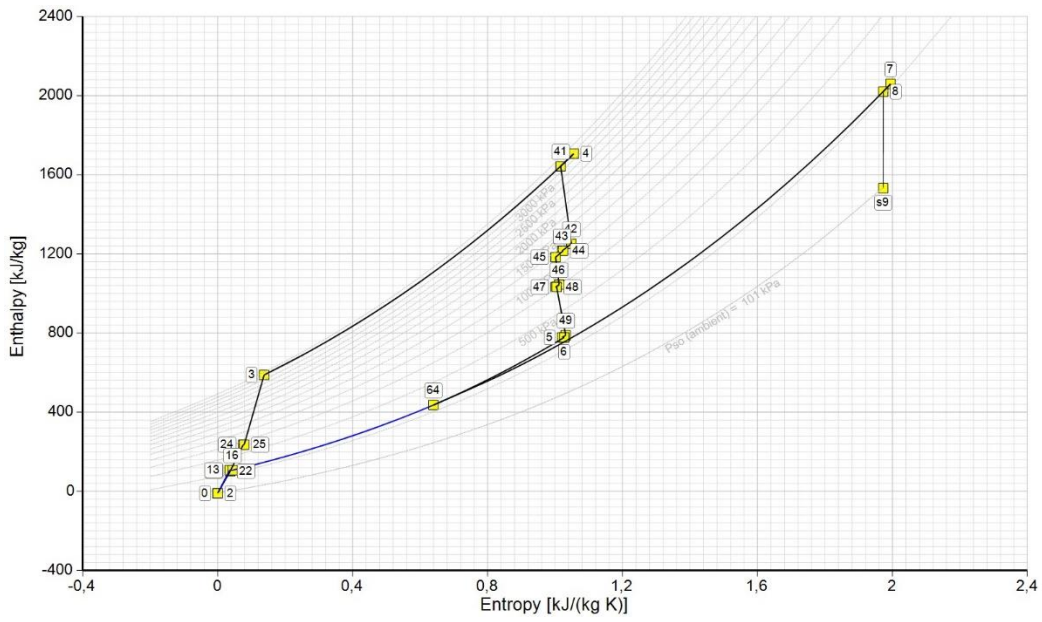


Figure 29. The relation between enthalpy and entropy.[GasTurb]

The figure 29 shows the enthalpy versus entropy relations at every part of the wet engine.

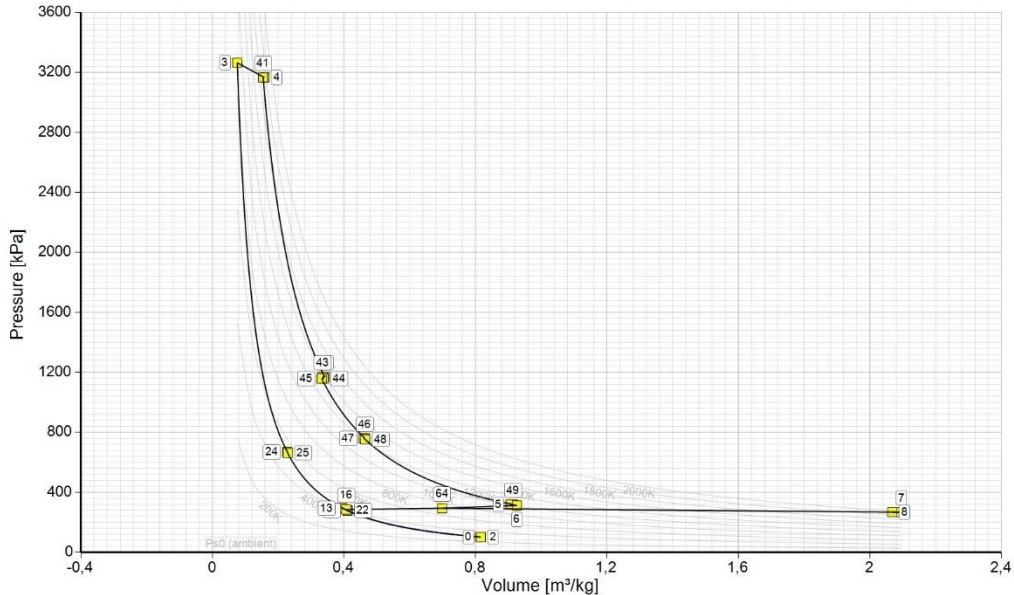


Figure 30. The relation between pressure and volume.[GasTurb]

The figure 30 represents the pressure versus volume relation. The variables can be seen at every part of the wet engine.

Using the formula 33, when  $\dot{m}_e = 72 \text{ kg/s}$ ,  $u_e = 166.055 \text{ m/s}$ ,  $\dot{m}_o = 75.6996 \text{ kg/s}$ ,  $u_o = 987.889 \text{ m/s}$ ,  $\dot{m}_f = 0.75123 + 3.12004 = 3.87127 \text{ kg/s}$  and  $h = 43.124 \text{ MJ/kg}$  the thermal efficiency can be found as 21.532% for the FireFly Jetx wet engine.

Station	W kg/s	T K	P kPa	WRstd kg/s	FN	=	43,89 kN
amb	288,15	101,325		72,000	TSFC	=	17,1148 g/(kN*s)
2	72,000	288,15	101,325	72,000	WF Burner	=	0,75123 kg/s
13	37,714	404,14	293,843	15,402	s NOx	=	1,37729
21	34,286	398,79	278,644	14,667	BPR	=	1,1000
22	34,286	398,79	278,644	14,667	Core Eff	=	0,4538
24	34,286	529,23	668,745	7,040	Prop Eff	=	0,0000
25	34,286	529,23	662,058	7,111	P3/P2	=	32,213
3	31,200	858,02	3263,944	1,671	P2/P1	=	1,00000
31	27,600	858,02	3263,944		P22/P21	=	1,00000
4	28,351	1745,00	3166,026	2,233	P25/P24	=	0,99000
41	30,066	1698,83	3166,026	2,336	P4/P3	=	0,97000
42	30,066	1391,08	1169,237		P44/P43	=	0,99000
43	31,780	1364,34	1169,237		P48/P47	=	0,99000
44	31,780	1364,34	1157,545		P6/P5	=	0,98000
45	33,151	1340,15	1157,545	6,258	P16/P13	=	0,97000
46	33,151	1227,51	759,625		P5/P2	=	0,91281
47	33,837	1218,19	759,625		P8/P64	=	1,00000
48	33,837	1218,19	752,029	9,374	P16/P6	=	0,91281
49	33,837	1015,13	318,626		A63	=	0,14366 m²
5	34,866	1007,26	318,626	20,730	A163	=	0,26906 m²
64	72,580	708,29	293,295		A64	=	0,41272 m²
8	72,580	708,29	293,295	39,312	A8	=	0,17132 m²
Bleed	0,171	858,02	3263,934		WBld/W2	=	0,00238
-----							
Efficiencies:							
Outer LPC							
Inner LPC							
IP Compressor							
HP Compressor							
Burner							
HP Turbine							
IP Turbine							
LP Turbine							
-----							
HP Spool mech Eff							
IP Spool mech Eff							
LP Spool mech Eff							
-----							
Con-Di Nozzle:							
A9*(Ps9-Pamb)							
-----							
hum [%]	0,0	war0	FHV	Fuel	A9/A8	=	1,07500
		0,00000	43,124	Generic	CFGid	=	0,98572

Figure 31. The results for new dry engine.[GasTurb]

As it can be seen from the figure 31, at sea level stationary conditions, our new dry engine gives these values after the simulation.

Table 18. The new dry engine main thermo-fluid variable.[GasTurb]

Units	St 2	St 21	St 24	St 25	St 3	St 4	St 43	St 45	St 47	St 48	St 5	St 6	St 13	St 16	St 64	St 7	St 8	St 9
Mass Flow	kg/s	72	34,2857	34,2857	34,2857	31,2	28,3512	31,7798	33,1512	33,8369	33,8369	34,8655	34,8655	37,7143	37,7143	72,5798	72,5798	72,5798
Total Temperature	K	288,15	398,794	529,225	529,225	856,022	1745	1364,34	1340,15	1218,19	1218,19	1007,26	1007,26	404,143	404,142	708,291	708,291	708,291
Static Temperature	K	274,407	379,922	505,07	505,07	852,078	1722,94	1314,99	1291,44	1172,89	1172,89	968,037	994,733	385,069	385,069	701,156	700,889	599,188
Total Pressure	kPa	101,325	278,644	668,745	662,058	3263,94	3166,03	1169,24	1157,54	759,625	752,029	318,626	312,254	293,843	285,027	293,295	293,295	293,295
Static Pressure	kPa	85,416	235,024	564,674	559,027	3177,34	2989,21	996,535	986,396	646,849	640,38	270,898	296,576	247,847	240,411	282,107	281,695	156,397
Velocity	m/s	166,055	195,102	224,137	224,137	114,87	239,264	350,558	347,637	332,127	332,127	303,385	172,08	196,402	196,402	125,462	127,781	485,331
Area	m²	0,398849	0,081544	0,039275	0,039671	0,020908	0,019605	0,034338	0,035839	0,053027	0,053562	0,11788	0,195069	0,085639	0,088288	0,412726	0,405671	0,164463
Mach Number		0,5	0,5	0,5	0,5	0,2	0,3	0,5	0,5	0,5	0,5	0,28	0,5	0,5	0,24	0,244481	1	1,31693
Density	kg/m³	1,08439	2,15506	3,89482	3,85584	12,9905	6,04413	2,64008	2,66087	1,92126	1,90207	0,974904	1,03867	2,42226	2,17499	1,40166	1,40015	0,909303
Spec Heat @ T	J/(kg*K)	1004,52	1013,4	1035,78	1035,78	1111,58	1297,12	1247,41	1241,87	1222,45	1222,45	1181,88	1181,88	1014,16	1014,16	1092,39	1092,39	1092,39
Spec Heat @ Ts	J/(kg*K)	1004,19	1011,75	1030,59	1030,59	1110,26	1295,11	1240,51	1234,95	1214,78	1214,78	1173,28	1179,24	1012,2	1012,2	1090,61	1090,55	1065,02
Enthalpy @ T	J/kg	-1002,3	104489	235194	235194	588176	1,7066466	1,2154461	1,1836566	1,0325766	1,0325766	777913	777913	106935	106935	429255	429255	429255
Enthalpy @ Ts	J/kg	-23819,4	82456,7	210075	210075	581579	1,6780266	1,15461	1,1232366	977412	977412	731891	731891	87648,1	87648,1	421385	421091	311482
Entropy Function @ T		-0,11924	1,02129	2,03117	2,03117	3,83265	6,99805	5,88134	5,79614	5,3831	5,3831	4,58214	4,58214	1,06854	1,06854	3,13732	3,13732	3,13732
Entropy Function @ Ts		-0,29004	0,851042	1,86202	1,86202	3,80575	6,94058	5,72152	5,63814	5,22239	5,22239	4,41987	4,53063	0,898305	0,898303	3,09843	3,09867	2,50854
Exergy	J/kg	4,6855E-3	100857	223444	222613	558545	1,4126866	931453	905878	754112	753281	493847	492176	106788	104269	257840	257840	257840
Gas Constant	J/(kg*K)	287,05	287,05	287,05	287,05	287,05	287,046	287,046	287,046	287,046	287,046	287,047	287,047	287,047	287,047	287,049	287,049	287,049
Fuel-Air-Ratio		0	0	0	0	0	0,027219	0,024211	0,023186	0,022706	0,022706	0,022021	0,022021	0	0	0,010459	0,010459	0,010459
Water-Air-Ratio		0	0	0	0	0	0	0	0	0	0	0	0	0	0	0	0	0
Inner Radius	m	0,112195	0,166709	0,150038	0,149831	0,153587	0,154828	0,154828	0,154828	0,147086	0,147086	0	0,236836	0,254184	0	0	0	0
Outer Radius	m	0,373983	0,231836	0,186948	0,187289	0,175056	0,173816	0,18682	0,188094	0,202115	0,202537	0,243222	0,249184	0,284619	0,304487	0,362456	0	0,23352
Axial Position	m	0,186992	0,186992	0,101605	1,07607	1,32989	1,46507	1,52836	1,55933	1,61477	1,69219	1,85122	2,1674	0,763424	2,1674	2,47189	0	2,72561

At every part of the new dry engine main thermo-fluid variable can be seen using the table 18.

Using the formula 33, when  $\dot{m}_e = 72 \text{ kg/s}$ ,  $u_e = 166.055 \text{ m/s}$ ,  $\dot{m}_o = 75.5798 \text{ kg/s}$ ,  $u_o = 606.3224 \text{ m/s}$ ,  $\dot{m}_f = 0.75123 \text{ kg/s}$  and  $h = 43.124 \text{ MJ/kg}$  the thermal efficiency can be found as 38.117% for the FireFly Jetx wet engine.

## Geometrical Comparison:

Table 19. The geometrical values of the overall engines.[GasTurb]

		Front LP Shaft Cone Length	m	0,01603			Front LP Shaft Cone Length	m	0,01543		
		Middle LP Shaft Length	m	1,25068			Middle LP Shaft Length	m	1,1263		
		Middle LP Shaft Radius	m	0,01789			Middle LP Shaft Radius	m	0,01848		
		Front IP Shaft Cone Length	m	0,00502			Front IP Shaft Cone Length	m	0,00503		
		Middle IP Shaft Length	m	0,34329			Middle IP Shaft Length	m	0,30760		
LP Shaft Thickness	m	0,005	Middle IP Shaft Radius	m	0,02789	LP Shaft Thickness	m	0,005	Middle IP Shaft Radius	m	0,02848
IP Shaft Thickness	m	0,005	Rear LP Shaft Cone Length	m	0,05325	IP Shaft Thickness	m	0,005	Rear LP Shaft Cone Length	m	0,04432
HP Shaft Thickness	m	0,005	Front HP Shaft Cone Length	m	0	HP Shaft Thickness	m	0,005	Front HP Shaft Cone Length	m	0
Shaft Material Density	kg/m³	8000	Rear HP Shaft Cone Length	m	0,13334	Shaft Material Density	kg/m³	8000	Rear HP Shaft Cone Length	m	0,11774
LP Spool Design Spd Incr [°]	0		Rear HP Shaft Length	m	0,10472	LP Spool Design Spd Incr [°]	0		Rear HP Shaft Length	m	0,08994
IP Spool Design Spd Incr [°]	0		Rear HP Shaft Radius	m	0,04073	IP Spool Design Spd Incr [°]	0		Rear HP Shaft Radius	m	0,03601
HP Spool Design Spd Incr [°]	0		Engine Length	m	4,21233	HP Spool Design Spd Incr [°]	0		Engine Length	m	4,58666
Net Mass Factor		1,3	Max Engine Diameter	m	0,81803	Net Mass Factor		1,3	Max Engine Diameter	m	0,81552
Net Mass Adder	kg	0	LP Shaft Mass	kg	6,36828	Net Mass Adder	kg	0	LP Shaft Mass	kg	5,82039
			IP Shaft Mass	kg	2,7205				IP Shaft Mass	kg	2,42971
			HP Shaft Mass	kg	4,89012				HP Shaft Mass	kg	3,79202
			Net Mass	kg	803,061				Net Mass	kg	764,611
			Total Mass	kg	1043,98				Total Mass	kg	993,994
			LP Spool Inertia	kg*m²	6,36814				LP Spool Inertia	kg*m²	5,73657
			IP Spool Inertia	kg*m²	0,99632				IP Spool Inertia	kg*m²	0,74290
			HP Spool Inertia	kg*m²	0,73728				HP Spool Inertia	kg*m²	0,39456

## Baseline Engine

FireFly Jetx Engine

The table 19 shows the geometrical values of the overall engines. It can be seen that total mass of the FireFly Jetx engine is 993.994 kg while baseline engine has 1043.98 kg mass.

Table 20. The geometrical variables of the inlet part of the engines.[GasTurb]

Number of Struts	8	Number of Struts	8
Strut Chord/Height	0	Strut Chord/Height	0
Gap Width/Height	0,2	Gap Width/Height	0,2
Cone Length/Radius	0,5	Cone Length	m 0,05609
Cone Angle [deg]	35	Cone Mass	kg 1,22108
Casing Length/Radius	0,5	Casing Mass	kg 8,78789
Casing Thickness	m 0,005	Strut Mass	kg 0
Casing Material Density	kg/m <sup>3</sup> 4000	Total Mass	kg 10,009
Inlet Mass Factor	1	Inlet Mass Factor	1

## Baseline Engine

FireFly Jetx Engine

The table 20 shows the geometrical variables of the inlet part of the engines. For the FireFly Jetx engine, these variables are without supersonic intake. Also, for more information can be checked the intake part of this project.

Table 21. The geometrical parameters of the fan part of the engines.[GasTurb]

Number of Stages	3
Inlet Guide Vanes (IGV)	0
IGV Profile Thickness [%]	5
IGV Material Density	kg/m <sup>3</sup> 4000
Annulus Shape Descriptor	0,3
Inlet Radius Ratio	0,3
Core Aspect Ratio Span/Ch	2,5
Inner Vane Aspect Ratio	2,5
Bypass Vane Aspect Ratio	2,5
Core Vane Gap/Chord Ratik	0,2
Bypass Gap/Chord Ratio	1,2
Rotor Pitch/Chord Ratio	0,5
Core Vane Pitch/Chord Rat	0,5
Core Exit Vane Gap/Chord	0,2
Core Exit Duct Radius Ratik	1
Bypass Vane Pitch/Chord R	0,5
Bypass Vane Lean Angle	5
Bypass Inner/Splitter Radiu	1,06
Disk Bore / Inner Inlet Radi	0,3
Rel Thickness Inner Air Seal	0,04
Casing Thickness	m 0,005
Casing Material Density	kg/m <sup>3</sup> 4000
Containment Ring Thicknes	5
Containment Ring Mat Den	kg/m <sup>3</sup> 800
Mean Bypass Vane Thickne	5
Byp Vane Material Density	kg/m <sup>3</sup> 4000
LP Compressor Mass Facto	1
Length	m 0,59260
Number of Inlet Guide Vane	0
Number of Bypass Stream	0
Number of Core Stream Va	0
Total Number of Blade and	230
Outer Casing Mass	kg 23,3027
Containment Ring Mass	kg 3,52526
Splitter Mass	kg 0
Bypass Vane Mass	kg 62,7124
Vane Mass	kg 99,669
Blade Mass	kg 11,5569
Inner Air Seal Mass	kg 153,747
Rotating Mass	kg 0
IGV Mass	kg 243,437
Total Mass	kg 5,22344
Polar Moment of Inertia	kg*m <sup>2</sup> 4,9879
Number of Stages	3
Inlet Guide Vanes (IGV)	0
IGV Profile Thickness [%]	5
IGV Material Density	kg/m <sup>3</sup> 4000
Annulus Shape Descriptor	0,3
Inlet Radius Ratio	0,3
Core Aspect Ratio Span/Ch	2,5
Inner Vane Aspect Ratio	2,5
Bypass Vane Aspect Ratio	2,5
Core Vane Gap/Chord Ratik	0,2
Bypass Gap/Chord Ratio	1,2
Rotor Pitch/Chord Ratio	0,5
Core Vane Pitch/Chord Rat	0,5
Core Exit Vane Gap/Chord	0,2
Core Exit Duct Radius Ratik	1
Bypass Vane Pitch/Chord R	0,5
Bypass Vane Lean Angle	5
Bypass Inner/Splitter Radu	1,06
Disk Bore / Inner Inlet Radi	0,3
Rel Thickness Inner Air Seal	0,04
Casing Thickness	m 0,005
Casing Material Density	kg/m <sup>3</sup> 4000
Containment Ring Thicknes	5
Containment Ring Mat Den	kg/m <sup>3</sup> 800
Mean Bypass Vane Thickne	5
Byp Vane Material Density	kg/m <sup>3</sup> 4000
LP Compressor Mass Facto	1
Length	m 0,57643
Number of Inlet Guide Vane	0
Number of Bypass Stream	0
Number of Core Stream Va	0
Total Number of Blade and	240
Outer Casing Mass	kg 22,5991
Containment Ring Mass	kg 3,50334
Splitter Mass	kg 0
Bypass Vane Mass	kg 0
Vane Mass	kg 58,6636
Blade Mass	kg 94,7031
Inner Air Seal Mass	kg 11,3731
Rotating Mass	kg 147,827
IGV Mass	kg 0
Total Mass	kg 232,74
Polar Moment of Inertia	kg*m <sup>2</sup> 4,9879

## Baseline Engine

**FireFly Jetx Engine**

From the table 21, the geometrical parameters of the fan part of the engines can be seen.

Table 22. The geometrical dimensions of the IPC part of the engines.[GasTurb]

Number of Stages	3	Number of Stages	3
Number of Variable Guide V	1	Number of Variable Guide V	1
Inlet Guide Vanes (IGV) 0,	1	Inlet Guide Vanes (IGV) 0,	1
IGV Profile Thickness [%]	5	IGV Profile Thickness [%]	5
IGV Material Density kg/m³	4000	IGV Material Density kg/m³	4000
Annulus Shape Descr -0..5..	-0,1	Annulus Shape Descr -0..5..	-0,1
Annulus Shape Descr -0..5..	-0,1	Annulus Shape Descr -0..5..	-0,1
Blade and Vane Sweep	0	Blade and Vane Sweep	0
First Stage Aspect Ratio	1,5	Length	m 0,28918
Last Stage Aspect Ratio	2	Total Number of Blade and	483
Blade Gapping: Gap/Chord	0,1	Casing Mass	kg 7,88514
Pitch/Chord Ratio	0,5	Total Vane Mass	kg 10,3458
Disk Bore / Inner Inlet Radii	0,2	Total Blade Mass	kg 11,2559
Rel Thickness Inner Air Seal	0,04	Inner Air Seal Mass	kg 1,97457
IP Compressor Mass Factor	1	Rotating Mass	kg 33,1588
Casing Thickness m	0,005	Total Mass	kg 53,1228
Casing Material Density kg/m³	4000	Polar Moment of Inertia	kg*m² 0,71708
Casing Thermal Exp Coeff E-6/K	10		
Casing Specific Heat J/(kg*K)	500		
Casing Time Constant	10		
Blade and Vane Time Const	0,5		
Platform Time Constant	1		
Design Tip Clearance [%]	1,5		
d Flow / d Tip Clear.	2		
d Eff / d Tip Clear.	2		
d Surge Margin / d Tip Clea	5		

Baseline Engine

Number of Stages	3	Number of Stages	3
Number of Variable Guide V	1	Number of Variable Guide V	1
Inlet Guide Vanes (IGV) 0,	1	Inlet Guide Vanes (IGV) 0,	1
IGV Profile Thickness [%]	5	IGV Profile Thickness [%]	5
IGV Material Density kg/m³	4000	IGV Material Density kg/m³	4000
Annulus Shape Descr -0..5..	-0,1	Annulus Shape Descr -0..5..	-0,1
Annulus Shape Descr -0..5..	-0,1	Annulus Shape Descr -0..5..	-0,1
Blade and Vane Sweep	0	Blade and Vane Sweep	0
First Stage Aspect Ratio	1,5	Length	m 0,25262
Last Stage Aspect Ratio	2	Total Number of Blade and	562
Blade Gapping: Gap/Chord	0,1	Casing Mass	kg 6,75148
Pitch/Chord Ratio	0,5	Total Vane Mass	kg 7,66216
Disk Bore / Inner Inlet Radii	0,2	Total Blade Mass	kg 8,53021
Rel Thickness Inner Air Seal	0,04	Inner Air Seal Mass	kg 1,52866
IP Compressor Mass Factor	1	Rotating Mass	kg 27,7064
Casing Thickness m	0,005	Total Mass	kg 43,5442
Casing Material Density kg/m³	4000	Polar Moment of Inertia	kg*m² 0,58666
Casing Thermal Exp Coeff E-6/K	10		
Casing Specific Heat J/(kg*K)	500		
Casing Time Constant	10		
Blade and Vane Time Const	0,5		
Platform Time Constant	1		
Design Tip Clearance [%]	1,5		
d Flow / d Tip Clear.	2		
d Eff / d Tip Clear.	2		
d Surge Margin / d Tip Clea	5		

FireFly Jetx Engine

The table 22 variables represent the geometrical dimensions of the intermediate-pressure compressor part of the engines.

Table 23. The parameters of the innerduct part between the LPC and HPC parts.[GasTurb]

Number of Struts	8	Number of Struts	8
Length/Inlet Inner Radius	0,4	Length/Inlet Inner Radius	0,4
Inner Annulus Slope@Exit [	0	Inner Annulus Slope@Exit [	0
Relative Strut Length [%]	60	Relative Strut Length [%]	60
Casing Thickness m	0,005	Casing Thickness m	0,005
Casing Material Density kg/m³	8000	Casing Material Density kg/m³	8000
Compr Interduct Mass Fact	1	Compr Interduct Mass Fact	1

Baseline Engine

Length/Inlet Inner Radius	0,4	Length	m 0,06001
Inner Annulus Slope@Exit [	0	Outer Casing Mass	kg 2,82367
Relative Strut Length [%]	60	Strut Mass	kg 0,85888
Casing Thickness m	0,005	Inner Casing Mass	kg 2,26154
Casing Material Density kg/m³	8000	Total Mass	kg 5,9441

FireFly Jetx Engine

The table 23 shows the geometrical parameters of the innerduct part of the engines between the LPC and HPC.

Table 24. The geometrical parameters for the HPC part of the engines.[GasTurb]

Number of Stages	6	Number of Stages	6
Number of Radial Stages	0	Number of Radial Stages	0
Number of Variable Guide V	1	Number of Variable Guide V	1
Inlet Guide Vanes (IGV) 0,	1	Inlet Guide Vanes (IGV) 0,	1
IGV Profile Thickness [%]	5	IGV Profile Thickness [%]	5
IGV Material Density kg/m³	4000	IGV Material Density kg/m³	4000
Annulus Shape Descriptor (	0,3	Annulus Shape Descriptor (	0,3
Given Radius Rat: In/Exit 0	0	Given Radius Rat: In/Exit 0	0
Inlet Radius Ratio	0,243	Inlet Radius Ratio	0,243
Exit Radius Ratio	0,9	Exit Radius Ratio	0,9
Blade and Vane Sweep	0	Blade and Vane Sweep	0
First Stage Aspect Ratio	1,5	Length (w/o Diffusor)	m 0,25562
Last Stage Aspect Ratio	2	Number of Inlet Guide Vane	85
Blade Gapping: Gap/Chord	0,1	Total Number of Blade and	2143
Pitch/Chord Ratio	0,5	Diffusor Length	m 0,03353
Disk Bore / Inner Inlet Radii	0,25	Casing Mass	kg 6,54713
Diffuser Area Ratio	1,5	Outer Casing Mass	kg 5,40239
Rel Thickness Inner Air Seal	0,04	Total Vane Mass	kg 4,15893
Compressor Mass Factor	1	Total Blade Mass	kg 5,07378
Outer Casing Thickness m	0,005	Inner Air Seal Mass	kg 1,02355
Outer Casing Material Densi kg/m³	4000	Rotating Mass	kg 25,3799
Casing Thickness m	0,005	IGV Mass	kg 0,57751
Casing Material Density kg/m³	4000	Exit Diffusor Mass	kg 1,58125
Rel Work of Radial End Sta	0,3	Total Mass	kg 43,6472
Duct Inner Radius Ratio	1	Polar Moment of Inertia	kg*m² 0,51850
Duct Length/Inlet Inner Ra	0		
Number of Duct Struts	8		
Relative Duct Strut Length	60		
Rad Diffusor/Rotor Blade L	0,5		
Rotor Inlet Swirl Angle	0		
Rotor Blade Backsweep Ang	20		
Diffusor Wall Thickness m	0,0025		
Casing Thermal Exp Coeff E-6/K	10		
Casing Specific Heat J/(kg*K)	500		
Casing Time Constant	10		

Baseline Engine

Number of Stages	6	Number of Stages	6
Number of Radial Stages	0	Number of Radial Stages	0
Number of Variable Guide V	1	Number of Variable Guide V	1
Inlet Guide Vanes (IGV) 0,	1	Inlet Guide Vanes (IGV) 0,	1
IGV Profile Thickness [%]	5	IGV Profile Thickness [%]	5
IGV Material Density kg/m³	4000	IGV Material Density kg/m³	4000
Annulus Shape Descriptor (	0,3	Annulus Shape Descriptor (	0,3
Given Radius Rat: In/Exit 0	0	Given Radius Rat: In/Exit 0	0
Inlet Radius Ratio	0,243	Inlet Radius Ratio	0,243
Exit Radius Ratio	0,9	Exit Radius Ratio	0,9
Blade and Vane Sweep	0	Blade and Vane Sweep	0
First Stage Aspect Ratio	1,5	Length (w/o Diffusor)	m 0,22468
Last Stage Aspect Ratio	2	Number of Inlet Guide Vane	85
Blade Gapping: Gap/Chord	0,1	Total Number of Blade and	2162
Pitch/Chord Ratio	0,5	Diffusor Length	m 0,02914
Disk Bore / Inner Inlet Radii	0,25	Casing Mass	kg 5,07728
Diffuser Area Ratio	1,5	Outer Casing Mass	kg 4,1796
Rel Thickness Inner Air Seal	0,04	Total Vane Mass	kg 4,15869
Compressor Mass Factor	1	Total Blade Mass	kg 3,45901
Outer Casing Thickness m	0,005	Inner Air Seal Mass	kg 0,69929
Outer Casing Material Densi kg/m³	4000	Rotating Mass	kg 17,9417
Casing Thickness m	0,005	IGV Mass	kg 0,39709
Casing Material Density kg/m³	4000	Exit Diffusor Mass	kg 1,21255
Rel Work of Radial End Sta	0,3	Total Mass	kg 31,6439
Duct Inner Radius Ratio	1	Polar Moment of Inertia	kg*m² 0,27799
Duct Length/Inlet Inner Ra	0		
Number of Duct Struts	8		
Relative Duct Strut Length	60		
Rad Diffusor/Rotor Blade L	0,5		
Rotor Inlet Swirl Angle	0		
Rotor Blade Backsweep Ang	20		
Diffusor Wall Thickness m	0,0025		
Casing Thermal Exp Coeff E-6/K	10		
Casing Specific Heat J/(kg*K)	500		
Casing Time Constant	10		

FireFly Jetx Engine

From the table 24, the geometrical parameters are owned by the high-pressure compressor part of the engines.

Table 25. The geometrical variables of the combustion part of the engines.[GasTurb]

Reverse Flow Design (0/1)	0	Reverse Flow Design (0/1)	0
Outer Casing Length/Lengt	2	Outer Casing Length/Lengt	2
Exit/Inlet Radius	1	Mean Radius, Exit	m [0,18622]
Length/Inlet Radius	1	Length	m 0,18622
Can Width/Can Length	0,4	Can Volume	m³ 0,00712
Inner Casing Thickness	m 0,002	Can Mass	kg 14,1392
Outer Casing Thickness	m 0,005	Can Surface Area / Mass	m²/kg 0,05
Casing Material Density	kg/m³ 8000	Fuel Injector Mass	kg 1,33748
Can Wall Thickness	m 0,005	Inner Casing Mass	kg 3,16153
Can Material Density	kg/m³ 8000	Outer Casing Mass	kg 10,7192
Can Thermal Exp Coeff	E-6/K 10	Total Mass	kg 29,3574
Can Specific Heat	J/(kg*K) 500	Can Heat Soakage	kW 0
Can Time Constant	1		
Mass of Fuel Inj. / Fuel Flow	2		
Burner Mass Factor	1		

Baseline Engine

Reverse Flow Design (0/1)	0	Reverse Flow Design (0/1)	0
Outer Casing Length/Lengt	2	Outer Casing Length/Lengt	2
Exit/Inlet Radius	1	Mean Radius, Exit	m [0,16432]
Length/Inlet Radius	1	Length	m 0,16432
Can Width/Can Length	0,4	Can Volume	m³ 0,00491
Inner Casing Thickness	m 0,002	Can Mass	kg 11,0484
Outer Casing Thickness	m 0,005	Can Surface Area / Mass	m²/kg 0,05
Casing Material Density	kg/m³ 8000	Fuel Injector Mass	kg 1,50247
Can Wall Thickness	m 0,005	Inner Casing Mass	kg 2,46425
Can Material Density	kg/m³ 8000	Outer Casing Mass	kg 8,35918
Can Thermal Exp Coeff	E-6/K 10	Total Mass	kg 23,3743
Can Specific Heat	J/(kg*K) 500	Can Heat Soakage	kW 0
Can Time Constant	1		
Mass of Fuel Inj. / Fuel Flow	2		
Burner Mass Factor	1		

FireFly Jetx Engine

The geometrical variables of the combustion part of the engines can be seen from the table 25.

Table 26. The geometrical values of the HPT part of the engines.[GasTurb]

Number of Stages = 1	no input	Number of Stages = 1	no input
Unshrouded/Shrouded Blad	0	Unshrouded/Shrouded Blad	0
Inner Radius: R_exit / R,inle	1	Inner Radius: R_exit / R,inle	1
Inner Annulus Slope@Inlet[	-30	Inner Annulus Slope@Inlet[	-30
Inner Annulus Slope@Exit [	0	Inner Annulus Slope@Exit [	0
First Stage Aspect Ratio	0,75	First Stage Aspect Ratio	0,75
Last Stage Aspect Ratio	1,5	Last Stage Aspect Ratio	1,5
Blade Gapping: Gap/Chord	0,25	Blade Gapping: Gap/Chord	0,25
Pitch/Chord Ratio	0,8	Pitch/Chord Ratio	0,8
Disk Bore / Inner Inlet Radi	0,23	Disk Bore / Inner Inlet Radi	0,23
Rel Thickness Inner Air Seal	0,04	Rel Thickness Inner Air Seal	0,04
HP Turbine Mass Factor	1	Total Vane Mass	kg 0,92355
Outer Casing Thickness	m 0,005	Total Blade Mass	kg 3,12658
Outer Casing Material Dens	kg/m³ 8000	Inner Air Seal Mass	kg 0
Casing Thickness	m 0,005	Rotating Mass	kg 10,9355
Casing Cooling Effectiveness	0,5	Total Mass	kg 20,1151
Casing Material Density	kg/m³ 8000	Polar Moment of Inertia	kg*m² 0,21877
Casing Thermal Exp Coeff	E-6/K 10		
Casing Specific Heat	J/(kg*K) 500		
Casing Time Constant	20		
Blade and Vane Time Const	2		
Platform Time Constant	5		
Design Tip Clearance [%]	1,5		
d Eff / d Tip Clear.	2		

Baseline Engine

Number of Stages = 1	no input	Number of Stages = 1	no input
Unshrouded/Shrouded Blad	0	Unshrouded/Shrouded Blad	0
Inner Radius: R_exit / R,inle	1	Inner Radius: R_exit / R,inle	1
Inner Annulus Slope@Inlet[	-30	Inner Annulus Slope@Inlet[	-30
Inner Annulus Slope@Exit [	0	Inner Annulus Slope@Exit [	0
First Stage Aspect Ratio	0,75	First Stage Aspect Ratio	0,75
Last Stage Aspect Ratio	1,5	Last Stage Aspect Ratio	1,5
Blade Gapping: Gap/Chord	0,25	Blade Gapping: Gap/Chord	0,25
Pitch/Chord Ratio	0,8	Pitch/Chord Ratio	0,8
Disk Bore / Inner Inlet Radi	0,23	Disk Bore / Inner Inlet Radi	0,23
Rel Thickness Inner Air Seal	0,04	Rel Thickness Inner Air Seal	0,04
HP Turbine Mass Factor	1	Total Vane Mass	kg 0,61746
Outer Casing Thickness	m 0,005	Total Blade Mass	kg 2,12047
Outer Casing Material Dens	kg/m³ 8000	Outer Casing Mass	kg 2,92834
Casing Thickness	m 0,005	Inner Air Seal Mass	kg 0
Casing Cooling Effectiveness	0,5	Rotating Mass	kg 7,69981
Casing Material Density	kg/m³ 8000	Total Mass	kg 14,6631
Casing Thermal Exp Coeff	E-6/K 10	Polar Moment of Inertia	kg*m² 0,11656
Casing Specific Heat	J/(kg*K) 500		
Casing Time Constant	20		
Blade and Vane Time Const	2		
Platform Time Constant	5		
Design Tip Clearance [%]	1,5		
d Eff / d Tip Clear.	2		

FireFly Jetx Engine

The table 26 shows the geometrical values of the high-pressure turbine part of the engines.

Table 27. The parameters of the innerduct part between the HPT and IPT parts.[GasTurb]

Number of Struts	0	Number of Struts	0
Exit/Inlet Inner Radius	1	Exit/Inlet Inner Radius	1
Length/Inlet Inner Radius	0,2	Length/Inlet Inner Radius	0,2
Inner Annulus Slope@Inlet[	0	Inner Annulus Slope@Inlet[	0
Inner Annulus Slope@Exit [	5	Inner Annulus Slope@Exit [	5
Relative Strut Length [%]	0	Relative Strut Length [%]	0
Casing Thickness	m 0,005	Casing Thickness	m 0,005
Casing Material Density	kg/m³ 8000	Casing Material Density	kg/m³ 8000
Turbine Interduct Mass Fac	1	Total Mass	kg 2,66506

Baseline Engine

Number of Struts	0	Number of Struts	0
Exit/Inlet Inner Radius	1	Exit/Inlet Inner Radius	1
Length/Inlet Inner Radius	0,2	Length/Inlet Inner Radius	0,2
Inner Annulus Slope@Inlet[	0	Inner Annulus Slope@Inlet[	0
Inner Annulus Slope@Exit [	5	Inner Annulus Slope@Exit [	5
Relative Strut Length [%]	0	Relative Strut Length [%]	0
Casing Thickness	m 0,005	Casing Thickness	m 0,005
Casing Material Density	kg/m³ 8000	Casing Material Density	kg/m³ 8000
Turbine Interduct Mass Fac	1	Total Mass	kg 1,20495

FireFly Jetx Engine

From the table 27, the geometrical parameters of the innerduct part between the HPT and IPT parts of the engines can be seen.

Table 28. The geometrical parameters for the IPT part of the engines.[GasTurb]

Number of Stages = 1	no input
Unshrouded/Shrouded Bla	1
Inner Radius: R_exit / R,inle	1
Inner Annulus Slope@Inlet[	0
Inner Annulus Slope@Exit [	0
First Stage Aspect Ratio	1,5
Last Stage Aspect Ratio	1,5
Blade Gapping: Gap/Chord	0,25
Pitch/Chord Ratio	0,5
Disk Bore / Inner Inlet Radi	0,3
Rel Thickness Inner Air Seal	0,04
IP Turbine Mass Factor	1
Casing Thickness	m 0,005
Casing Cooling Effectivenes	0,5
Casing Material Density	kg/m³ 8000
Casing Thermal Exp Coeff	E-6/K 10
Casing Specific Heat	J/(kg*K) 500
Casing Time Constant	20
Blade and Vane Time Const	2
Platform Time Constant	5
Design Tip Clearance [%]	1,5
d Eff / d Tip Clear.	2

Baseline Engine

Number of Stages = 1	no input
Unshrouded/Shrouded Bla	1
Inner Radius: R_exit / R,inle	1
Inner Annulus Slope@Inlet[	0
Inner Annulus Slope@Exit [	0
First Stage Aspect Ratio	1,5
Last Stage Aspect Ratio	1,5
Blade Gapping: Gap/Chord	0,25
Pitch/Chord Ratio	0,5
Disk Bore / Inner Inlet Radi	0,3
Rel Thickness Inner Air Seal	0,04
IP Turbine Mass Factor	1
Casing Thickness	m 0,005
Casing Cooling Effectivenes	0,5
Casing Material Density	kg/m³ 8000
Casing Thermal Exp Coeff	E-6/K 10
Casing Specific Heat	J/(kg*K) 500
Casing Time Constant	20
Blade and Vane Time Const	2
Platform Time Constant	5
Design Tip Clearance [%]	1,5
d Eff / d Tip Clear.	2

FireFly Jetx Engine

The table 28 depicts the geometrical parameters for the intermediate-pressure turbine part of the engines.

Table 29. The parameters of the innerduct part between the IPT and LPT parts.[GasTurb]

Number of Struts	8
Exit/Inlet Inner Radius	1
Length/Inlet Inner Radius	0,5
Inner Annulus Slope@Inlet[	0
Inner Annulus Slope@Exit [	-5
Relative Strut Length [%]	60
Casing Thickness	m 0,005
Casing Material Density	kg/m³ 8000
Turbine Interduct Mass Fac	1

Baseline Engine

Number of Struts	8
Exit/Inlet Inner Radius	1
Length/Inlet Inner Radius	0,5
Inner Annulus Slope@Inlet[	0
Inner Annulus Slope@Exit [	-5
Relative Strut Length [%]	60
Casing Thickness	m 0,005
Casing Material Density	kg/m³ 8000
Turbine Interduct Mass Fac	1

FireFly Jetx Engine

The table 29 demonstrates the geometrical parameters for the innerduct part between the IPT and LPT parts of the engines.

Table 30. The geometrical parameters for the LPT part of the engines.[GasTurb]

Number of Stages = 2	no input
Unshrouded/Shrouded Bla	1
Inner Radius: R_exit / R,inle	0,95
Inner Annulus Slope@Inlet[	0
Inner Annulus Slope@Exit [	0
First Stage Aspect Ratio	1,5
Last Stage Aspect Ratio	1,5
Blade Gapping: Gap/Chord	0,25
Pitch/Chord Ratio	0,5
Disk Bore / Inner Inlet Radi	0,4
Rel Thickness Inner Air Seal	0,04
LP Turbine Mass Factor	1
Casing Thickness	m 0,005
Casing Cooling Effectivenes	0,5
Casing Material Density	kg/m³ 8000
Casing Thermal Exp Coeff	E-6/K 10
Casing Specific Heat	J/(kg*K) 500
Casing Time Constant	20
Blade and Vane Time Const	2
Platform Time Constant	5
Design Tip Clearance [%]	1,5
d Eff / d Tip Clear.	2

Baseline Engine

Number of Stages = 2	no input
Unshrouded/Shrouded Bla	1
Inner Radius: R_exit / R,inle	0,95
Inner Annulus Slope@Inlet[	0
Inner Annulus Slope@Exit [	0
First Stage Aspect Ratio	1,5
Last Stage Aspect Ratio	1,5
Blade Gapping: Gap/Chord	0,25
Pitch/Chord Ratio	0,5
Disk Bore / Inner Inlet Radi	0,4
Rel Thickness Inner Air Seal	0,04
LP Turbine Mass Factor	1
Casing Thickness	m 0,005
Casing Cooling Effectivenes	0,5
Casing Material Density	kg/m³ 8000
Casing Thermal Exp Coeff	E-6/K 10
Casing Specific Heat	J/(kg*K) 500
Casing Time Constant	20
Blade and Vane Time Const	2
Platform Time Constant	5
Design Tip Clearance [%]	1,5
d Eff / d Tip Clear.	2

FireFly Jetx Engine

The table 30 illustrates the geometrical parameters for the low-pressure turbine part of the engines.

Table 31. the geometrical variables of the exhaust part after the LPT part.[GasTurb]

Number of Struts	8	Number of Struts	8
Strut Chord/Height	0,5	Strut Chord/Height	0,5
Strut Lean Angle	5	Length	m 0,34315
Gap Width/Height	0,2	Cone Length	m 0,12490
Cone Angle [deg]	15	Outer Casing Mass	kg 21,4534
Cone Length/Inlet Radius	0,75	Strut Mass	kg 3,03771
Casing Length/Inlet Radius	1,3	Cone Mass	kg 2,76292
Bypass Radius/Flange Radii	1	Front Cover Mass	kg 1,25628
Inner Casing Thickness	m 0,002	Total Mass	kg 28,5103
Outer Casing Thickness	m 0,005		
Casing Material Density	kg/m³ 8000		
Exhaust Duct Mass Factor	1		

Baseline Engine

Number of Struts	8	Number of Struts	8
Strut Chord/Height	0,5	Strut Chord/Height	0,5
Strut Lean Angle	5	Length	m 0,31618
Gap Width/Height	0,2	Cone Length	m 0,11031
Cone Angle [deg]	15	Outer Casing Mass	kg 18,3436
Cone Length/Inlet Radius	0,75	Strut Mass	kg 2,95744
Casing Length/Inlet Radius	1,3	Cone Mass	kg 2,22981
Bypass Radius/Flange Radii	1	Front Cover Mass	kg 0,97998
Inner Casing Thickness	m 0,002	Total Mass	kg 24,5108
Outer Casing Thickness	m 0,005		
Casing Material Density	kg/m³ 8000		
Exhaust Duct Mass Factor	1		

FireFly Jetx Engine

The table 31 shows the geometrical variables of the exhaust part after the LPT part of the engines.

Table 32. The geometrical parameters of the bypass part of the engines.[GasTurb]

Number of Struts	8	Number of Struts	8
Flat Point Pos in % of Leng	50	Flat Point Pos in % of Leng	50
Flat Point Radius/Inlet Radi	1,1	Outer Casing Length	m 1,21667
Strut Inlet Pos in % of Len	5	Inner Casing Length	m 1,21667
Relative Strut Length [%]	10	Outer Casing Mass	kg 46,9815
Mean Strut Thickness	m 0,002	Inner Casing Mass	kg 32,0501
Strut Material Density	kg/m³ 4000	Strut Mass	kg 0,40817
Inner Casing Thickness	m 0,004	Total Mass	kg 79,4398
Outer Casing Thickness	m 0,005		
Casing Material Density	kg/m³ 4000		
Bypass Duct Mass Factor	1		

Baseline Engine

Number of Struts	8	Number of Struts	8
Flat Point Pos in % of Leng	50	Flat Point Pos in % of Leng	50
Flat Point Radius/Inlet Radi	1,1	Outer Casing Length	m 1,08779
Strut Inlet Pos in % of Len	5	Inner Casing Length	m 1,08779
Relative Strut Length [%]	10	Outer Casing Mass	kg 40,2709
Mean Strut Thickness	m 0,002	Inner Casing Mass	kg 34,4222
Strut Material Density	kg/m³ 4000	Strut Mass	kg 0,33419
Inner Casing Thickness	m 0,004	Total Mass	kg 75,0273
Outer Casing Thickness	m 0,005		
Casing Material Density	kg/m³ 4000		
Bypass Duct Mass Factor	1		

FireFly Jetx Engine

The table 32 indicates the geometrical parameters of the bypass part of the engines.

Table 33. The geometrical dimensions of mixer part of the engines.[GasTurb]

Length/Diameter	0,5	Length/Diameter	0,5
Number of Chutes	15	Number of Chutes	15
Chute Height [%]	70	Chute Height [%]	70
Chute Thickness	m 0,001	Chute Mass	kg 3,63462
Chute Material Density	kg/m³ 8000	Casing Mass	kg 14,3574
Casing Thickness	m 0,005	Cone Mass	kg 0
Casing Material Density	kg/m³ 4000	Total Mass	kg 17,992
Mixer Mass Factor	1	Mixer Mass Factor	1

Baseline Engine

Length/Diameter	0,5	Length/Diameter	0,5
Number of Chutes	15	Number of Chutes	15
Chute Height [%]	70	Chute Height [%]	70
Chute Thickness	m 0,001	Chute Mass	kg 3,2647
Chute Material Density	kg/m³ 8000	Casing Mass	kg 12,9046
Casing Thickness	m 0,005	Cone Mass	kg 0
Casing Material Density	kg/m³ 4000	Total Mass	kg 16,1693
Mixer Mass Factor	1	Mixer Mass Factor	1

FireFly Jetx Engine

The table 33 shows the geometrical dimensions of mixer part of the engines.

Table 34. The geometrical variables of the afterburner part of the engines.[GasTurb]

Length/Diameter	1,7	Length	m 1,28655
Mass of Fuel Inj. / Fuel Flow	2	Flame Holder Mass	kg 6,57595
Casing Thickness	m 0,005	Fuel Injector Mass	kg 6,94215
Casing Material Density	kg/m³ 4000	Casing Mass	kg 61,1763
Liner Thickness	m 0,003	Liner Mass	kg 69,6443
Liner Material Density	kg/m³ 8000	Total Mass	kg 144,339
Reheat Mass Factor	1		

Baseline Engine

Length/Diameter	1,7	Length	m 1,22177
Mass of Fuel Inj. / Fuel Flow	2	Flame Holder Mass	kg 5,93045
Casing Thickness	m 0,005	Fuel Injector Mass	kg 6,24007
Casing Material Density	kg/m³ 4000	Casing Mass	kg 55,1712
Liner Thickness	m 0,003	Liner Mass	kg 62,808
Liner Material Density	kg/m³ 8000	Total Mass	kg 130,15
Reheat Mass Factor	1		

FireFly Jetx Engine

The table 34 exhibits the geometrical variables of the afterburner part of the engines.

Table 35. The geometrical parameters of the nozzle part of the engines.[GasTurb]

Std/Plug/Power Gen Exh 1	1	Overall Length	m 0,26487
Inl Section Length/Outer R	inactive	Inlet Section Length	m 0
Conv Length/Inl Section R	0,7	Convergent Length	m 0,26487
Cone Angle [deg]	inactive	Divergent Length	m 0
Cone Length/Inlet Radius	inactive	Convergent Cone Angle [d	5,826
Inlet Section Area Ratio	inactive	Divergent Cone Angle [deg	0
Divergent Length/Throat R	inactive	Inlet Section Mass	kg 0
Inner Casing Thickness	m 0,002	Convergent Section Mass	kg 24,4168
Outer Casing Thickness	m 0,005	Divergent Section Mass	kg 0
Casing Material Density	kg/m³ 8000	Inner Casing Mass	kg 0
Nozzle Mass Factor	1	Outer Casing Mass	kg 24,4168
		Total Mass	kg 24,4168

Baseline Engine

Std/Plug/Power Gen Exh 1	1	Overall Length	m 0,89299
Inl Section Length/Outer R	inactive	Inlet Section Length	m 0
Conv Length/Inl Section R	0,7	Convergent Length	m 0,25154
Cone Angle [deg]	inactive	Divergent Length	m 0,64145
Cone Length/Inlet Radius	inactive	Convergent Cone Angle [d	8,72837
Inlet Section Area Ratio	inactive	Divergent Cone Angle [deg	1,05476
Divergent Length/Throat R	1	Inlet Section Mass	kg 0
Inner Casing Thickness	m 0,002	Convergent Section Mass	kg 21,7487
Outer Casing Thickness	m 0,005	Divergent Section Mass	kg 52,6667
Casing Material Density	kg/m³ 8000	Inner Casing Mass	kg 0
Nozzle Mass Factor	1	Outer Casing Mass	kg 74,4154
		Total Mass	kg 74,4154

FireFly Jetx Engine

The table 35 shows the geometrical parameters of the nozzle part of the engines. Detailed analysis of the nozzle part with CFD calculations can be found in the nozzle and the CFD analysis parts of this report (See Appendix B.1).

### Parametric:

The parametric tool is also used during optimization. The graphs below the main design parameters such as BPR, FPR, TET, and OPR were compared for the different ranges. The grey parts represent the net thrust either above 75 kN or below 73 kN, which are out of our goal. The thin and more frequent dashed lines and colors show the TSFC values. Also, the little black square represents our design point.

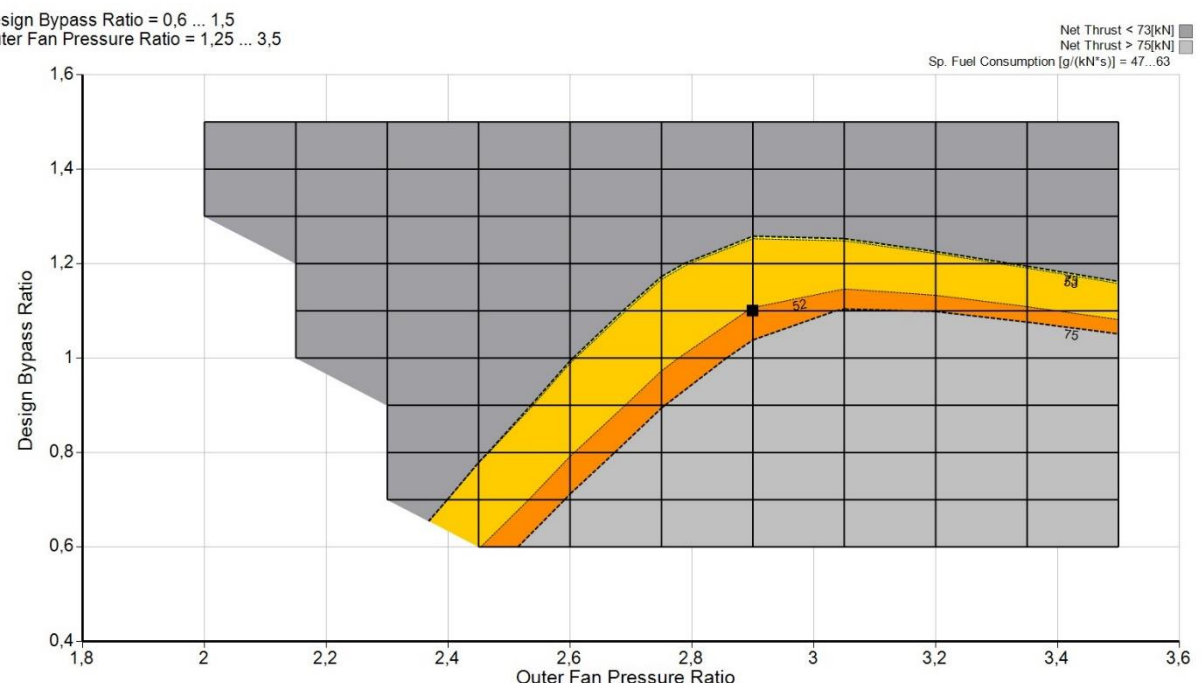


*Figure 32. The relation between design bypass ratio and outer fan pressure ratio.[GasTurb]*

The figure 32 shows the relation between BPR ranges from 0.4 to 1.6 versus outer FPR ranges from 1.8 to 3.6.

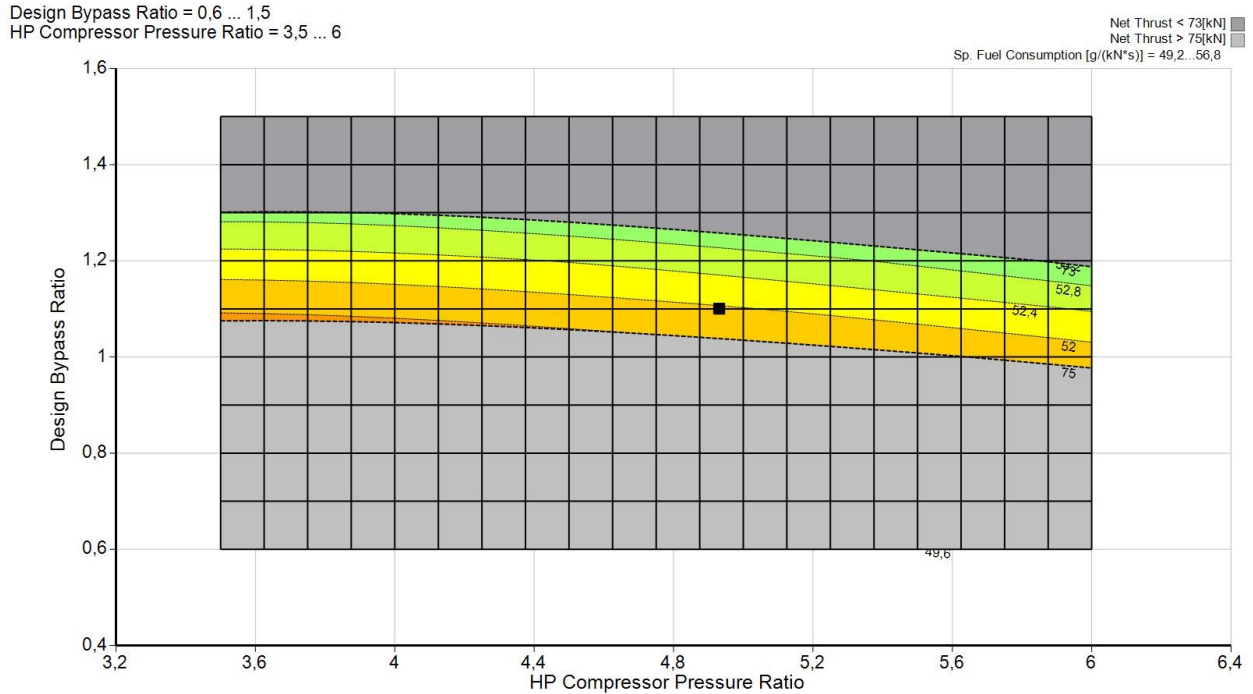


*Figure 33. The relation between design bypass ratio and HP compressor pressure ratio.[GasTurb]*

The figure 33 shows the relation of BPR (range: 0.4-1.6) versus HPCPR (range: 3.2-6.4).

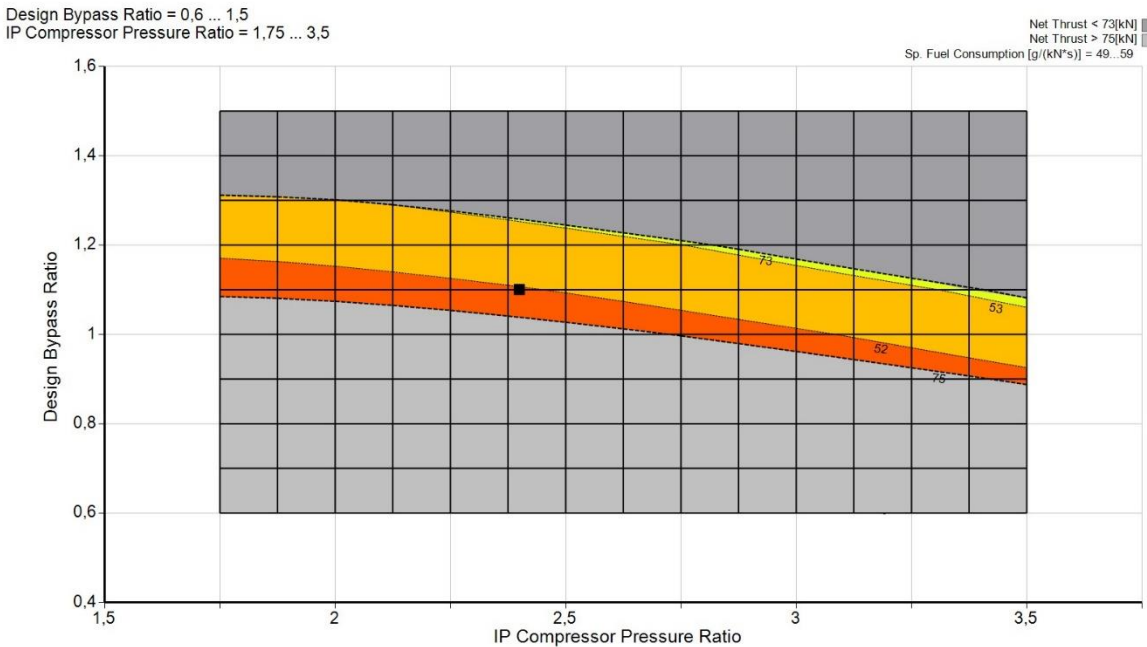


*Figure 34. The relation between design bypass ratio and IP compressor pressure ratio.[GasTurb]*

The figure 34 illustrates the relation between BPR (0.4-1.6) and IPCPR (1.5-3.75).

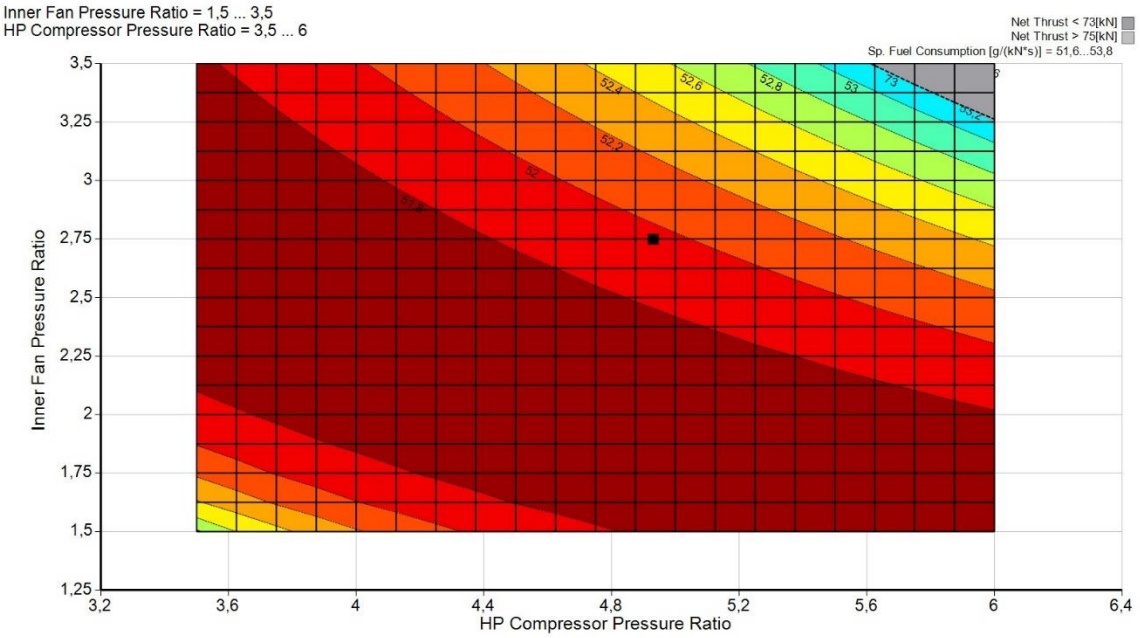


*Figure 35. The relation between inner fan pressure ratio and HP compressor pressure ratio.[GasTurb]*

The figure 35 depicts the relation between inner FPR and HPCPR. The range for the inner FPR is from 1.25 to 3.5, and for the HPCPR, it is from 3.2 to 6.4.

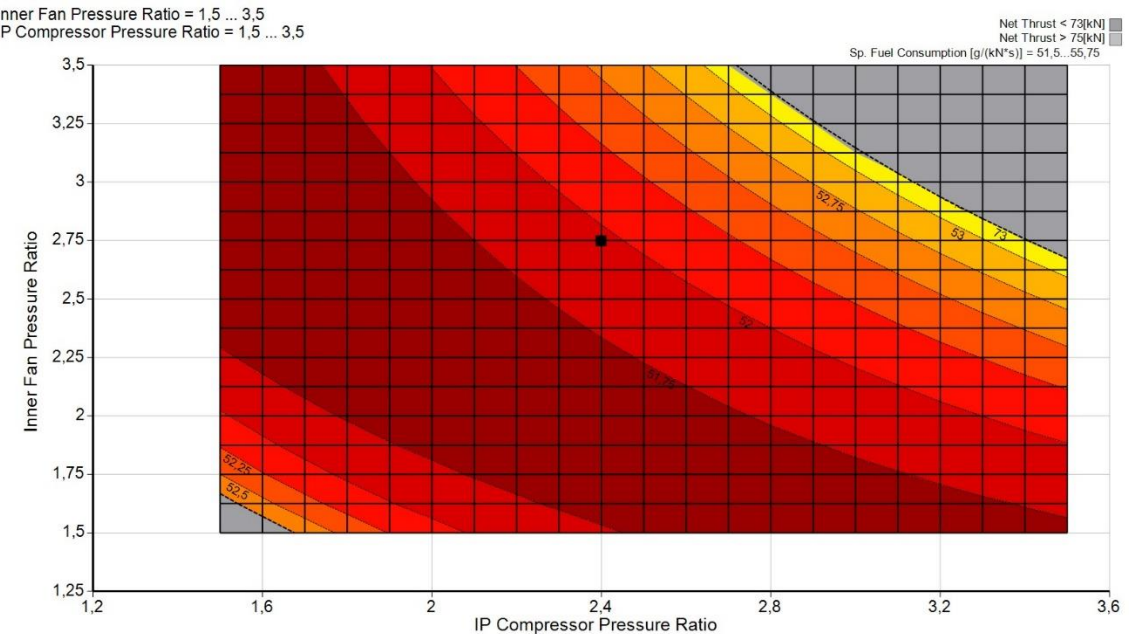


*Figure 36. The relation between inner fan pressure ratio and IP compressor pressure ratio.[GasTurb]*

The figure 36 depicts the relation between the inner FPR (1.25-3.5) and IPCPR (1.2-3.6).

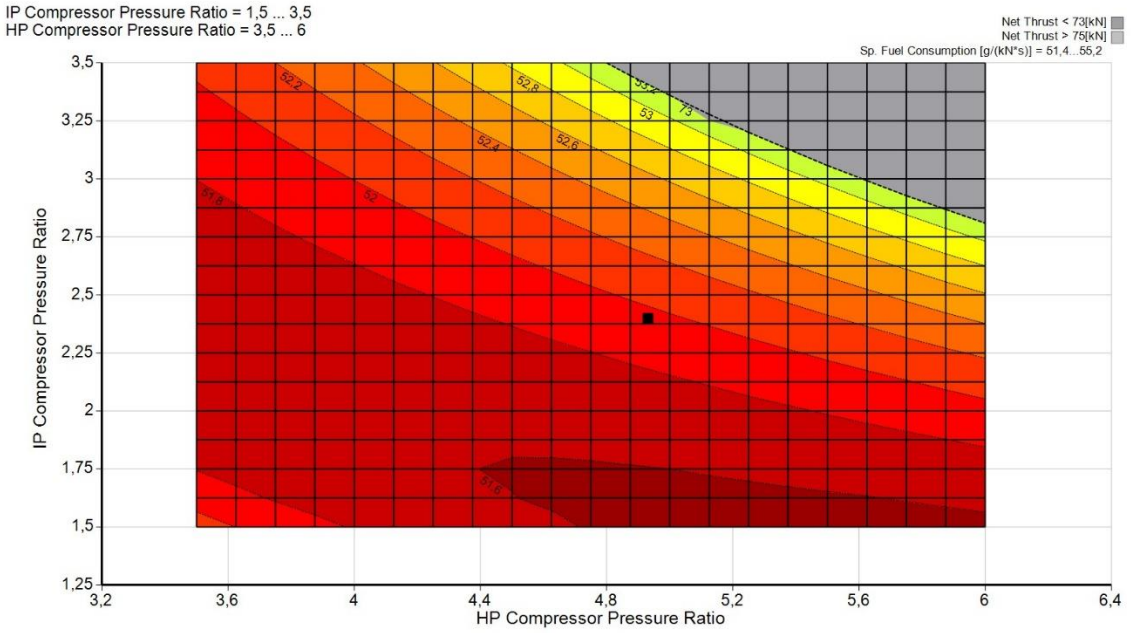


*Figure 37. The relation between IP compressor pressure ratio and HP compressor pressure ratio.[GasTurb]*

The figure 37 exhibits the relation between IPCPR (range: 1.25-3.5) and HPCPR (range: 3.2-6.4).

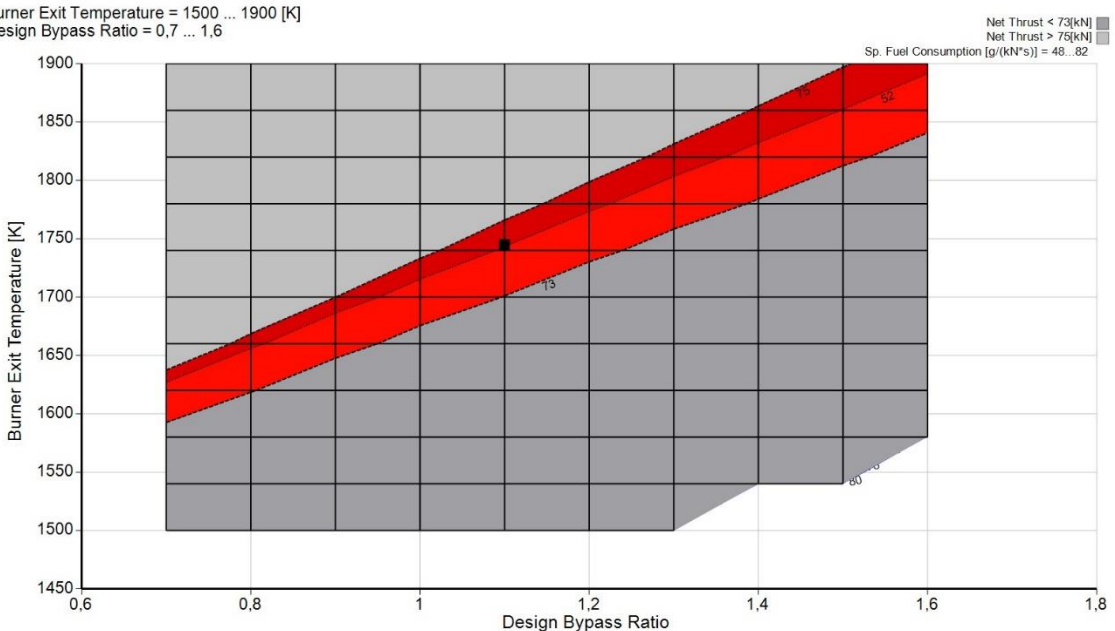


*Figure 38. The relation between burner exit temperature and design bypass ratio.[GasTurb]*

The figure 38 demonstrates the relation between TET (1450-1900) and BPR (0.6-1.8).

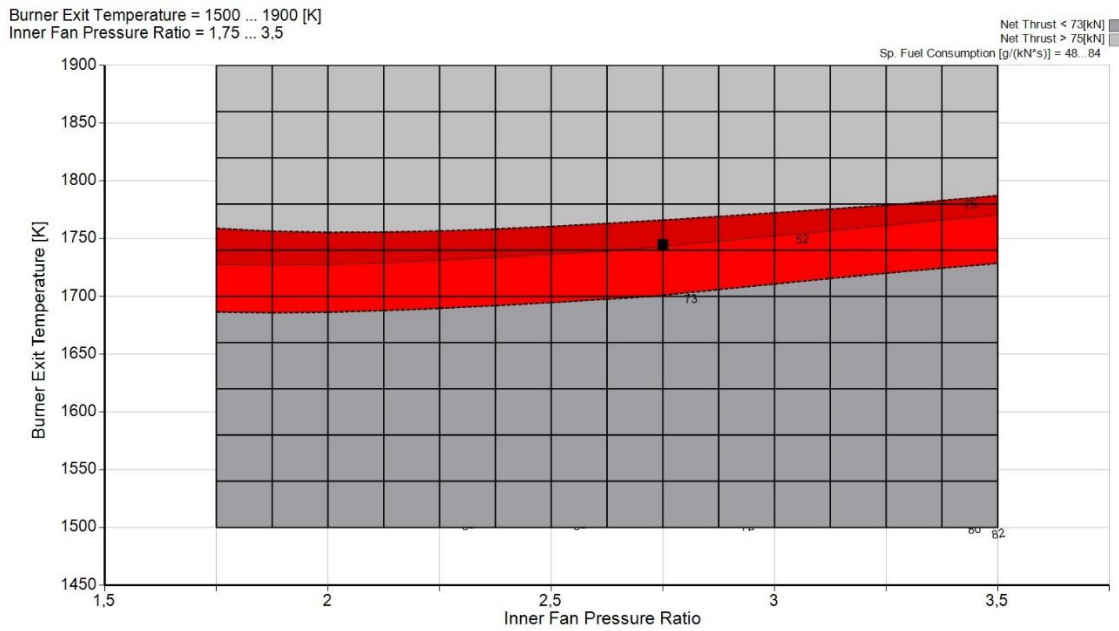


*Figure 39. The relation between burner exit temperature and inner fan pressure ratio.[GasTurb]*

The figure 39 demonstrates the relation between the TET ranges from 1450 to 1900 and inner FPR ranges from 1.5 to 3.75.

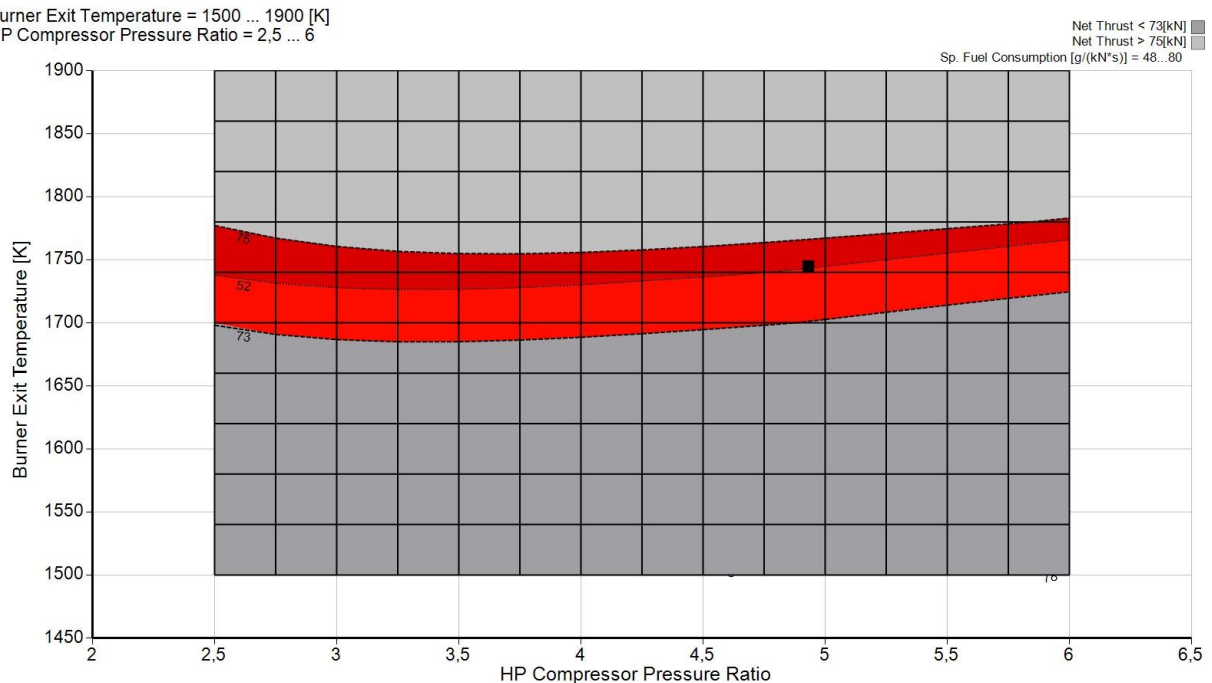


*Figure 40. The relation between burner exit temperature and HP compressor pressure ratio.[GasTurb]*

The figure 40 shows the relation between the TET (range:1450-1900) and HPCPR (range: 2-6.5).

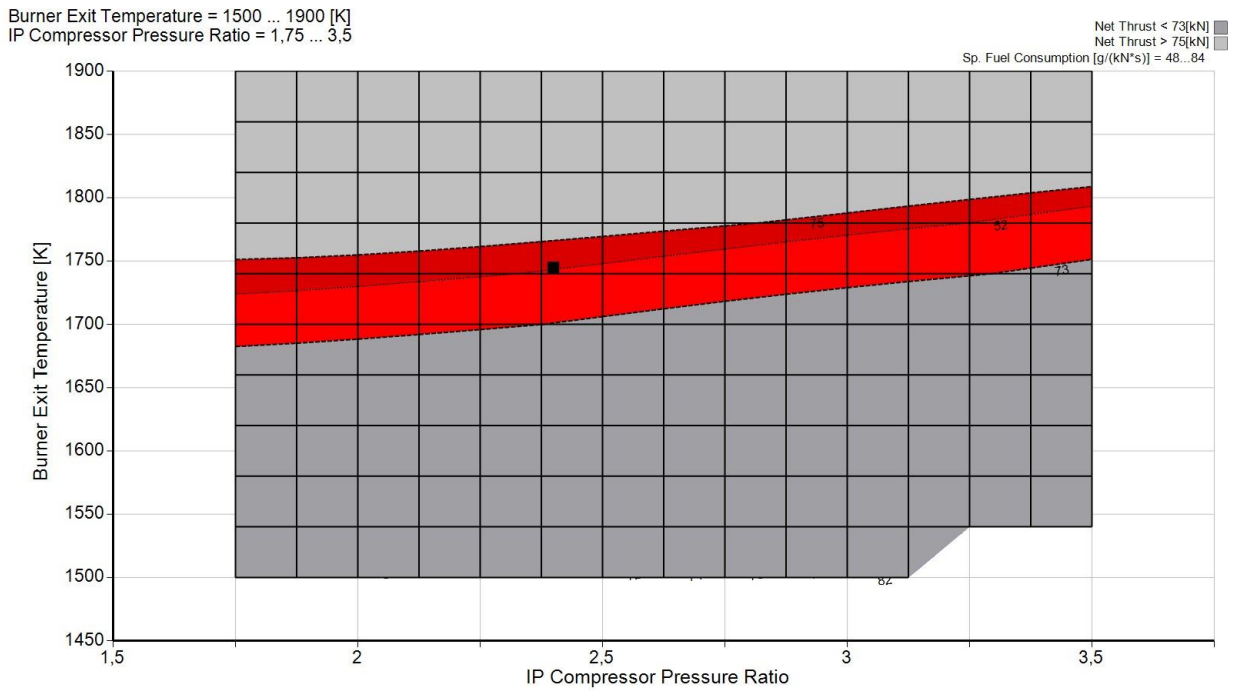


*Figure 41. The relation between burner exit temperature and IP compressor pressure ratio.[GasTurb]*

The figure 41 demonstrates the relation between the TET (1450-1900) and IPCPR (1.5-3.75).

## B) CFD Analysis

### B.1. CFD Analysis for Convergent-Divergent Nozzle

**ANSYS**  
2021 R1  
ACADEMIC

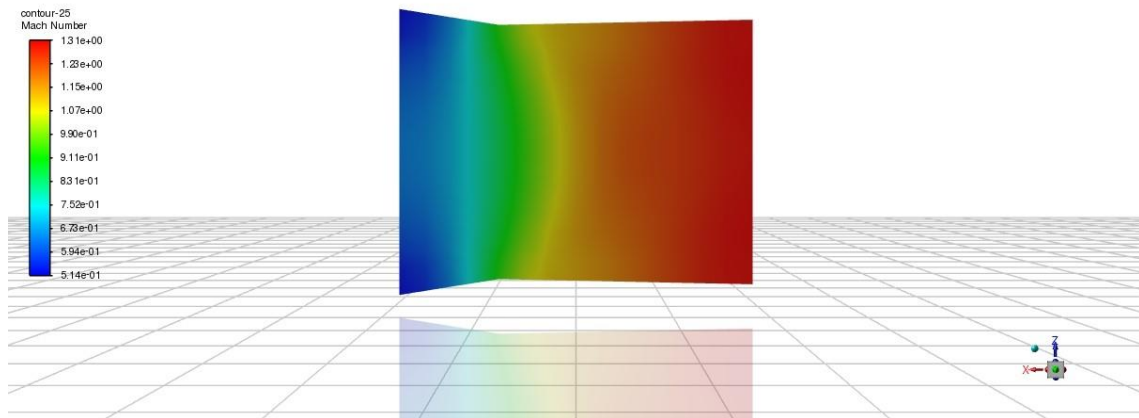


Figure 42. Mach Number for the ConDi Nozzle.[ANSYS]

The Mach value in section 7 that we calculated for our engine is 0.534, and the Mach value in section 9 is 1.306 with afterburner. As it can be seen from the CFD analysis in figure 42, the minimum Mach number is 0.52, and the maximum Mach number is 1.31. As a result, the calculated values are compatible with each other. All calculations are made at sea level and cruise speed.

**ANSYS**  
2021 R1  
ACADEMIC

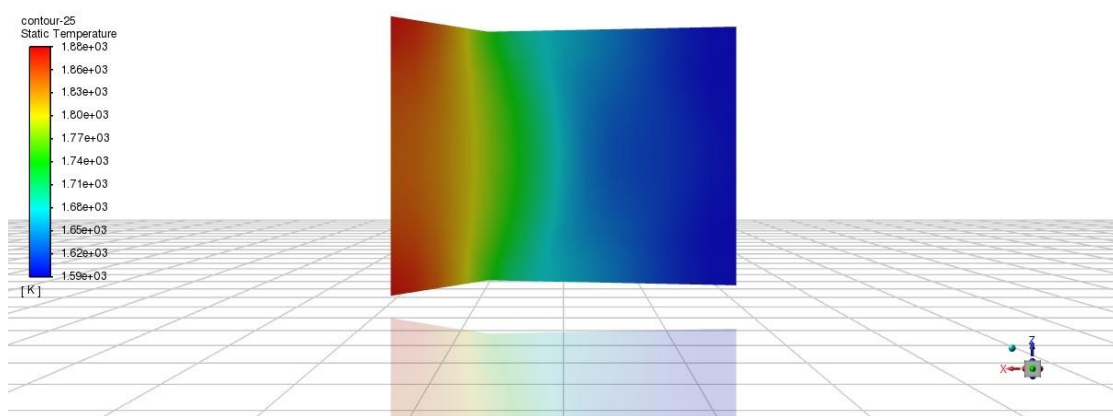


Figure 43. Static temperature for the ConDi Nozzle.[ANSYS]

The values we found with GasTurb 13 in Sections 7, 8, and 9 are respectively 1879.56 K, 1698.14 K and 1565.49 K. As it can be seen from the CFD analysis in figure 43, the maximum static temperature value in section 7 is 1880 K, the static value in section 6 is 1700 K, and finally, the minimum static temperature value in section 9 is 1560 K. With these results, It can be easily understood that the values we found in wet condition and CFD values are consistent.

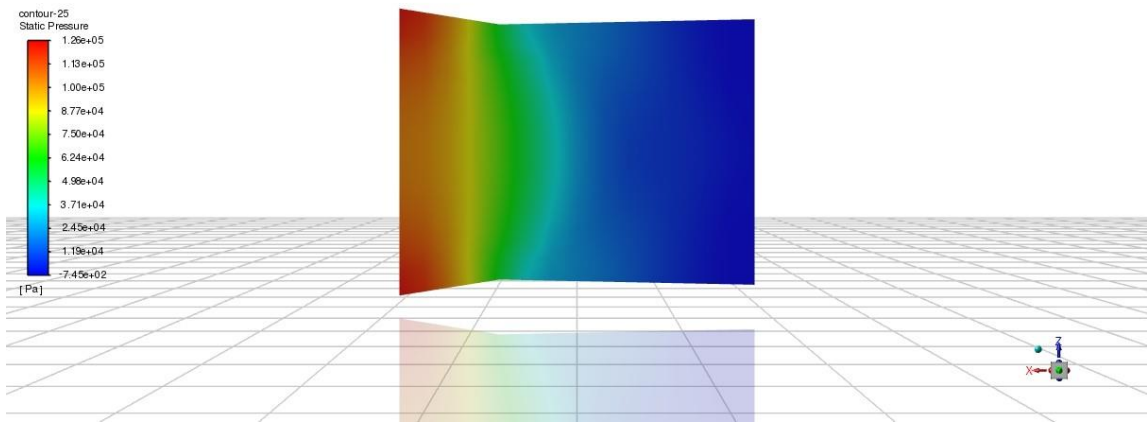


Figure 44. Static pressure for the ConDi Nozzle.[ANSYS]

The static pressure values have been obtained using GasTurb 13. These values are 223.759 kPa for section 7, 147.23 kPa for section 8, and 100.526 kPa for section 9. As seen in the figure 44, our values are minimum -0.745 kPa and maximum 126 kPa. However, we need to add 101.325 kPa to these values because the program which we used to prepare the CFD extracted the gage pressure itself. When we add 101.325 kPa to the values, we found in the CFD analysis, and our new values will be a minimum of 100.58 kPa and a maximum of 227.325 kPa. These results are almost the same and reasonable as the values in GasTurb 13.

## C) CAD Design

### C.1. CAD Drawing for the Combustion Chamber

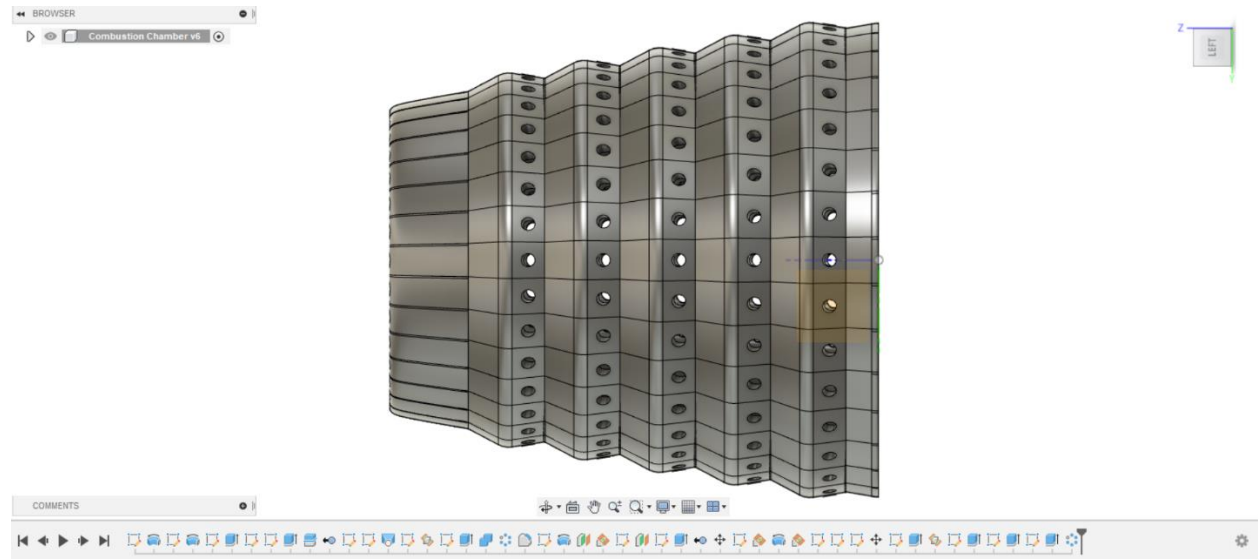


Figure 45. The view of the combustion chamber.[Fusion 360]

The figure 45 shows the view of the combustion chamber. This part of the engine has been drawn by using Fusion 360.

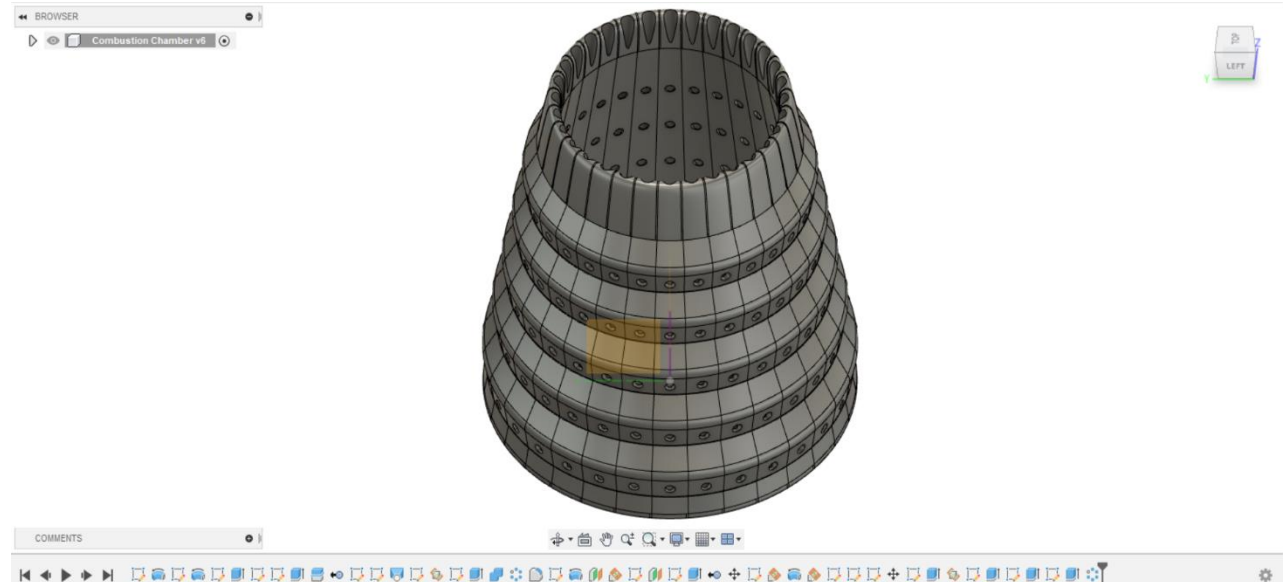
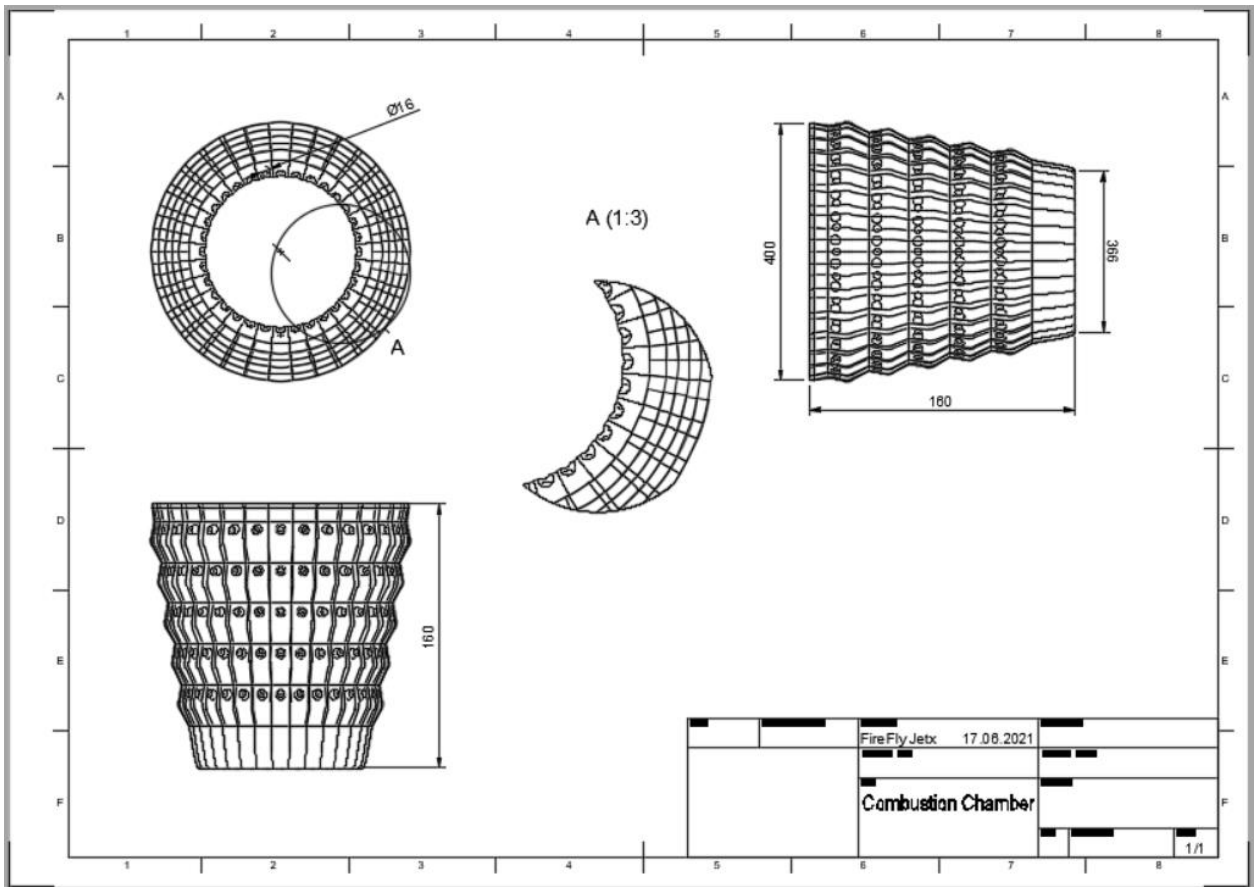


Figure 46. The view of the combustion chamber.[Fusion 360]

The figure 46 depicts the view of the combustion chamber. This part of the engine has been drawn by using Fusion 360.



*Figure 47. The view of technical drawing for the combustion chamber.[Fusion 360]*

The figure 47 shows the technical drawing view of the combustion chamber. This part of the engine has been drawn by using Fusion 360.

## C.2. CAD Drawing for the Blade

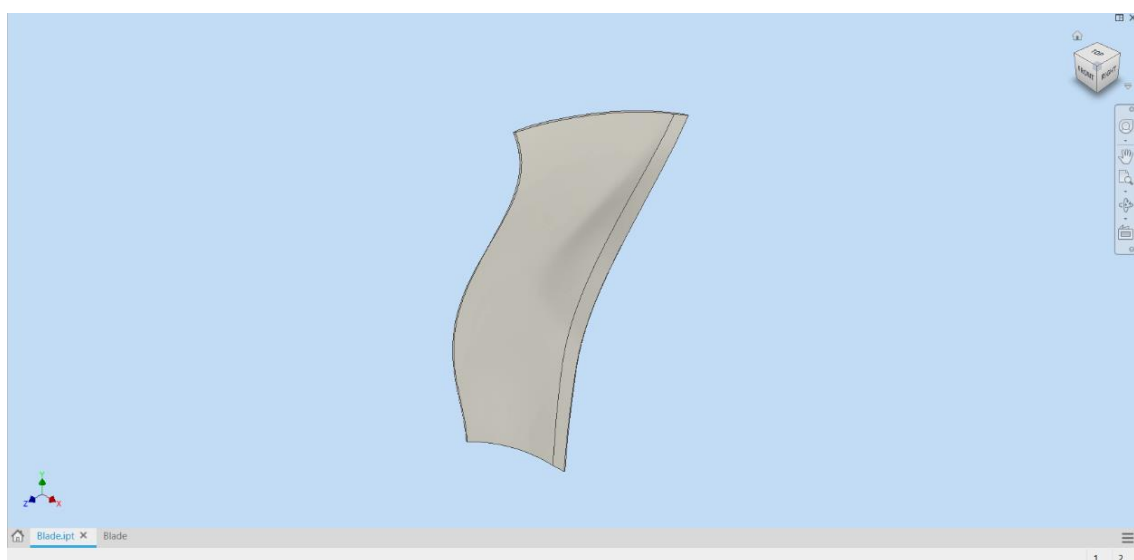


*Figure 48. The view of blade.[Inventor Professional]*

The figure 48 indicates the view of the blade. This part of the fan has been drawn by using Inventor Professional.

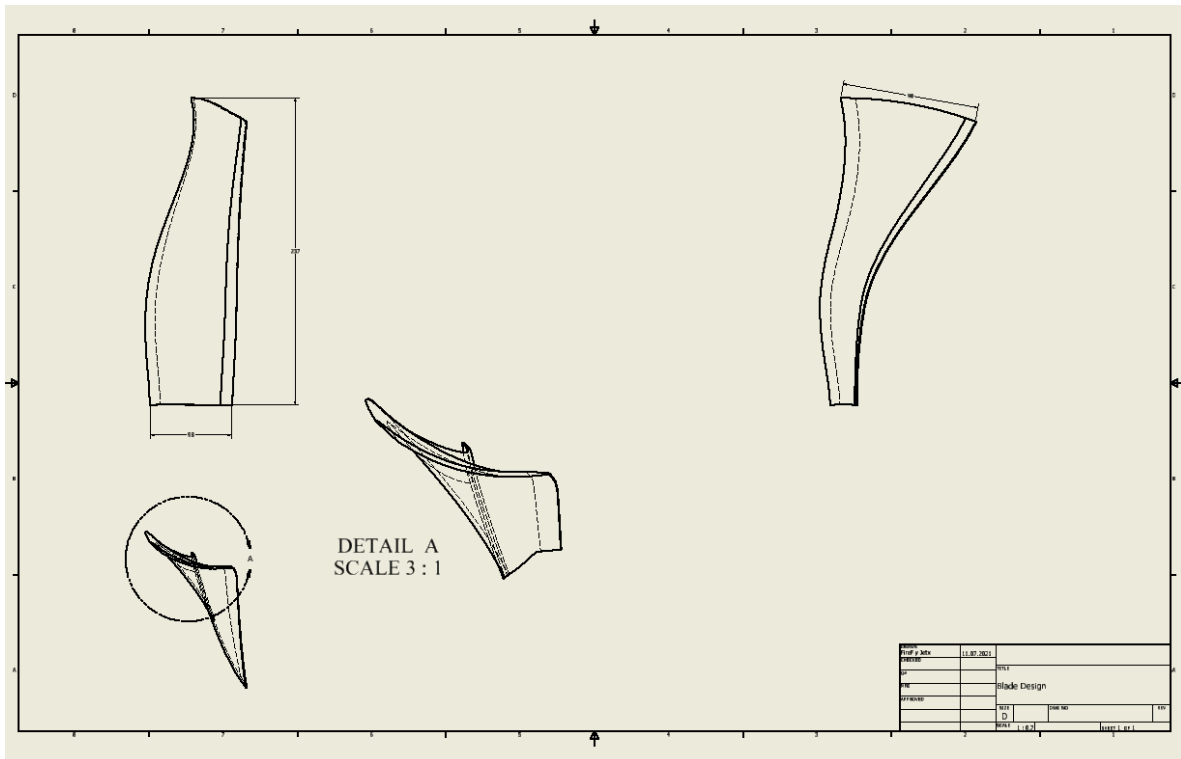


Figure 49. The technical drawing view for the blade.[Inventor Professional]

The figure 49 illustrates the technical drawing view for the blade. This part of the fan has been drawn by using Inventor Professional.

### C.3. CAD Drawing for the ConDi Nozzle

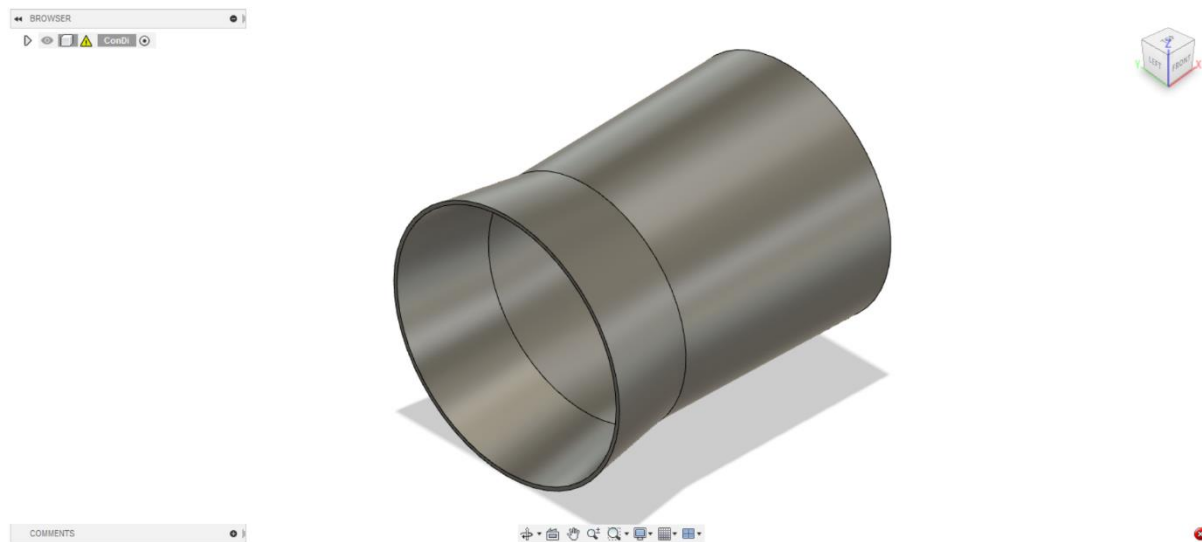


Figure 50. The view of for the ConDi nozzle.[Fusion 360]

The figure 50 shows the view of for the ConDi nozzle. This part of the engine has been drawn by using Fusion 360.

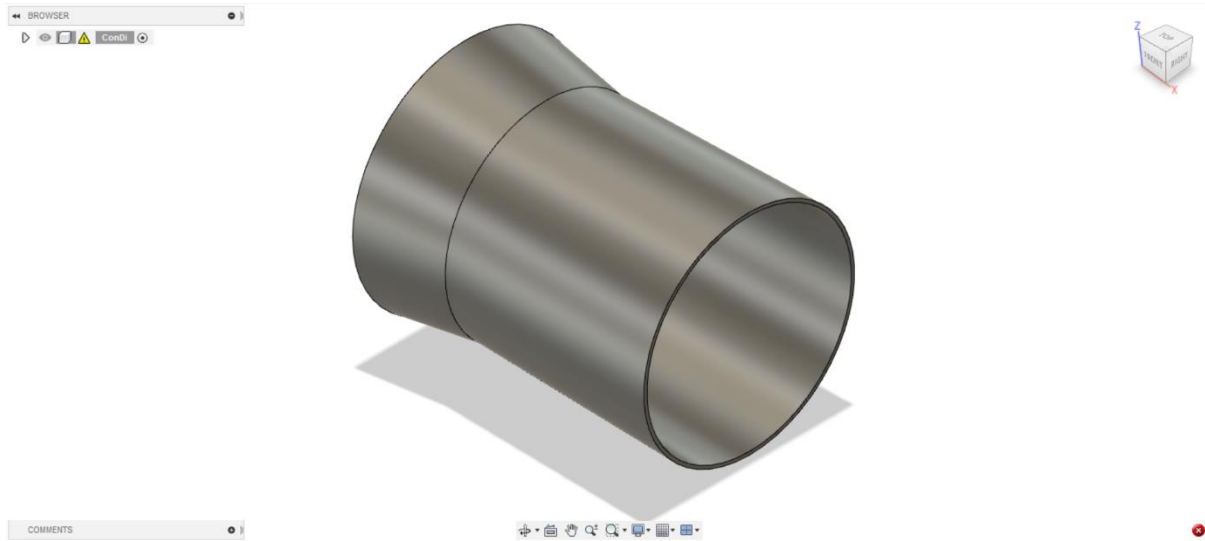


Figure 51. The view of for the ConDi nozzle.[Fusion 360]

The figure 51 exhibits the view of for the ConDi nozzle. This part of the engine has been drawn by using Fusion 360.

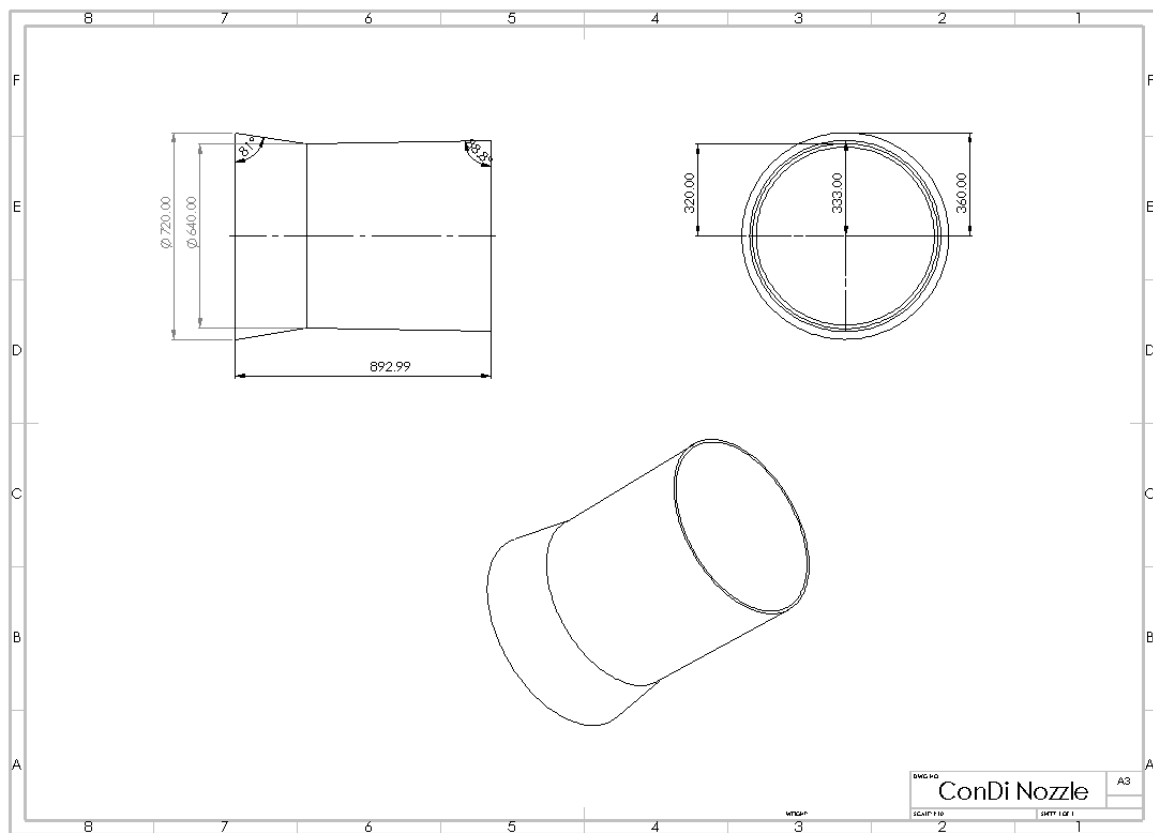


Figure 52. The ConDi nozzle dimensions with afterburner.[SolidWorks]

The figure 52 demonstrates the ConDi nozzle dimensions with afterburner. This part of the engine has been drawn by using SolidWorks.